Sumario

ENFOQUE UTE REVISTA
Facultad Ciencias de la Ingeniería e Industrias
eISSN:13906542

Editorial

It is a pleasure to present Volume 16, Issue 1 of the Enfoque UTE journal, which features a selection of high-quality research articles. It is worth mentioning that the articles included in this edition have undergone a rigorous peer review process by national and international experts. After this thorough process, we have selected six articles that make up the current issue.

In this issue we are pleased to present the paper by Mera et al. which is a contribution to the study of the environmental impact of road transportation. This study presents an evaluation of the effects of idling and power demand on fuel consumption and CO_2 emissions from taxis. The study evaluates the impact of idling, traffic, and ecodriving on fuel consumption and well-to-wheel (WTW) CO_2 emissions in urban taxi operations under real traffic conditions in Ecuador. Five scenarios were examined: baseline, eco-driving, low traffic, start-stop technology, and a combined scenario. The results shows that urban driving resulted in the highest WTW CO_2 emissions (354 gCO_2/km) compared with rural and highway driving. In the case of the combined scenario, which merges lower power demand with start-stop technology, achieved the greatest improvements, reducing WTW CO_2 emissions and fuel consumption by 15% compared to the baseline scenario. These findings underscore the potential of ecodriving and start-stop technology in reducing fuel consumption and emissions.

Continuing with our line of engineering contributions, the paper presented by Gallardo et al., investigates the efficacy of submerged vanes as a technique for stabilizing riverine structures and reducing local scour around bridge piers. The study examined acrylic vanes placed at a 15° angle upstream of a square bridge pier in a sedimentation channel at the National Polytechnic School in Quito, Ecuador. According to the experiments, these vanes considerably decreased average silt flow downstream by 40% and maximum scour depth by up to 60%. The findings suggest that submerged vanes are not only effective but also cost-efficient, making them a promising alternative to traditional scour protection methods such as riprap or aprons.

In the electrical and electronics area, the Enfoque UTE journal presents the paper developed by Naranjo et al. The paper aims to analyze the challenges in the Coca Codo Sinclair hydropower in Ecuador. The study identifies structural problems, geological problems, and environmental impacts including erosion and sedimentation. The authors recommend urgent action on remediation works, with a combination of investments in repairs and maintenance activities, improvements in management and governance of the project.

Continuing with the exploration of innovative technologies, we present the paper by Carrillo et al., which investigates Artificial Intelligence methods for automatic bandwidth adjustment in wireless networks, focusing on their impact on improving Quality of Service (QoS) and user experience. This study explores automatic bandwidth adjustment techniques using supervised learning methods, assessing their effectiveness in wireless networks. Results indicate that Random Forest is the most effective method, followed by Naive Bayes, Logistic Regression, and SVM, while KNN and neural networks showed limited performance. The research underscores the importance of these techniques in optimizing traffic management and ensuring service quality.

Moving into the environmental area, Chumi et al. present the bioremediation of water contaminated with motor oil by biological surfactants produced by Streptococcus thermophilus bacteria, using cheese whey as a carbon source. In this paper, the ecotoxicity test with Daphnia magna confirmed that the biosurfactant is environmentally friendly.

We also present the paper by Susunagua et al., which analyzes the greenhouse gas emissions generated by commercial grills in the metropolitan area of Veracruz, Mexico, and their impact on climate change. The study is focused on CO_2, CH_2, and N_2O generated by cooking processes using firewood and charcoal. Surveys reveal 74.18% of establishments use charcoal, while 25.81% use firewood, resulting in total emissions of 11,612.65 tons/year of CO_2 equivalent. These emissions contribute significantly to climate change and highlight the need for inclusion in local regulations and climate change agendas. The findings provide essential data for addressing environmental impacts in this region.

We invite readers to explore these six contributions, each of which reflects the dedication of their respective authors to advancing scientific knowledge across a diverse range of fields. These studies not only deepen our understanding of key topics but also offer practical solutions to pressing global challenges.

Dr. Oscar Martínez Mozos
Universidad Politécnica de Madrid
Editor-in-Chief

Dr. Diego Guffanti Martínez
Universidad UTE
Editor-in-Chief

ENFOQUE UTE REVISTA
Facultad Ciencias de la Ingeniería e Industrias
elSSN:13906542

Editorial

Es un placer presentar el Volumen 16, Número 1 de la revista Enfoque UTE, que incluye una selección de artículos de investigación de alta calidad. Cabe destacar que los artículos incluidos en esta edición han pasado por un riguroso proceso de revisión por pares realizado por expertos nacionales e internacionales. Tras este exhaustivo proceso, hemos seleccionado seis artículos que conforman el número actual.

En esta edición nos complace presentar el artículo de Mera et al., que constituye una contribución al estudio del impacto ambiental del transporte terrestre. Este estudio evalúa los efectos del ralentí y la demanda de potencia sobre el consumo de combustible y las emisiones de CO_2 en taxis. Se examinan cinco escenarios: línea base, conducción ecológica, tráfico reducido, tecnología start-stop y un escenario combinado. Los resultados muestran que la conducción urbana genera las mayores emisiones de CO_2 (354 gCO_2/km) en comparación con la conducción rural y en carretera. El escenario combinado, que integra una menor demanda de potencia con tecnología start-stop, logra las mayores mejoras, reduciendo las emisiones de CO_2 y el consumo de combustible en un 15 % respecto al escenario base. Estos hallazgos destacan el potencial de la conducción ecológica y la tecnología start-stop para disminuir el consumo de combustible y las emisiones.

Continuando con nuestra línea de contribuciones en ingeniería, el artículo presentado por Gallardo et al. investiga la eficacia de las aletas sumergidas como técnica para estabilizar estructuras fluviales y reducir la socavación local alrededor de pilares de puentes. El estudio analizó aletas acrílicas colocadas en un ángulo de 15° aguas arriba de un pilar cuadrado en un canal de sedimentación de la Escuela Politécnica Nacional en Quito, Ecuador. Los experimentos demostraron que estas aletas redujeron considerablemente el flujo de sedimentos aguas abajo en un 40 % y la profundidad máxima de socavación hasta en un 60 %. Los hallazgos sugieren que las aletas sumergidas no solo son efectivas, sino también rentables, lo que las convierte en una alternativa prometedora a los métodos tradicionales de protección contra la socavación como el enrocado o las losas.

En el área de electricidad y electrónica, la revista Enfoque UTE presenta el artículo desarrollado por Naranjo et al. Este trabajo analiza los desafíos en la hidroeléctrica Coca Codo Sinclair en Ecuador. El estudio identifica problemas estructurales, geológicos e impactos ambientales como la erosión y la sedimentación. Los autores recomiendan acciones urgentes en obras de remediación, combinando inversiones en reparaciones y actividades de mantenimiento, así como mejoras en la gestión y gobernanza del proyecto.

Continuando con la exploración de tecnologías innovadoras, presentamos el artículo de Carrillo et al., que investiga métodos de Inteligencia Artificial para el ajuste automático de ancho de banda en redes inalámbricas, con énfasis en su impacto en la mejora de la Calidad de Servicio (QoS) y la experiencia del usuario. Este estudio explora técnicas de ajuste automático de ancho de banda utilizando métodos de aprendizaje supervisado. Los resultados indican que Random Forest es el método más efectivo, seguido de Naive Bayes, Regresión Logística y SVM, mientras que KNN y las redes neuronales mostraron un desempeño limitado. La investigación resalta la importancia de estas técnicas para optimizar la gestión del tráfico y garantizar la calidad del servicio.

En el ámbito ambiental, Chumi et al. presentan la biorremediación de agua contaminada con aceite de motor mediante surfactantes biológicos producidos por bacterias *Streptococcus thermophilus*, utilizando suero de leche como fuente de carbono. En este trabajo, la prueba de ecotoxicidad con *Daphnia magna* confirmó que el biosurfactante es amigable con el medio ambiente.

También presentamos el artículo de Susunagua et al., que analiza las emisiones de gases de efecto invernadero generadas por las parrillas comerciales en el área metropolitana de Veracruz, México, y su impacto en el cambio climático. El estudio se centra en el CO_2, CH_2 y N_2O generados por procesos de cocción utilizando leña y carbón. Las encuestas revelan que el 74.18 % de los establecimientos usan carbón y el 25.81 % leña, resultando en emisiones totales de 11 612.65 toneladas/año de CO_2 equivalente. Estas emisiones contribuyen significativamente al cambio climático y destacan la necesidad de incluirlas en las normativas locales y agendas de cambio climático. Los hallazgos proporcionan datos esenciales para abordar los impactos ambientales en esta región.

Invitamos a los lectores a explorar estas seis contribuciones, cada una de las cuales refleja la dedicación de sus respectivos autores al avance del conocimiento científico en una variedad de campos. Estos estudios no solo profundizan nuestra comprensión de temas clave, sino que también ofrecen soluciones prácticas a los desafíos globales más apremiantes.

Dr. Oscar Martínez Mozos
Universidad Politécnica de Madrid
Editor en Jefe

Dr. Diego Guffanti Martínez
Universidad UTE
Editor en Jefe

Effect of idling and power demand on fuel consumption and CO_2 emissions from taxis

Mera Zamir[1], Rosero Fredy[2], Rosero Ramiro[3], Tapia Fausto[4], Sergio Ibarra-Espinosa[5]

Abstract — **Urban driving worldwide is characterized by frequent vehicle idling due to traffic congestion, which significantly impacts fuel consumption and vehicle emissions. While strategies such as eco-driving techniques and start-stop systems have been studied extensively in various regions, limited research has been conducted to assess their effects in Latin America. This study evaluates the impact of idling, traffic, and ecodriving on fuel consumption and well-to-wheel (WTW) CO_2 emissions in urban taxi operations under real traffic conditions in Ecuador. Real-world driving data were collected using on-board diagnostics (OBD). A key innovation of this research is the assessment of alternative scenarios, with reduced idling times and power demand, based on the Vehicle Specific Power (VSP) approach. As result, five scenarios were examined: baseline, eco-driving, low traffic, start-stop technology, and a combined scenario. The results shows that urban driving resulted in the highest WTW CO_2 emissions (354 gCO_2/km) compared with rural and highway driving. The combined scenario, which merges lower power demand with start-stop technology, achieved the greatest improvements, reducing WTW CO_2 emissions and fuel consumption by 15% compared to the baseline scenario. Annually, the combined scenario could avoid 3.68 tons of CO_2 emitted per vehicle and fuel savings of 870 USD. These findings underscore the potential of ecodriving and start-stop technology in reducing fuel consumption and emissions to mitigate the environmental impact of road transportation.**

Keywords: **taxis; ecodriving; well-to-wheel CO_2 emissions; on-board diagnosis; idling; vehicle specific power (VSP).**

Resumen — **La conducción urbana a nivel mundial se caracteriza por el frecuente tiempo en ralentí de los vehículos, debido a la congestión del tráfico. Esto impacta significativamente en el consumo de combustible y las emisiones de los vehículos. Si bien se han estudiado ampliamente estrategias como las técnicas de conducción ecológica y los sistemas start-stop en varias regiones, se ha realizado poca investigación para evaluar sus efectos en América Latina. Este estudio evalúa el impacto del ralentí, el tráfico y la conducción ecológica en el consumo de combustible y las emisiones de CO_2 de pozo a rueda (WTW) en las operaciones de taxis urbanos bajo condiciones de tráfico real en Ecuador. Se recopilaron datos de conducción real utilizando diagnóstico a bordo (OBD). Una innovación clave de esta investigación es la evaluación de escenarios alternativos, con tiempos ralentí y demanda de potencia reducidos, basada en el enfoque de Potencia Específica del Vehículo (VSP). Como resultado, se examinaron cinco escenarios: línea base, conducción ecológica, bajo tráfico, tecnología start-stop, y un escenario combinado. Los resultados muestran que la conducción urbana resultó en las mayores emisiones de CO_2 WTW (354 gCO_2/km) en comparación con la conducción rural y en carretera. El escenario combinado, que fusiona una menor demanda de potencia con la tecnología start-stop, logró mayores mejoras, reduciendo las emisiones de CO_2 WTW y el consumo de combustible en un 15% en comparación con el escenario base. Anualmente, el escenario combinado podría evitar 3.68 toneladas de CO_2 emitidas por vehículo y ahorrar 870 USD en combustible. Estos hallazgos subrayan el potencial de la conducción ecológica y la tecnología de arranque y parada para reducir el consumo de combustible y las emisiones, contribuyendo a mitigar el impacto ambiental del transporte por carretera.**

Palabras Clave: **taxis; ecoconducción; emisiones de CO_2 de pozo a la rueda; diagnóstico a bordo; ralentí; potencia específica del vehículo.**

I. INTRODUCTION

THE global challenge of climate change has driven nations worldwide to adopt severe policies aimed at curbing the rise in global temperatures. The Intergovernmental Panel on Climate Change (IPCC) warns that if the current rate of warming continues, the planet is likely to experience a 1.5 °C increase in human-induced global warming by 2040 [1]. A major strategy to mitigate climate change involves reducing emissions from the road transport sector, either through the promotion of cleaner vehicle technologies or the implementation of efficient emissions control systems [2]. In Latin America and the Caribbean (LAC), road transport represents 95% of the total energy consumption in the transport sector, with cars and light commercial vehicles accounting for over 55% of this demand [3]. Ecuador faces a significant challenge with its road transport sector, which contributes approximately 14.3 million tons of CO_2 emissions annually [4]. The country's fuel subsidies, which cover 68% of the annual fuel costs for road transporta-

1. Zamir Mera, Ph.D. Faculty of Applied Sciences, Universidad Técnica del Norte, 100105 Ibarra, Ecuador (e-mail: zamera@utn.edu.ec). ORCID number https://orcid.org/0000-0003-2897-8847.

2. Rosero Fredy, Ph.D. Faculty of Applied Sciences, Universidad Técnica del Norte, 100105 Ibarra, Ecuador (e-mail: farosero@utn.edu.ec). ORCID number https://orcid.org/0000-0003-0971-1944.

3. Rosero Ramiro, MSc. Faculty of Applied Sciences, Universidad Técnica del Norte, 100105 Ibarra, Ecuador (e-mail: rarosero@utn.edu.ec). ORCID number https://orcid.org/0000-0002-3094-0197.

4. Tapia Fausto, MSc. Faculty of Applied Sciences, Universidad Técnica del Norte, 100105 Ibarra, Ecuador (e-mail: fetapia@utn.edu.ec). ORCID number https://orcid.org/0000-0001-7681-2564.

5. Sergio Ibarra-Espinosa, PhD. Cooperative Institute for Research in Environmental Sciences, University of Colorado-Boulder, Boulder, CO, United States (e-mail: sergio.ibarra-espinosa@noaa.gov), and Global Monitoring Laboratory, National Oceanic and Atmospheric Administration (NOAA), Boulder, CO, United States. ORCID number https://orcid.org/0000-0002-3162-1905.

Manuscript Received: 07/10/2024
Revised: 14/11/2024
Accepted: 26/11/2024
DOI: https://doi.org/10.29019/enfoqueute.1100
Section Editor: Víctor Suntaxi

tion, exacerbate the issue by encouraging higher fuel consumption and emissions. Adjusting these subsidies could play a pivotal role in making the road transport system more sustainable. However, the lack of a comprehensive and low-cost methodology for estimating fuel consumption across Latin America further complicates efforts to address this issue. Despite these challenges, the implementation of fuel-saving strategies could potentially result in savings of over 550 million barrels of oil by 2030 [5]. Addressing vehicle emissions and fuel consumption is not only critical for mitigating environmental damage but also for improving public health.

Nowadays, some of the most urbanized regions in the world include Northern America (82% of its population living in urban areas as of 2018), Latin America and the Caribbean (LAC) with 81%, followed by Europe (74%), and Oceania (68%). Meanwhile, Asia's urbanization level has reached nearly 50%, and Africa remains predominantly rural, with only 43% of its population living in cities [6]. In LAC, rapid urbanization has placed immense pressure on mobility systems, which often lack the capacity and infrastructure to meet the growing demands of urban populations. This has led to a reliance on inefficient transportation solutions such as taxis and motorcycles, which are typically low-capacity and inefficiently routed [7]. The prevalence of these modes of transport complicates efforts to manage energy consumption and implement effective fuel-saving policies. In many urban areas, taxis have become the preferred mode of transportation, contributing significantly to traffic congestion, especially during peak hours. This congestion leads to increased idling and stop-start driving, both of which result in higher fuel consumption and elevated CO_2 emissions [8]. As a result, addressing the inefficiencies in urban transport systems, particularly in terms of vehicle emissions and energy use, is crucial for enhancing sustainability and reducing the environmental impact in these rapidly urbanizing regions. Effective policy interventions, such as optimizing public transportation and adjusting transportation subsidies, are critical to tackling these challenges and improving urban mobility in LAC and countries like Ecuador.

Vehicle performance is influenced by various internal factors such as technology, powertrain configuration, and fuel type, as well as external factors like regulations, driving behavior, traffic conditions, and road quality. In urban environments, traffic congestion significantly increases vehicle emissions due to the high frequency of idling and repeated acceleration and deceleration cycles. To mitigate the problems related to traffic congestion, several studies have explored strategies like reducing idling times, implementing eco-driving techniques, and utilizing start-stop systems, which collectively offer substantial fuel savings by minimizing unnecessary braking and acceleration. Idling alone accounts for 6% to 8% of CO_2 emissions, 0.2% to 0.5% of CO emissions by volume, and hydrocarbon emissions can reach up to 2.5 parts per million (ppm) during idle periods [9]. Eco-driving, which involves maintaining a steady speed, avoiding harsh braking, and minimizing idling, has demonstrated average fuel savings of 6% per trip with only a 1.5% increase in travel time [10]. These benefits are seen across different vehicle types and driving environments, highlighting the potential of eco-driving to contribute to emission reduction goals without significantly disrupting traffic flow.

Start-stop systems, which automatically shut off the engine when the vehicle is stationary, can further reduce fuel consumption to zero during idle periods, effectively eliminating associated emissions. Despite the proven benefits, these technologies remain underutilized in LAC, where emissions regulations typically do not address CO_2 emissions. The absence of CO_2 limits allows vehicles with higher fuel consumption and carbon footprints to continue entering the market, undermining progress toward carbon neutrality [11]. Additionally, the lack of stringent regulations reduces incentives for automakers to adopt fuel-saving technologies, such as hybridization, engine downsizing, and start-stop systems, which could play a pivotal role in reducing emissions and improving energy efficiency in the region. Addressing this regulatory deficiency is crucial for aligning the LAC region with global emission reduction targets and fostering a transition toward cleaner, more efficient transportation systems.

In recent years, the global automotive industry has seen considerable variation in the fuel consumption of newly registered light-duty vehicles (LDVs), which averaged 7.2 liters of gasoline-equivalent per 100 kilometers (L/100 km) in 2017. Significant disparities in fuel consumption exist between countries, with advanced economies like Australia, Canada, and the United States, where gasoline prices are below USD 1 per liter, averaging higher fuel consumption rates of 7.9 to 9 L/100 km. In contrast, countries with higher fuel prices, such as those in the European Union, Japan, and Korea, achieve lower fuel consumption figures, ranging from 5.2 to 6.5 L/100 km. Emerging economies also show variation, with average consumption between 6.5 and 8.5 L/100 km, although India stands out as an exception with a notably lower rate of 5.6 L/100 km [12].

The variation in fuel consumption across regions is largely driven by factors such as fuel pricing, regulatory frameworks, and the adoption of fuel-efficient technologies. These disparities highlight the urgent need for tailored policies that address the unique challenges of each region in reducing fuel consumption and vehicle emissions. In emerging economies, where regulatory structures and technological adoption may lag, there is a critical demand for standardized and cost-effective methodologies to evaluate fuel consumption. One such approach is the Vehicle Specific Power (VSP) methodology, which provides a valuable tool for estimating fuel economy and mobile source emissions by analyzing the relationship between driving patterns and vehicle performance [13]. VSP offers a detailed understanding of how factors like acceleration, road grade, and speed influence fuel consumption, making it an essential framework for developing fuel-saving strategies, particularly in regions where conventional testing infrastructure may be limited.

A key gap in the existing literature is the limited research on the effects of idling on fuel consumption and emissions in taxis, particularly in high-altitude cities. While some studies have explored vehicle performance using OBD systems, these are few and often limited in scope, highlighting the need for more accessible, low-cost equipment for widespread application. Additionally, there is a lack of studies that specifically

examine the impact of eco-driving techniques and the use of start-stop systems on fuel consumption in urban taxi fleets. Although the VSP approach has shown promise in analyzing fuel economy and emissions, its application in studies across LAC has been limited.

This study investigates the effects of idling, traffic conditions, and eco-driving on fuel consumption and well-to-wheel (WTW) CO_2 emissions of taxis in urban environments, leveraging real-world driving data collected through the On-Board Diagnostics (OBD) system. The innovative aspect of this research is the application of the Vehicle Specific Power (VSP) methodology to simulate alternative vehicle operation scenarios, including eco-driving techniques and start-stop system use. By integrating the Well-to-Tank approach, the study provides a comprehensive analysis of fuel consumption and emissions, offering key insights into strategies for enhancing taxi performance and minimizing environmental impact, especially in high-altitude urban areas. Five scenarios—eco-driving, low traffic conditions, start-stop technology, and a combined approach—were evaluated using VSP to assess the performance of a representative vehicle in Ecuador. This approach highlights the potential benefits of adopting these strategies to significantly reduce fuel consumption and CO_2 emissions in urban taxi fleets.

The structure of this paper is organized as follows: Section 2 details the methodology, including the tested vehicles, measurement campaign, and the definition of operating modes. It also explains the VSP approach, emissions modeling, and the simulation scenarios. Section 3 presents and analyzes the results, discussing their implications for fuel efficiency and emissions reduction in urban taxi fleets. Finally, Section 5 offers the concluding remarks, summarizing key findings and their relevance to improving vehicle performance and reducing environmental impacts in urban settings.

II. METHODOLOGY

A. Tested vehicles

Two gasoline-powered passenger vehicles representative of the Ecuadorian fleet was selected to assess emissions and fuel consumption in real-world conditions. The vehicles were modeled as an average vehicle, using the VSP methodology.

Over the past decade, the Chevrolet Aveo and Chevrolet Sail has been among the most used for taxi services in various cities across Ecuador. The Chevrolet Aveo was the best-selling model in its segment in Ecuador, with approximately 70,000 units sold between 2009 and 2019, and reported by the Association of Automotive Companies of Ecuador [14]; its successor, the Chevrolet Sail, became the top-selling vehicle in the same segment, with 10,000 units sold between 2019 and 2023 [15]. The purpose of selecting these models is to compare the technological development in emissions of the current vehicle with its predecessor, as both share similar technical characteristics. The characteristics, including displacement, weight, engine torque and power are typical of the country's automotive segment. Additional details about the vehicle can be found in Table I.

TABLE I
TECHNICAL SPECIFICATIONS OF THE TESTED VEHICLES

Vehicle parameter	**Vehicle 1**	**Vehicle 2**
Fuel type	Gasoline	Gasoline
Model name	Aveo Emotion	Sail
Model year	2011	2021
Gross vehicle weight (kg)	1592	1470
Engine displacement (cm^3)	1598	1498
Engine maximum power ($kW@min^{-1}$)	76@5800	81@6000
Engine peak torque ($Nm@min^{-1}$)	145@3600	141@4000
Fuel injection type	Indirect	Indirect
Compression ratio	9.5:1	10.5:1

Notably, the tested vehicles underwent a comprehensive preventive and corrective maintenance program to ensure the reliability of the study's results.

B. Measuring campaign

The measuring campaign was performed in the city of Ibarra, located in Ecuador and serving as the capital of Imbabura Province. The selection of Ibarra as the study site is based on a thorough analysis of its mobility landscape and the rapid growth of its automotive fleet, making it an ideal representation of intermediate high-altitude cities in Ecuador and Latin America. According to the United Nations (UN) definition and various studies, the population of intermediate cities ranges from 20,000 to 500,000 inhabitants, depending on factors such as population density and the country's urban system [16]. Ibarra, situated in a valley at an altitude of 2,200 meters above sea level, currently has an estimated population of 221,000 residents, a number that continues to rise [17]. Additionally, the province has seen a significant 55% increase in its automotive fleet from 2013 to 2022.

The vehicles were driven by professional drivers during real-world taxi trips. The driving profiles from passenger cars were derived from real-world data collected at 1-second intervals. As shown in Fig. 1, these profiles are recorded using a GPS+GLONASS logger GL-770 [18]. The speed data was smoothed, and road grade was adjusted using altitude profiles, following the methodology outlined in Regulation EU 2018/1832 [19].

To record engine operating parameters and vehicle fuel consumption data, an OBD interface device ELM 327 [20] was connected to the Torque Pro mobile phone application. The ELM 327 was connected to the OBD2 diagnostic port to read engine operating parameters in real time from the engine control unit (ECU). Simultaneously, these parameters were transmitted via Bluetooth from the ELM 327 to the Torque Pro mobile application for recording and further synchronizing process.

Fig. 1. Tested vehicle equipped and equipment for field data collection.

Long stops higher than 300s were removed from data because they represent stops at the taxis stands. During the tests, a minimum altitude of 2155 meters above sea level was reported. The total positive elevation gain during the test was 343 meters, indicating significant changes in the road levels, particularly in rural and highway segments, which is typical of high-altitude locations

C. Definition of operating modes

The driving mode is described as [21]; however, we used 2 km/h as threshold to define not idling driving modes (Eq. 1-2-3-4).

Idle $v \leq 2\ km/h$; otherwise (1)

Cruise $-0.1\ m/s^2 < a > 0.1\ m/s^2$ (2)

Acceleration $a \geq 0.1\ m/s^2$ (3)

Deceleration $a \leq -0.1\ m/s^2$ (4)

D. Vehicle specific power and emissions modelling

The tractive power refers to the instantaneous power supplied by the engine to alter the kinetic and potential energies of the vehicle, while also counteracting rolling resistance and aerodynamic drag. As a mass-independent parameter, tractive power is commonly expressed as Vehicle Specific Power (VSP) in units of W kg^{-1}. VSP is widely utilized in emissions research and modeling, including the Motor Vehicle Emission Simulator (MOVES) model employed by the United States Environmental Protection Agency (EPA). The formulation of VSP is described in references [22], [23] (Eq. 5).

$$VSP = \frac{P_{wheel}}{m} = v \cdot (a(1+\varepsilon_i) + g \cdot \alpha + g \cdot C_R) + \frac{1}{2}\rho_a \cdot v^3 \left(\frac{C_D \cdot A}{m}\right) \quad (5)$$

where m corresponds to the vehicle mass, v is speed (in m s^{-1}), a is acceleration (in m s^{-2}), $\varepsilon_i \sim 0.1$ is the mass factor for rotational masses, g = 9.81 m s^{-2} is the acceleration of gravity, α is the road grade, C_R is the rolling resistance coefficient (dimensionless), C_D is the drag coefficient (dimensionless), ρ_a is the air density (1.207 kg m^{-3} at 20 °C and 1.013 bar), and A is the cross-sectional area (in m^2). VSP values are binned in 14 modes, establishing different VSP modes and derived power usage, as presented in Table II [24], [25], [26], [27].

TABLE II
VSP MODE AND POWER USAGE LEVEL

	VSP mode	Power usage	VSP range
	[W kg^{-1}]		[W kg^{-1}]
1	VSP < -2	Deceleration	VSP < 0
2	-2 ≤ VSP < 0		
3	0 ≤ VSP < 1	Idle	0 ≤ VSP < 1
4	1 ≤ VSP < 4	Normal usage-low power	1 ≤ VSP < 10
5	4 ≤ VSP < 7		
6	7 ≤ VSP < 10		
7	10 ≤ VSP < 13	Normal usage-high power	10 ≤ VSP < 19
8	13 ≤ VSP < 16		
9	16 ≤ VSP < 19		
10	19 ≤ VSP < 23	Extra-high power	VSP ≥ 19
11	23 ≤ VSP < 28		
12	28 ≤ VSP < 33		
13	33 ≤ VSP < 39		
14	VSP ≥ 39		

The emissions outcomes from the conventional VSP method depend on the average emission level of each of the 14 VSP modes. The instantaneous emission p (in g) of the pollutant i is equal to the average emission $\bar{p}$ (in g) of the VSP mode k [28] (Eq. 6).

$$p_i = \bar{p}_{i,k} \quad (6)$$

The total emission P (in g) of the pollutant i are computed using the number of datapoints for each VSP mode as (Eq. 7):

$$P_i = \sum_{k=1}^{14} N_k \cdot \bar{p}_{i,k} \quad (7)$$

where k is the VSP mode, N the number of data points, and $\bar{p}$ is the VSP-mode average emission (g).

E. Simulation scenarios

1. Baseline scenario

In the baseline scenario for this study, the real-world fuel consumption is used to derive the CO_2 emissions and the fuel consumption. The baseline scenario is crucial in evaluating the impact of alternative scenarios or experimental conditions presented below.

2. Ecodriving scenario

In the Eco driving scenario, VSP power usage levels categorized as 'normal usage-high power', and 'extra-high power' were substituted with a minimum level of 'normal usage-low power'. Thus, VSP values exceeding 4 W/kg were replaced with the corresponding emissions and fuel consumption values specific to the VSP bin 4 category. This alternative scenario aims to evaluate the potential impact of less aggressive driving behavior on overall emissions and fuel efficiency.

3. Low traffic scenario

In this scenario, all vehicle stops lasting longer than 60 seconds were excluded from the dataset. The average stop time in urban driving and traffic can vary depending on traffic density, signal timings, and road conditions. In congested urban environments, stop times can be significantly higher, especially during peak hours, where idle times exceed 30-60 seconds per stop [29].

4. Start-stop scenario

In the start-stop scenario, vehicle stops larger than 2 seconds were removed from the dataset. The fuel consumption by restart of the engine after the start-stop action was assumed to be increased by 3%.

5. Combined strategies scenario

This scenario evaluated the combined effects of ecodriving and start-stop scenarios. Since a start-stop device turns off the vehicle during traffic congestions, long stops and congestion become less relevant for the comparison in terms of GHG emissions.

F. Emission Factors

1. Well-to-wheel emissions

The WTW CO_2 emissions were computed from the fuel consumption and based on the emission values reported by the ICCT in the 'Global comparison of the life-cycle greenhouse gas emissions of combustion engine and electric passenger cars' [30]. The reported values were 19.9 gCO_2/MJ and 73.4 gCO_2/MJ for WTT and TTW emissions for gasoline, respectively. The low heat value for the gasoline (LHV) was 32.1 MJ/lt. The well-to-tank (WTT) emissions of gasoline —primarily related to petroleum extraction, processing, and transportation— along with the tank-to-wheel (TTW) emissions from fuel combustion in vehicles. The WTT emissions were calculated by integrating these TTW figures with the well-to-wheel (WTW) emissions outlined in the European Union's Fuel Quality Directive [31] and the U.S. Renewable Fuel Standard Program [32]. The TTW emissions are based on data from a report by a consortium consisting of the European Commission's Joint Research Centre, EUCAR, and Concawe [33].

2. Distance-specific emission factors

For pollutant j and road section k, the raw distance-specific emission factor (in mg km^{-1}) was computed as (Eq. 8).

$$EF_{j,k} = \frac{\sum \dot{m}_{j,k} \cdot \Delta t}{s_k} \tag{8}$$

where $\dot{m}_{j,k}$ is the instantaneous emission (in mg s^{-1}) during the distance s (in km), and Δt is the sampling time of 1 s.

G. Fuel cost and annual mileage

Fuel savings were calculated based on the reduction in fuel consumption per kilometer for each scenario and the current average price for the gasoline in Ecuador. The analysis assumes an annual mileage of 70,000 km/year or 200 km/day, typical for taxis [34]. As of August 2024, under Presidential Decree No. 308 [35], gasoline prices in the country were liberalized, allowing for price adjustments tied to international oil prices. However, the decree guarantees a maximum monthly increase of 5% and a maximum reduction of 10% in the price. While prices fluctuate, the average cost over recent months has been 2.68 USD per gallon or 0.71 USD per liter of gasoline. The calculation is done only for urban driving since taxis are most of the time used in this area.

III. RESULTS AND DISCUSSION

A. Vehicle activity

These results provide a comprehensive overview of the vehicle's performance across different driving conditions and altitude variations, which will be used for subsequent emissions analysis. The distribution of time spent across different driving environments was 67% in urban, 27% in rural, and 6% in highway driving, while the distance corresponded to 64% in urban settings, 26% in rural areas, and 10% on highways.

The time spent in different driving modes was categorized into four distinct phases: idle, deceleration, acceleration, and cruising. Overall, 34% of the total testing time was spent in idle mode, 25% in deceleration, 29% in acceleration, and 12% in cruise mode.

Fig 2 illustrates the time share across driving modes in urban environment for baseline, ecodriving, low traffic, start stop, and combined scenarios. The smoothed acceleration mode (light yellow) represents the conditions where high power demand observations were replaced by low power demand values. The vehicle spent 33% idling, 25% decelerating, 29% accelerating, and 13% cruising under the baseline scenario. As reference, the idling time of NEDC and WLTC driving cycles, corresponds to 22.6% and 13.4%, respectively [36]. This study shows that overall idling time in real-world conditions is higher than driving

cycles. These values reflect the more frequent stops and starts typical of city driving characterized by frequent stops at traffic lights and congestion under low speeds.

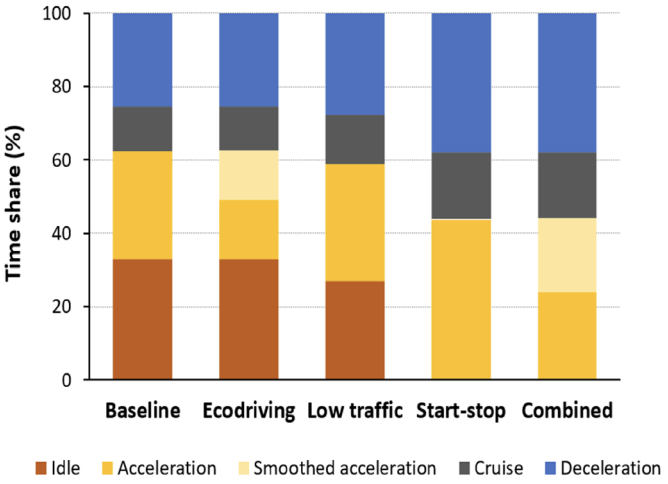

Fig. 2. Time share for each driving mode for the evaluated scenarios in urban zone.

For the ecodriving scenario, part of the acceleration conditions under high power demand is replaced by smoothed accelerations, which becomes 13% of the driving time. In the low traffic scenario, idle time further decreases to around 26%. With fewer prolonged stops, vehicles spend more time cruising and reduced total travel time to destiny. This result indicates that reduced traffic congestion allows for more continuous vehicle movement, thus increasing overall efficiency.

In the **start-stop** scenario, designed to eliminate idle time through the use of start-stop technology, acceleration time dominates this scenario. However, in heavy urban traffic with frequent short stops, the effectivity of this system may be reduced due to the frequent restarting of the engine, potentially diminishing its overall benefits [37]. The **combined** scenario leads to no idle time like to the start-stop scenario and 20% of the time in smoothed acceleration mode. The redistribution of time shares for acceleration and deceleration reflects the smoother driving associated with ecodriving, in conjunction with the elimination of unnecessary idling through start-stop functionality. This scenario represents the optimal configuration for urban driving, merging both strategies to achieve significant improvements in fuel efficiency and emissions reduction.

1. Stops

Fig. 3 presents the distribution of stop time recorded during the urban driving test. The histogram illustrates a highly skewed distribution with the majority of stop times concentrated in the lower range. The stop time data predominantly falls below 50 seconds, with a peak between 0 and 10 seconds. As stop time increases, the frequency sharply decreases, indicating that most stops during the test were of short duration.

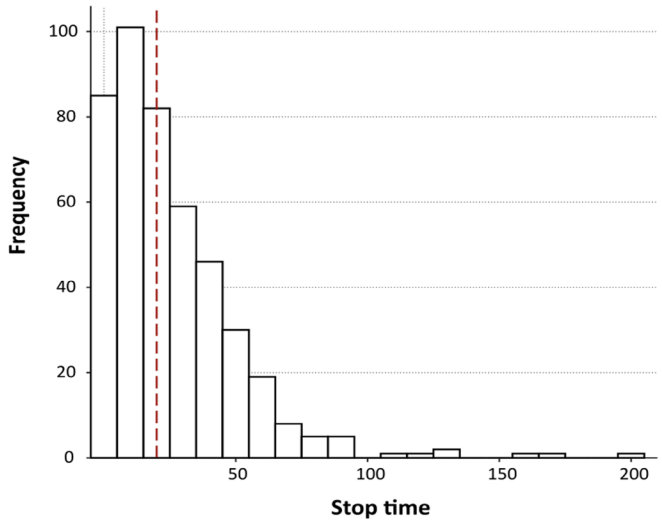

Fig. 3. Frequency distribution for the stop time in urban driving.

Additionally, the dashed vertical line represents the median of 20.5 s, which is positioned within the lower part of the distribution, reaffirming the preponderance of shorter stops. Few instances of stop times exceed 100 seconds. These results suggest that in typical urban driving conditions, stops tend to be brief, but outliers representing prolonged stops occur infrequently.

B. VSP distributions

Fig. 4 shows the frequency distributions for the VSP modes for each scenario. The VSP modes do not exceed bin 10, reflecting the urban driving patterns in these scenarios. The baseline scenario exhibits the highest frequency of observations in bin 3. This idling frequency significantly decreases in the low traffic, start-stop, and combined scenarios. Note that Fig. 4 shows the VSP mode distributions during the engine operation. Additionally, VSP mode 4 is more prevalent in the ecodriving scenario, and subsequently in the combined scenario, due to the shift from higher power demand bins to VSP mode 4.

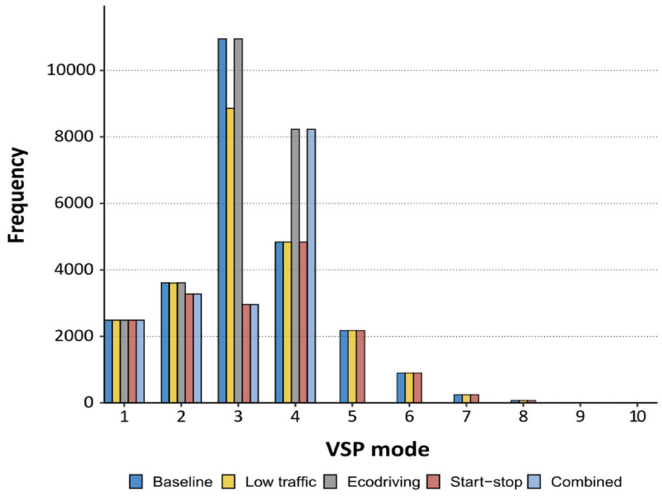

Fig. 4. Frequency distribution of VSP mode for the evaluated scenarios in urban driving, during the engine operation.

C. Baseline fuel consumption and emissions

For comparison, and the use along this study, the average vehicle across all driving conditions had an overall fuel consumption of 11.2 L/100km. Considering the driving zone, the average vehicle achieved 11.8 L/100km in urban driving, 10.8 L/100km in rural driving, and 8.2 L/100km on highways.

Taking the average vehicle, Fig. 5 presents the well-to-wheel (WTW) CO_2 emissions for three driving zones: urban, rural, and highway. The emissions are divided into two components: fuel consumption and fuel production, with total emissions reported in grams of CO_2 per kilometer (gCO_2/km).

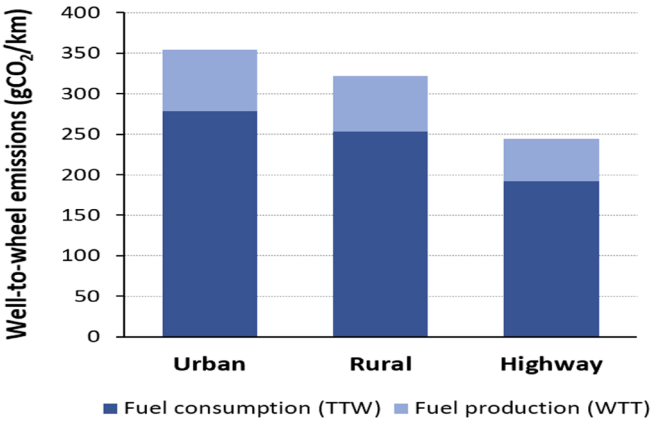

Fig. 5. WTW CO_2 emissions for urban, rural, and highway driving zones.

As is shown, CO_2 emissions from fuel consumption is higher than fuel production. Fuel consumption emissions represent 79% of WTW emissions. The urban driving exhibits the highest total WTW emissions, having 354 gCO_2/km. Of this total, 279 gCO_2/km, is attributed to fuel consumption, while the remaining emissions from fuel production. This high emission level in urban settings can be linked to frequent idling, stop-and-go traffic, and the relatively low average speeds characteristic of city driving. These conditions lead to less efficient fuel combustion, thereby increasing both fuel consumption and overall emissions.

In contrast, the rural driving shows a slight reduction in WTW emissions, reaching 322 gCO_2/km. This reduction can be explained by the typically higher speeds and fewer stop-start events in rural driving, which allow for more efficient fuel use.

The highway driving zone demonstrates the lowest WTW emissions, falling below 244 gCO_2/km. The efficiency gains associated with highway driving can be attributed to sustained higher speeds and fewer interruptions, allowing the engine to operate in their optimal fuel efficiency range for extended periods [38]. Additionally, highway driving involves less acceleration and deceleration, which further enhances fuel efficiency.

Overall, these results illustrate the substantial variability in WTW CO_2 emissions across different driving environments. Urban driving, with its frequent stops, lower speeds, and higher idling times, is associated with the highest emissions, underscoring the need for targeted interventions such as enhanced traffic management, eco-driving practices, and the adoption of start-stop systems to reduce fuel consumption in cities.

D. Fuel consumption and emissions in alternative scenarios

Fig. 6 and Fig. 7 provide a comparison of fuel consumption (in L/100km) and well-to-wheel CO_2 emissions (in gCO_2/km) across five evaluated scenarios in urban driving: baseline, ecodriving, low Traffic, start-stop, and combined scenario. In Fig. 7, WTW emissions are divided into fuel consumption and fuel production, with percentage reductions from the Baseline scenario indicated for each alternative.

The baseline scenario has the highest emissions, while each strategy leads to progressively lower emissions, with the combined approach yielding the largest reduction of 15% in emissions and fuel consumption. Together, these figures demonstrate that implementing fuel-saving techniques and technologies can simultaneously improve fuel consumption and reduce environmental impact.

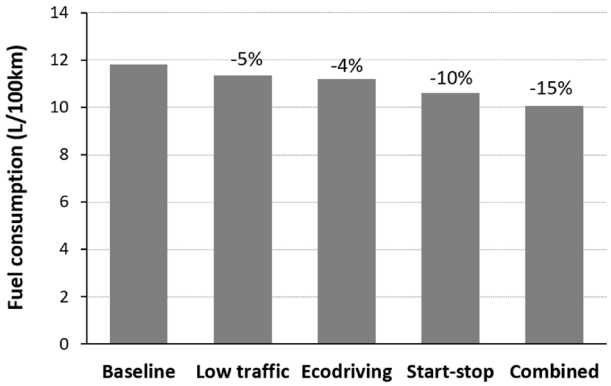

Fig. 6. Comparison of fuel consumption for the evaluated scenarios in urban driving.

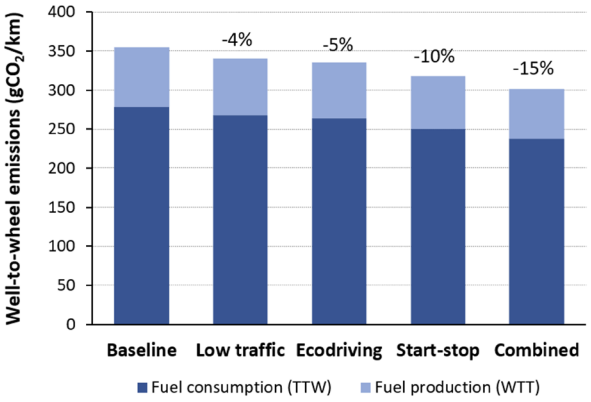

Fig. 7. Comparison of WTW CO_2 emissions for the evaluated scenarios in urban driving.

The ecodriving scenario, achieved a 4% reduction in total WTW CO_2 emissions compared to the Baseline. This relatively modest reduction can be attributed to improvements in fuel efficiency through better driving practices, represented in this study by a driving style with reduced power demand. In the low traffic scenario, where stops longer than 60 seconds are removed, WTW emissions decreased by 5%. The reduction in fuel consumption under low traffic conditions has a direct impact on the overall emissions, especially in urban areas where idling is common.

Consequently, the start-stop scenario demonstrates a 10% reduction in WTW CO_2 emissions and fuel consumption. This significant reduction is achieved by utilizing start-stop technology to eliminate idle fuel consumption. The near-complete elimination of idling substantially reduces fuel consumption, leading to a more noticeable decrease in overall emissions compared to ecodriving or low traffic scenarios. A reduction of 2.5–4.8% in CO_2 emissions were found under the NEDC and WLTC cycles and 4–7% in a report for the revision of Regulation (EC) No 443/2009 on CO_2 emissions from cars [36]. This could be explained because real-world emissions can differ in longer vehicle stops, and the tested vehicles are Euro 3 technology, with expected lower fuel efficiency. Fonseca et al. reported CO_2 emission reduction of more than 20% for diesel passenger cars equipped with the stop/start system. Those results were consistent regardless of the variability in driving style, the grade and type of streets, traffic congestion, and the engine operating temperature [39].

The combined scenario, which integrates both ecodriving techniques and start-stop technology, delivers the most substantial reduction in WTW CO_2 emissions and fuel consumption, achieving a 15% decrease compared to the baseline. This scenario benefits from both smoother driving patterns, which improve fuel efficiency, and the elimination of idling using start-stop systems.

E. Fuel cost and avoided emissions

The annual fuel consumption for an average vehicle in urban driving is estimated at 8,279 liters, costing approximately 5,861 USD. The projected fuel savings per taxi for each evaluated scenario are as follows: 233 USD for the low traffic scenario, 306 USD for the ecodriving scenario, 596 USD for the start-stop scenario, and 870 USD for the combined scenario. At the same time the avoided emissions per taxi in one year are 0.98, 1.30, 2.52, and 3.68 tons of CO_2 for the low traffic, ecodriving, start-stop, and combined scenarios, respectively. The avoided emissions are diminished from a total of 24.8 tons of CO_2 emissions released under the baseline scenario.

IV. CONCLUSIONS

The study provides an assessment of fuel consumption and WTW CO_2 emissions of a representative average taxi under different driving or technology scenarios related to the idling in urban driving. The study uses real-world fuel consumption obtained from ODB data.

Urban driving is the least efficient zone, with frequent idling (33% of driving time) and the highest well-to-wheel (WTW) CO_2 emissions at 354 gCO_2/km, representing 24.8 tons of CO_2 emissions per vehicle-year. This contrasts with rural and highway driving, where emissions are lower due to fewer stops and more sustained speeds. In general, emissions from fuel consumption (TTW) accounts 79% of WTW emissions

The analysis of alternative driving scenarios highlights the potential for emission reductions and fuel savings. The baseline scenario recorded the highest emissions and fuel consumption (11.8 L/100km in urban settings), while the low traffic scenario reduced WTW emissions and fuel consumption by 4%), due to fewer long stops. The ecodriving scenario led to an 5% reduction in emissions by reducing the power demand. The start-stop scenario, which nearly eliminated idle time, reduced emissions and fuel consumption by 10%. The most significant gains were observed in the combined scenario, which merged ecodriving techniques with start-stop technology, resulting in a 15% decrease in emissions to 301 gCO_2/km and fuel consumption to 10.1 L/100km, which avoids 3.68 tons of C_2 per vehicle each year.

In terms of economic impact, the combined scenario yielded the highest annual fuel savings, reducing costs by 870 USD from the 5,861 USD of the baseline scenario, where the fuel consumption is estimated at 8,279 liters.

Overall, these findings highlight the potential of ecodriving practices and start-stop systems to change the distribution of driving modes, particularly in urban settings where idling and strong acceleration is prevalent. As result, fuel consumption and emissions are mitigated by reducing idle time and the power demand, consequently increasing the share of cruise time. The Combined scenario demonstrates the greatest potential for improving efficiency by combining both smoother driving techniques and the elimination of idling. This suggests that urban driving strategies that encourage consistent vehicle motion, alongside the use of start-stop systems, could play a crucial role in reducing the environmental impact of urban transportation.

ACKNOWLEDGMENT

The authors thank to Anthony Champutiz and Luis Cuyago for the contribution in the experimental campaign of the study.

REFERENCES

[1] IPCC, Global Warming of 1.5°C: IPCC Special Report on Impacts of Global Warming of 1.5°C above Pre-industrial Levels in Context of Strengthening Response to Climate Change, Sustainable Development, and Efforts to Eradicate Poverty, 1st ed. Cambridge University Press, 2022. https://doi.org/10.1017/9781009157940

[2] L. Kinsella, A. Stefaniec, A. Foley and B. Caulfield, "Pathways to decarbonising the transport sector: The impacts of electrifying taxi fleets," *Renewable and Sustainable Energy Reviews*, vol. 174, p. 113160, Mar. 2023. https://doi.org/10.1016/j.rser.2023.113160

[3] International Energy Agency, Latin America Energy Outlook 2023. OECD, 2023. https://doi.org/10.1787/fd3a6daa-en

[4] J. C. Sierra, "Estimating Road transport fuel consumption in Ecuador," *Energy Policy*, vol. 92, pp. 359-368, May 2016. https://doi.org/10.1016/j.enpol.2016.02.008

[5] M. F. Chavez-Rodriguez, P. Carvajal, J. Martínez, A. Egüez, R. Gonzalez, R. Schaeffer, A. Szklo, A. Lucena and S. Arango, "Fuel saving strategies in the Andes: Long-term impacts for Peru, Colombia and Ecuador," *Energy Strategy Reviews*, vol. 20, pp. 35-48, Apr. 2018. https://doi.org/10.1016/j.esr.2017.12.011

[6] "Total and urban population – UNCTAD Handbook of Statistics 2023." Accessed: Oct. 04, 2024. [Online]. Available: https://hbs.unctad.org/total-and-urban-population/

[7] Inter-American Development Bank, "The Experience of Latin America and the Caribbean in Urbanization: Knowledge Sharing Forum on Development Experiences: Comparative Experiences of Korea and Latin America and the Caribbean," *Inter-American Development Bank*, Mar. 2015. https://doi.org/10.18235/0007004

[8] S. Ma, Y. Zheng and O. Wolfson, "Real-Time City-Scale Taxi Ridesharing," *IEEE Trans. Knowl. Data Eng.*, vol. 27, no. 7, pp. 1782–1795, Jul. 2015. https://doi.org/10.1109/TKDE.2014.2334313

[9] M. Karrouchi, M. Rhiat, I. Nasri, I. Atamane, K. Hirech, A. Messaoudi, M. Melhaoui and K. Kassmi, "Practical investigation and evaluation of the Start/Stop system's impact on the engine's fuel use, noise output, and pollutant emissions," *e-Prime - Advances in Electrical Engineering, Electronics and Energy*, vol. 6, p. 100310, Dec. 2023. https://doi.org/10.1016/j.prime.2023.100310

[10] M. Miotti, Z. Needell, S. Ramakrisnan, J. Heywood and J. Trancik, "Quantifying the impact of driving style changes on light-duty vehicle fuel consumption," *Transportation Research Part D: Transport and Environment*, vol. 98, p.102918, 2021. https://doi.org/10.1016/j.trd.2021.102918

[11] P. Fan, H. Yin, H. Lu, Y, Wu, Z. Zhai, L. Yu and G. Song, "Which factor contributes more to the fuel consumption gap between in-laboratory vs. real-world driving conditions? An independent component analysis," *Energy Policy*, vol. 182, p. 113739, Nov. 2023. https://doi.org/10.1016/j.enpol.2023.113739

[12] "Fuel Economy in Major Car Markets".

[13] R. A. Rodríguez, "Influence of driving patterns on vehicle emissions: A case study for Latin American cities," *Transportation Research Part D Transport and Environment*, vol. 43(C), p. 192, 2016. https://doi.org/10.1016/j.trd.2015.12.008

[14] AEADE, "Anuario 2019." 2019. [Online]. Available: https://www.aeade.net/sdm_downloads/anuario-2019/

[15] AEADE, "Anuario 2023." 2023. [Online]. Available: https://www.aeade.net/sdm_downloads/anuario-2023/

[16] J.-C. Bolay and A.-L. Kern, "Intermediate Cities," in *The Wiley Blackwell Encyclopedia of Urban and Regional Studies*, John Wiley & Sons, Ltd, 2019, pp. 1-5. https://doi.org/10.1002/9781118568446.eurs0163.

[17] National Institute of Statistics and Censuses, "INEC: Población y Demografía." [Online]. Available: https://www.ecuadorencifras.gob.ec/censo-de-poblacion-y-vivienda/,

[18] Transystem Inc., "GPS GL-770." Accessed: Oct. 01, 2024. [Online]. Available: http://www.transystem.com.tw/www/product.php?b=G&m=pe&cid=4&sid=14&id=150

[19] European Commission, "Commission Regulation (EU) 2018/1832 of 5 November 2018 amending Directive 2007/46/EC of the European Parliament and of the Council, Commission Regulation (EC) No 692/2008 and Commission Regulation (EU) 2017/1151 for the purpose of improving the emission." *Official Journal of the European Union.* 1832, 301, 2018. [Online]. Available: http://data.europa.eu/eli/reg/2018/1832/oj

[20] ELM Electronics, "ELM 327." Accessed: Oct. 01, 2024. [Online]. Available: https://www.elm327.com/

[21] S. Kumar Pathak, V. Sood, Y. Singh and S. A. Channiwala, "Real world vehicle emissions: Their correlation with driving parameters," *Transportation Research Part D: Transport and Environment*, vol. 44, pp. 157-176, May 2016. https://doi.org/10.1016/j.trd.2016.02.001

[22] H. C. Frey, K. Zhang and N. M. Rouphail, "Vehicle-Specific Emissions Modeling Based upon on-Road Measurements," *Environ. Sci. Technol.*, vol. 44, no. 9, pp. 3594-3600, May 2010. https://doi.org/10.1021/es902835h

[23] J. L. Jimenez-Palacios, "Understanding and Quantifying motor vehicle emissions with vehicle specific power and TILDAS Remote Sensing," Massachusetts Institute of Technology, 1999. [Online]. Available: https://dspace.mit.edu/handle/1721.1/44505

[24] R. A. Varella, G. Duarte, P. Baptista, L. Sousa and P. Mendoza Villafuerte, "Comparison of data analysis methods for european real driving emissions regulation," *SAE Technical Paper,* vol. 6, no. Euro 6, 2017, https://doi.org/10.4271/2017-01-0997

[25] R. A. Varella, G. A. Gonçalves, G. Duarte and T. L. Farias, "Cold-Running NO x Emissions comparison between conventional and hybrid powertrain configurations using real world driving data," *SAE Technical Paper*, no. x, 2016. https://doi.org/10.4271/2016-01-1010

[26] H. Frey, A. Unal, J. Chen, S. Li and C. Xuan, "Methodology for developing modal emission rates for EPA's multi-scale motor vehicle & equipment emission system," State University for US EPA, Ann Arbor, MI, no. October, pp. 18-20, 2002.

[27] R. A. Varella, M. V. Faria, P. Mendoza-Villafuerte, P. C. Baptista, L. Sousa and G. O. Duarte, "Assessing the influence of boundary conditions, driving behavior and data analysis methods on real driving CO2 and NOx emissions," *Science of The Total Environment,* vol. 658, pp. 879-894, Mar. 2019. https://doi.org/10.4271/2016-01-1010 10.1016/j.scitotenv.2018.12.053

[28] Z. Mera, R. Varella, P. Baptista, G. Duarte and F. Rosero, "Including engine data for energy and pollutants assessment into the vehicle specific power methodology," *Applied Energy*, vol. 311, p. 118690, Apr. 2022. https://doi.org/10.1016/j.apenergy.2022.118690

[29] Q. Cheng, Z. Liu, J. Lu, G. List, P. Liu and X. S. Zhou, "Using frequency domain analysis to elucidate travel time reliability along congested freeway corridors," *Transportation Research Part B: Methodological*, vol. 184, p. 102961, Jun. 2024. https://doi.org/10.1016/j.trb.2024.102961

[30] G. Bieker, "A global comparison of the life-cycle greenhouse gas emissions of combustion engine and electric passenger cars," International Council on Clean Transportation, 2021. [Online]. Available: https://theicct.org/publication/a-global-comparison-of-the-life-cycle-greenhouse-gas-emissions-of-combustion-engine-and-electric-passenger-cars/

[31] Council of the European Union, "Council Directive (EU) 2015/652 of 20 April 2015 laying down calculation methods and reporting requirements pursuant to Directive 98/70/EC of the European Parliament and of the Council relating to the quality of petrol and diesel fuels," *Official Journal of the European Union, L107*., 2015. [Online]. Available: https://eur-lex.europa.eu/legal-content/EN/TXT/PDF/?uri=CELEX:32015L0652&from=DE

[32] U.S. EPA, "40 CFR Part 80. Regulation of Fuels and Fuel Additives: Changes to Renewable Fuel Standard Program.," U.S. Environmental Protection Agency, 2010. [Online]. Available: https://www.govinfo.gov/content/ pkg/FR-2010-03-26/pdf/2010-3851.pdf

[33] M. Prussi, M. Yugo, L. Prada, M. Padella, R. Edwards and L. Lonza, "JEC well to-tank report v5. Well-to-Wheels analysis of future automotive fuels and powertrains in the European context," Publications Office of the European Union, 2020. [Online]. Available: https://data.europa.eu/ doi/10.2760/959137

[34] D. Sarango and P. Moncayo, "Determinación del indicador kilómetros vehículo recorrido (KVR) para la ciudad de Cuenca," Universidad Salesiana, 2016. [Determination of the vehicle kilometers traveled (VKT) indicator for Cuenca city]. Available: https://dspace.ups.edu.ec/bitstream/123456789/12152/1/UPS-CT006103.pdf

[35] President of the Republic of Ecuador, "Decree No. 308. Codified regulation for the pricing of hydrocarbon derivatives." 2024. [Online]. Available: https://www.comunicacion.gob.ec/wp-content/uploads/2024/06/DE_308_20240526132045.pdf

[36] A. Dimaratos, D. Tsokolis, G. Fontaras, S. Tsiakmakis, B. Ciuffo and Z. Samaras, "Comparative Evaluation of the Effect of Various Technologies on Light-duty Vehicle CO2 Emissions over NEDC and WLTP," *Transportation Research Procedia*, vol. 14, pp. 3169-3178, 2016. https://doi.org/10.1016/j.trpro.2016.05.257

[37] I. Shancita, H. H. Masjuki, M. A. Kalam, I. M. Rizwanul Fattah, M. M. Rashed and H. K. Rashedul, "A review on idling reduction strategies to improve fuel economy and reduce exhaust emissions of transport vehicles," *Energy Conversion and Management,* vol. 88, pp. 794–807, Dec. 2014. https://doi.org/10.1016/j.enconman.2014.09.036

[38] F. Rosero, X. Rosero and Z. Mera, "Developing fuel efficiency and co2 emission maps of a vehicle engine based on the On-Board Diagnostic (OBD) Approach," *Enfoque UTE*, vol. 15, no. 1, pp. 7-15, Jan. 2024. https://doi.org/10.29019/enfoqueute.1002

[39] N. Fonseca, J. Casanova and M. Valdés, "Influence of the stop/start system on CO2 emissions of a diesel vehicle in urban traffic," *Transportation Research Part D: Transport and Environment,* vol. 16, no. 2, pp. 194-200, Mar. 2011. https://doi.org/10.1016/j.trd.2010.10.001

Experimental Analysis of the Effectiveness of Submerged Vanes in Mitigating Local Scour at Quadratic Bridge Piers

Karina Gallardo[1], Khaled Hamad-Mohamed[2], and Jorge Escobar-Ortiz[3]

Abstract — **The use of submerged vanes has been experimentally validated as an effective method for controlling local scour and stabilizing riverine structures. This study evaluates the efficacy of submerged vanes in mitigating local erosion around a square bridge pier. Four experiments were conducted under controlled conditions in the sedimentation channel of the Laboratory of the Faculty of Civil and Environmental Engineering at the National Polytechnic School in Quito, Ecuador. Acrylic submerged vanes were installed upstream of the pier at a 15° attack angle relative to the flow direction, aiming to modify the velocity distribution and sediment transport dynamics. The experimental results showed that submerged vanes reduced the maximum scour depth by up to 60% compared to tests without vanes, with an average reduction of approximately 58%. This significant reduction was attributed to the generation of vortices that redistributed sediment, resulting in shallower and more stable scour holes. Furthermore, the average sediment transport downstream decreased by approximately 40%, further validating the vanes' efficiency in controlling erosive processes. The vanes demonstrated consistent effectiveness across varying flow rates and sedimentation conditions, underscoring their practical adaptability. By modifying flow dynamics and reducing bed shear stress, the vanes provided reliable scour protection regardless of the hydraulic conditions tested. This study highlights the submerged vanes' potential as a viable, economical, and innovative solution for protecting riverine infrastructures, particularly bridge piers, against erosive forces. Their scalability and adaptability to different hydraulic conditions make them suitable for mitigating scour in river systems with high sediment transport activity and for retrofitting existing infrastructure to enhance its stability. This research contributes to the body of knowledge on local scour mitigation by presenting a replicable experimental methodology and emphasizing the practical applicability of submerged vanes. in hydraulic engineering. The findings suggest that submerged vanes are not only effective but also cost-efficient, making them a promising alternative to traditional scour protection methods such as riprap or aprons.**

Keywords: **local scoure; vortices; submerged vanes; sediment transport.**

Resumen — **El uso de paneles sumergidos ha sido validado experimentalmente como un método efectivo para controlar la erosión local y estabilizar estructuras fluviales. Este estudio evalúa la eficacia de los paneles sumergidos en la mitigación de la erosión local alrededor de una pila de puente cuadrada. Se realizaron cuatro experimentos bajo condiciones controladas en el canal de sedimentación del Laboratorio de la Facultad de Ingeniería Civil y Ambiental de la Escuela Politécnica Nacional en Quito, Ecuador. Los paneles sumergidos de acrílico se instalaron aguas arriba de la pila con un ángulo de ataque de 15° respecto a la dirección del flujo, con el objetivo de modificar la distribución de velocidades y la dinámica del transporte de sedimentos. Los resultados experimentales mostraron que los paneles sumergidos redujeron la profundidad máxima de socavación en hasta un 60% en comparación con las pruebas sin paneles, con una reducción promedio de aproximadamente 58%. Esta reducción significativa se atribuyó a la generación de vórtices que redistribuyeron el sedimento, resultando en cavidades de socavación más someras y estables. Además, el transporte promedio de sedimentos aguas abajo disminuyó aproximadamente un 40%, lo que valida aún más la eficiencia de los paneles en el control de los procesos erosivos. Los paneles demostraron una efectividad consistente frente a diferentes caudales y condiciones de sedimentación, subrayando su adaptabilidad práctica. Al modificar la dinámica del flujo y reducir las tensiones cortantes del lecho, los paneles proporcionaron una protección confiable contra la socavación, independientemente de las condiciones hidráulicas evaluadas. Este estudio destaca el potencial de los paneles sumergidos como una solución viable, económica e innovadora para proteger infraestructuras fluviales, particularmente pilas de puentes, contra fuerzas erosivas. Su escalabilidad y adaptabilidad a diferentes condiciones hidráulicas los hacen adecuados para mitigar la socavación en sistemas fluviales con alta actividad de transporte de sedimentos y para reacondicionar infraestructuras existentes, mejorando su estabilidad. Esta investigación contribuye al cuerpo de conocimiento sobre la mitigación de la socavación local al presentar una metodología experimental replicable y resaltar la aplicabilidad práctica de los paneles sumergidos.**

Palabras Clave: **Erosión local; vórtices; paneles sumergidos; transporte de sedimentos.**

I. INTRODUCTION

SCOUR remains one of the most critical challenges in civil engineering, being the leading cause of structural settlement in the vicinity of bridge piers. Predicting scour depth, unders-

Authors acknowledge the support provided by Escuela Politécnica Nacional. *Corresponding author:*jorge.escobaro@epn.edu.ec

1. Karina Gallardo Author is with the Centro de Investigaciones y Estudios de Ingeniería de los Recursos Hídricos & Departamento de Ingeniería Civil y Ambiental at Escuela Politécnica Nacional, Quito 170517, Ecuador. (e-mail: yrak1989@hotmail.com). ORCID: https://orcid.org/0000-0003-4365-3813

2. Khaled Hamad-Mohamed Author is with the Centro de Investigaciones y Estudios de Ingeniería de los Recursos Hídricos & Departamento de Ingeniería Civil y Ambiental at Escuela Politécnica Nacional, Quito 170517, Ecuador. (e-mail: khaled.hamad@epn.edu.ec). ORCID: https://orcid.org/0000-0001-9365-9602

3. Jorge Escobar-Ortiz Author is with the Centro de Investigaciones y Estudios de Ingeniería de los Recursos Hídricos & Departamento de Ingeniería Civil y Ambiental at Escuela Politécnica Nacional, Quito 170517, Ecuador. (e-mail: jorge.escobaro@epn.edu.ec). ORCID: https://orcid.org/0000-0003-3862-1657

Manuscript Received: 23/07/2024
Revised: 19/11/2024
Accepted: 28/11/2024
DOI: https://doi.org/10.29019/enfoqueute.1072
Section Editor: Diana Zuleta

tanding its mechanisms, and defining the equilibrium dimensions of scour holes are fundamental for the hydraulic design of bridges, ensuring their stability under varying channel and flow conditions [1]. These considerations require a comprehensive understanding of key parameters such as sediment size, flow velocity, and the geometric characteristics of bridge piers, as they directly influence the structural safety of hydraulic infrastructure [2].

Local erosion around bridge piers occurs due to the removal of bed material, creating a localized flow action that significantly lowers the riverbed around the pier. This process involves two subprocesses: active and passive erosion. The active phase originates at the bottom of the scour hole upstream of the pier, driven by the horseshoe vortex—a flow structure with a horizontal axis whose size depends on the water level [3]. The passive phase, characterized by the intermittent collapse of scour hole walls, is entirely dictated by the dynamics of the active phase. These flow structures amplify bed material displacement and exacerbate scour depth, particularly under clear-water conditions [4]; [5]. The complexity of these subprocesses underscores the need for targeted mitigation strategies to reduce local shear stress and stabilize sediment dynamics.

Traditional methods for mitigating scour, such as riprap, concrete aprons, groins, and spurs, have been widely used in hydraulic engineering. While effective, these methods often come with limitations such as high construction costs, reduced adaptability to dynamic flow conditions, and potential ecological disruption [2]. Comparative analyses reveal that submerged vanes offer a more economical and adaptable alternative, particularly in environments with complex sediment transport dynamics [6]. Unlike riprap, which can be dislodged during high-flow events, submerged vanes actively modify flow patterns to reduce bed shear stresses, making them less prone to failure [7]; (Brian Barkdoll et al., 1999).

Submerged vanes have emerged as a viable and cost-effective solution for controlling sediment transport and mitigating local scour [7]. These structures generate secondary circulation, altering velocity distributions and reducing bed stresses (Hamidi et al., 2024).

Experimental studies and numerical simulations have highlighted the importance of optimized design parameters, such as angles of attack and vane placement, in minimizing scour depth. For instance, dual submerged vanes have been shown to reduce scour depth by up to 33% when positioned at specific angles and distances relative to the pier diameter [8]; [9]. Similarly, [5] demonstrated that incorporating collars at the leading edges of submerged vanes effectively prevents local scour, further enhancing their stability and efficiency.

While submerged vanes present clear advantages, challenges remain, particularly in highly turbulent flows or sediment transport systems dominated by coarse materials [5]; [10]. Studies have shown that rectangular vanes often underperform under these conditions, necessitating alternative designs to enhance their stability and effectiveness. For instance, modifications such as tapered or angled vane configurations have demonstrated improved flow redirection and sediment redistribution capabilities, particularly in reducing shear stresses near bridge piers [11] [12] further highlighted that the application of curved vanes significantly enhances scour mitigation in systems dominated by coarse sediments.

Furthermore, most existing studies focus on circular bridge piers, leaving a significant gap in understanding scour mitigation around square piers. Square piers, with their sharp edges, exacerbate turbulence and increase vortex strength, making them particularly vulnerable to scour [13]; [14]. The three-dimensional nature of the flow around square piers further complicates the problem, as increased velocity gradients form horseshoe and wake vortices that intensify bed material displacement [3].

This study addresses these gaps by exploring the use of submerged vanes specifically designed for square bridge piers. Experimental findings highlight that the strategic placement of vanes upstream of the pier can reduce scour depth by up to 30%, particularly in sharp bend configurations [15]. Additionally, recent reviews emphasize the importance of optimizing vane dimensions and configurations, such as aspect ratios and angles of attack, to maximize sediment control and hydraulic stability [16]. By tailoring vane design and positioning to clear-water conditions, this research aims to achieve equilibrium states that balance erosion control and sediment deposition, offering a practical and sustainable methodology for improving hydraulic stability.

II. MATERIALS AND METHODS

The experimentation was conducted in the channel of the Hydraulic Teaching Laboratory of the Faculty of Civil and Environmental Engineering at the National Polytechnic School (EPN), Quito, Ecuador. The channel features a closed water circuit driven by a pump, capable of reproducing conditions from the incipient movement of particles to bed washout. Discharge flow rates were measured using weirs, and the channel's inclination can vary from 0 to 10%. Figure 1 shows the channel, which is 1.55 m long, 78 mm wide, and 110 mm deep.

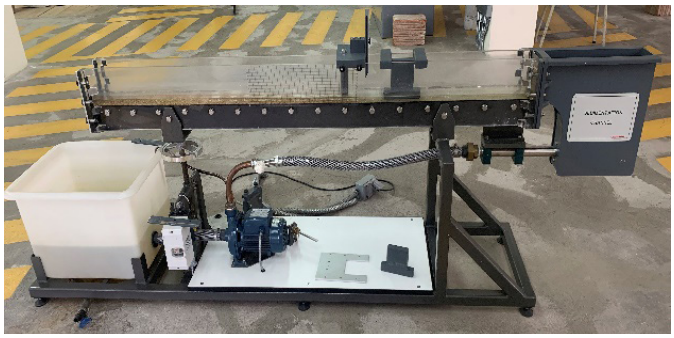

Fig. 1. Sediment Transport Demonstration Channel (Sedimentation Channel Operation Instructions, 2004, Cussons brand).

The design conditions of the submerged vanes experimented with in this research depended on the scenario in which the process was conducted. The primary objective was to mitigate the local scour hole that forms at the bridge pier, generating vortices that affect downstream flow. The height of the vane depended on the draft, as well as the spacing between vanes and the walls of the sedimentation channel, ensuring sufficient sediment redistribution to stabilize the scour hole.

Four systematically designed tests were conducted to evaluate the influence of submerged vanes on local scour around a square bridge pier. Each test was performed under controlled laboratory conditions to ensure reproducibility and accuracy. The submerged vanes were installed upstream of the pier at a 15° attack angle relative to the flow direction. [7] established that this angle optimizes secondary circulation, reducing bed shear stress and enhancing sediment redistribution. Subsequent studies, including [5], [11], and [4], validated that angles below 20° effectively promote horizontal vortices while maintaining manageable hydraulic resistance. Additionally, [8] demonstrated that dual submerged vanes positioned at optimal angles can reduce scour depth by up to 33%, making them a viable solution for real-world applications.

During the experiments, the water draft was systematically varied while maintaining a constant flow rate, ensuring that clear-water conditions prevailed. This approach allowed for consistent development of the scour hole until equilibrium was achieved. Discharge flow rates were measured using a rectangular weir at the channel's outlet, and the Hegly equation (1921) was applied to ensure accuracy. Calibration of the weir was verified before each test to minimize measurement errors.

Boundary conditions were carefully controlled to prevent external influences on erosion evolution. Following [17], the pier's dimensions were set at least 10% of the channel width, using a 10 mm square wooden pier. Quartz sand with a characteristic diameter of 0.74 mm and σg < 3 was selected, as its uniformity facilitates reproducibility and aligns with sediment properties commonly used in hydraulic studies. The sand was distributed uniformly along the channel, with the bridge pier placed at its center, 50 cm from the starting point.

The channel allowed for control of critical variables, such as flow rate and inclination, essential for simulating real-world conditions. Using square piers ensured that the study addressed challenges unique to their geometry, as sharp edges exacerbate turbulence and increase vortex strength [13]; [14].

The submerged vanes were designed using the equations proposed by [7] to modify flow dynamics effectively and reduce local scour depth. The attack angle of 15° was selected based on its hydraulic efficiency demonstrated in prior studies. This choice balances efficiency with practical implementation, avoiding the excessive flow resistance associated with larger angles [11]; [12]. Additionally, [9] highlighted the importance of proper vane spacing and alignment for maximizing sediment redistribution in controlled conditions.

The variation of the water draft in the tests allows observing the effect of different flow levels on local erosion. Maintaining a constant flow rate ensures that observed differences are due to the influence of the submerged vanes and not changes in flow. This approach strengthens the reliability of the results, isolating the impact of the submerged vanes from other potential variables.

Table 1 presents the boundary conditions with the different drafts and scenarios conducted in each test

TABLE I
BOUNDARY CONDITIONS FOR DIFFERENT WATER DRAFTS

	Calado (d)		A	Rh	Q	v	Fr	Re
	cm	m	m^2	m	m^3/s	m/s		
E1	4.5	0.045	0.0036	0.0212	0.0019	0.517	0.778	38424
E2	5	0.05	0.0040	0.0222	0.0019	0.465	0.665	36290
E3	5.5	0.055	0.0044	0.0232	0.0019	0.423	0.576	34380
E4	6	0.06	0.0048	0.0240	0.0019	0.388	0.506	32661

The submerged panels were dimensioned according to the equilibrium scour hole characteristics observed in each test, following the equations proposed by [7]. These equations ensure that the panels are optimally sized to modify flow dynamics effectively, promoting sediment redistribution while minimizing local scour depth. These equations were used to determine the optimal dimensions of the submerged vanes, considering the draft of each test, the spacing between vanes and the channel walls, and the distance from the edge of the pier to the edge of the submerged vanes.

The equations used are as follows (Eq. 1-2-3-4-5):

$$H = \frac{1}{3h} \tag{1}$$

$$L = 3H \tag{2}$$

$$ds = 15H \tag{3}$$

$$dn = 3H \tag{4}$$

$$db = 1.5H \tag{5}$$

Where:

H: Height of the submerged panel.
L: Length of the submerged panel.
ds: Distance from the edge of the pier to the start of the panel.
dn: Distance between vanes.
db: Distance from the channel wall to the submerged panel.

Table 2 establishes the dimensions of the submerged vanes tested for each trial.

TABLE II
DIMENSIONS OF SUBMERGED VANES

	Sizing of submerged vanes (α=15°)				
	H m	L m	ds m	dn m	db m
E1	0.015	0.045	0.1125	0.020	0.020
E2	0.017	0.05	0.125	0.020	0.020
E3	0.018	0.055	0.1375	0.020	0.020
E4	0.020	0.06	0.15	0.020	0.020

The implementation of the submerged vanes in each of the tests is shown in Figure 2.

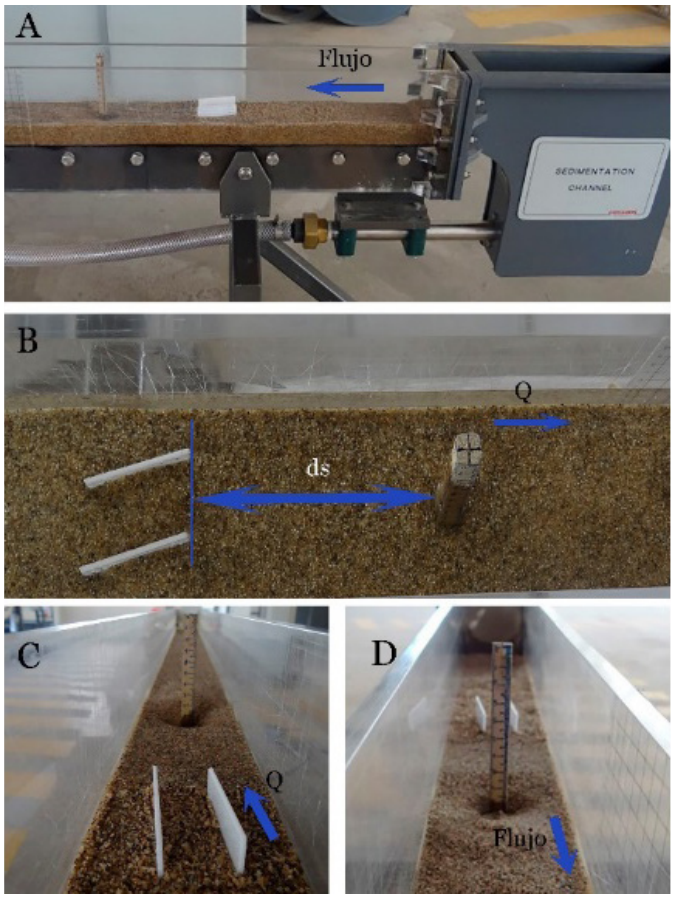

Fig. 2. Equilibrium State Scour Hole (a) left side view, (b) top view, (c) upstream view, (d) downstream view.

III. RESULTS AND DISCUSSION

Test E1

In test E1, the evolution of the erosive phenomenon was observed during the first hours of the test. The development of the horseshoe vortex initiated the active subprocess, followed by the collapse of the scour hole walls in the form of intermittent collapses, as shown in Figure 3. The scour hole reached its equilibrium state at 10 hours into the test. The early-stage aggressiveness of the erosion process highlights the dominance of vortices under lower drafts, which amplify bed shear stress and sediment mobilization. These findings align with the work of [2], emphasizing the critical role of draft height in influencing local scour dynamics. Additionally, the observed trends are consistent with the studies of [10], which demonstrate the importance of hydrodynamic parameters in shaping scour morphology.

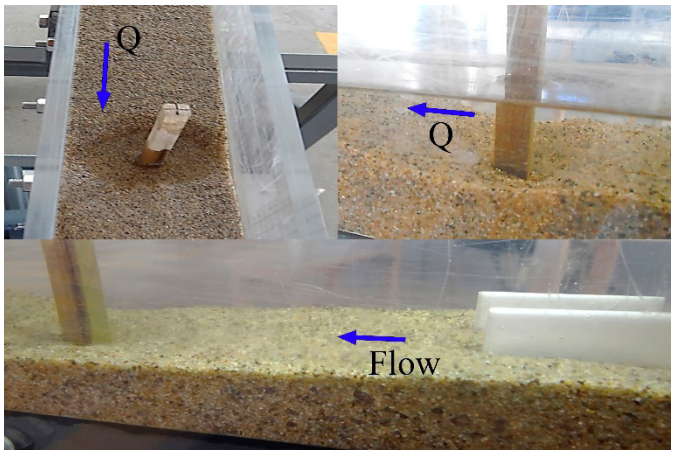

Fig. 3. Equilibrium State Scour Hole E1.

Test E2

In test E2, the onset of movement was ensured to maintain clear-water conditions throughout the process of local erosion evolution. The erosive phenomenon reached its equilibrium state at 13 hours into the test. It was observed that the erosion process occurred more rapidly during the initial hours, both in the formation of the scour hole and in sediment transport downstream of the pier, as shown in Figure 4. Compared to test E1, the erosion rate deceleration observed in the latter stages indicates a stabilization process driven by increasing draft height, which reduces flow turbulence near the bed. These results support the hypothesis of [5], which states that drafts exceeding the critical depth minimize sediment disturbance and enhance sediment stability.

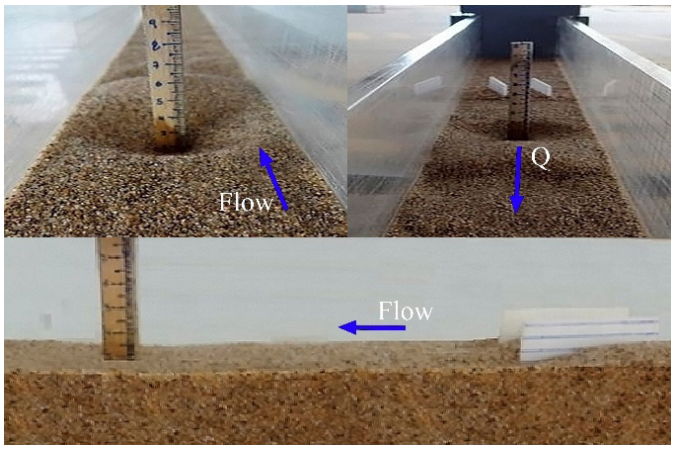

Fig. 4. Equilibrium State Scour Hole E2.

Test E3

In test E3, clear-water conditions were maintained to ensure comparability with the previous tests. In this case, the erosive phenomenon was less aggressive due to a greater draft, resulting in lower bed stress and smaller characteristic vortices. The erosive phenomenon reached its equilibrium state at 14 hours into the test, as shown in Figure 5. The reduced erosion rates confirm the theoretical relationship between draft height and vortex intensity, as described by [7]. These findings are further corroborated by the results of [8], who demonstrated a significant reduction in scour depth under controlled hydrodynamic parameters.

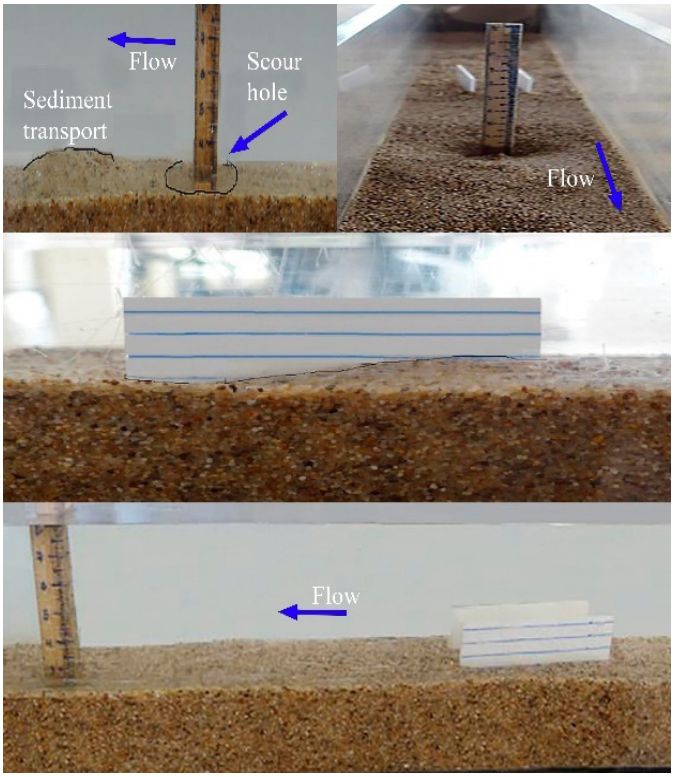

Fig. 5. Equilibrium State Scour Hole.

Test E4

In the final test, the pier was positioned at the point of incipient motion, as in the previous experiments. With a greater draft, the flow velocity and bed stress were lower, resulting in a slower and less aggressive development of the erosive phenomenon. Despite this, the formation of the horseshoe vortex in front of the pier and the wake vortex downstream was observed, causing sediment transport. Figure 6 shows the development of the erosive phenomenon at 16 hours into the test when it reached its equilibrium state. The slower progression of scour and reduced depth highlight the stabilizing effects of higher drafts. This behavior aligns with the studies of [18] and [12], confirming the critical role of draft height in controlling scour dynamics.

Fig. 6. Equilibrium State Scour Hole.

Table 3 presents the conditions for each experiment once the erosive phenomenon had developed, as well as the maximum experimental scour depth (ds). The results reveal a direct correlation between draft height and scour depth, with lower drafts generating deeper scour holes. This behavior agrees with established theories [2] and demonstrates the critical role of flow velocity and turbulence intensity in shaping scour morphology.

Error margins were calculated by repeating each experiment three times under identical conditions. The standard deviation of ds across trials ranged between ±0.1 cm and ±0.2 cm, indicating high repeatability and reliability of the experimental methodology.

TABLE III
EXPERIMENTAL RESULTS

Experiment with bridge pier						
Exp.	**Draft m**	**Flow m3/s**	**Velocity m/s**	**Froude**	**Reynolds**	**ds Exp.**
E1	0.045	0.0019	0.52	0.78	38424	3
E2	0.05	0.0019	0.47	0.66	36290	2.6
E3	0.055	0.0019	0.42	0.58	34380	2.1
E4	0.06	0.0019	0.39	0.51	32661	1.2

The implementation of submerged vanes significantly reduced scour depth, achieving an average protection efficiency of 58% across all tests. These findings confirm their ability to alter flow patterns and mitigate bed shear stress effectively, as summarized in Table 4.

TABLE IV
PROTECTION EFFICIENCY OF SUBMERGED VANES

Exp.	dsexp cm	dsw/vanes cm	Protection Efficiency (%)
E1	3	1.2	60
E2	2.6	1.1	57
E3	2.1	0.9	57
E4	1.2	0.6	50

Table 5 compares experimental results with theoretical methods, showing that the FHWA (HEC-18) method [19] produced results closest to the experimental data, with deviations within ±10%. Other methods, such as [2], tended to overestimate scour depth due to assumptions of higher turbulence intensity.

TABLE V
EROSION CALCULATION METHODS

Exp	ds exp cm	ds cm M.FHWA	ds cm M. Larras	ds cm M. Coleman	ds cm M. Melville
E1	3	3,7	6,641	6,9	9
E2	2,6	3,6	6,641	7,5	10
E3	2,1	3,5	6,641	8,1	11
E4	1,2	2,4	6,641	8,7	12

The results confirm the high effectiveness of submerged vanes in reducing the depth of the scour hole around bridge piers. This effectiveness stems from their ability to modify flow patterns, redistribute velocities, and reduce the erosive capacity of the flow. These findings are consistent with prior studies that demonstrate the efficacy of submerged vanes in mitigating local erosion [7]; [20]. Furthermore, the comparative analysis using various methods for calculating maximum erosion revealed that the FHWA (HEC-18) method provides predictions closest to the experimental results, with deviations within ±10%, validating its application under clear-water conditions [19]. These results reinforce the potential of submerged vanes as a scalable and practical solution for mitigating local scour.

However, practical implementation, especially in large-scale applications, poses certain challenges. A significant limitation is the cost associated with the fabrication and installation of vanes, particularly when durable materials are required to withstand harsh environmental conditions and prolonged submersion. Durability under highly turbulent flows or in environments dominated by coarse sediment transport is another critical concern, as these factors can lead to increased wear and reduced efficiency over time [12].

Scaling up submerged vane deployment also introduces logistical complexities, such as precise alignment during installation and maintaining optimal spacing to ensure effective sediment redistribution. Innovative approaches, such as modular vane designs or materials with enhanced erosion resistance, could help address these challenges. Additionally, field studies in diverse hydraulic environments would provide valuable insights into their real-world performance, offering a clearer picture of their adaptability and long-term effectiveness.

Despite these challenges, the adaptability, proven performance, and cost-effectiveness of submerged vanes underscore their potential as a practical solution for mitigating local scour. Future research should focus on cost-benefit analyses, exploring ways to reduce manufacturing costs, optimize vane configurations for various hydraulic conditions, and test their performance in field-scale implementations. Addressing these aspects will enhance their applicability and ensure their scalability as a robust solution for protecting hydraulic structures against local scour.

IV. CONCLUSIONS

The study determined that the erosive phenomenon develops continuously over a period known as the equilibrium state. During this phase, the vortices gradually diminish, leading to a cessation of interactions between the active and passive subprocesses of scour. This stabilization ultimately results in equilibrium in downstream sediment transport.

The results obtained for maximum erosion, calculated using the different methods presented in Table 5, revealed discrepancies when compared to the experimental results. These differences arise from limitations in accurately determining velocities near the onset of local erosion and the specific conditions under which the calculation methods were developed. Despite these discrepancies, the FHWA (HEC-18) method provided predictions closest to the experimental results, validating its application under clear-water conditions. This reinforces its practicality as a reliable tool for preliminary design in scenarios where site-specific hydraulic conditions resemble those of the controlled experiments.

Laboratory tests clearly demonstrated that submerged vanes can induce significant changes in flow velocity distribution, effectively modifying the depth and shape of the local scour hole around square bridge piers. This behavior is attributed to the reduction in bed shear stresses caused by the vanes. Specifically, the implementation of two submerged vanes upstream of the bridge pier generated vortices that influenced a broader area of the channel cross-section, ensuring complete coverage of the scour hole in all experiments. The evolution of the active and passive subprocesses varied across tests, influenced by the water draft, which controlled the vortex intensity. Consequently, the formation and equilibrium time of the scour hole differed, with a corresponding reduction in shear stress observed in each case. This systematic variation highlights the adaptability of submerged vanes to varying hydraulic conditions, providing a flexible tool for site-specific sediment management strategies.

From a practical perspective, the use of submerged vanes presents a promising solution for mitigating local scour in real-

world applications. These vanes could be strategically implemented in river systems with high sediment transport activity, especially in areas with sharp bends or regions experiencing significant turbulence where traditional methods, such as riprap or aprons, are less effective. Furthermore, their adaptability makes them suitable for retrofitting existing bridge infrastructure in locations where erosion poses an ongoing threat. However, practical challenges such as precise alignment during installation and ensuring structural integrity under fluctuating hydraulic loads remain areas that require further exploration. However, practical challenges such as precise alignment during installation and ensuring structural integrity under fluctuating hydraulic loads remain areas that require further exploration. Addressing these factors will be essential for maximizing the vanes' effectiveness in field applications.

Future research should focus on addressing the economic and material challenges associated with large-scale implementation. Optimizing the panel design for durability in highly turbulent flows and coarse sediment transport conditions is crucial. Cost-benefit analyses and long-term performance evaluations will also be essential to promote their widespread adoption. Moreover, developing guidelines for scaling laboratory results to real-world scenarios will help standardize the use of submerged vanes in hydraulic engineering projects. Additionally, field studies in diverse hydraulic settings will help validate laboratory findings and provide critical insights into real-world performance, especially under variable sediment and flow conditions.

In summary, submerged vanes have proven to be an effective, economical, and practical technique for controlling local erosion around square bridge piers. Their ability to modify flow patterns, reduce shear stress, and enhance structural stability under varied flow conditions highlights their potential as a sustainable and innovative solution in hydraulic engineering. Their demonstrated scalability and efficiency position them as a viable alternative to traditional erosion control measures, capable of addressing the limitations of existing approaches. This positions submerged vanes as a transformative tool for future scour mitigation practices.

REFERENCES

[1] A. Amini and N. Solaimani, "The effects of uniform and nonuniform pile spacing variations on local scour at pile groups," *Marine Georesources & Geotechnology*, vol. 36, no. 7, pp. 861-866, 2018. https://doi.org/10.1080/1064119X.2017.1392658

[2] B. W. Melville, *Bridge Scour*, vol. 112. Water Resources Publications, 2000.

[3] M. Fernàndez Nualart, "Estudio de la evolución temporal de la erosión local en pilas de puente a largo plazo," 2004.

[4] N. Safaripour, M. Vaghefi and A. Mahmoudi, "An experimental comparison of 3D velocity components around single and twin piers installed in a sharp bend under the influence of upstream implemented vanes," *Appl Water Sci*, vol. 14, no. 5, May 2024. https://doi.org/10.1007/s13201-024-02177-4

[5] U. P. Gupta, C. S. P. Ojha and N. Sharma, "Enhancing utility of submerged vanes with collar," *Journal of Hydraulic Engineering*, vol. 136, no. 9, pp. 651-655, 2010. https://doi.org/10.1061/(ASCE)HY.1943-7900.0000212

[6] B. Ghorbani and J. A. Kells, "Effect of submerged vanes on the scour occurring at a cylindrical pier," *Journal of Hydraulic Research*, vol. 46, no. 5, pp. 610-619, 2008. https://doi.org/10.3826/jhr.2008.3003

[7] A. J. Odgaard and Y. Wang, "Sediment management with submerged vanes. I: Theory," *Journal of Hydraulic Engineering*, vol. 117, no. 3, p. 267, 1991.

[8] M. Hamidi, M. Sadeqlu and A. Mahdian Khalili, "Investigating the design and arrangement of dual submerged vanes as mitigation countermeasure of bridge pier scour depth using a numerical approach," *Ocean Engineering*, vol. 299, p. 117270, May 2024. https://doi.org/10.1016/j.oceaneng.2024.117270

[9] M. Shafai Bejestan and R. Azizi, "Experimental investigation of scour depth at the edge of different submerged vanes shapes," 2012.

[10] N. Safaripour, M. Vaghefi and A. Mahmoudi, "Experimental study of the effect of submergence ratio of double submerged vanes on topography alterations and temporal evaluation of the maximum scour in a 180-degree bend with a bridge pier group," *International Journal of River Basin Management*, vol. 20, no. 4, pp. 427-441, 2022. https://doi.org/10.1080/15715124.2020.1837144

[11] R. Azizi and S. Bajestan, "Iranian Hydraulic Association Journal of Hydraulics Performance Evaluation of Submerged Vanes by Flow-3D Numerical Model," *Journal of Hydraulics*, vol. 15, no. 1, p. 2020, 2020. https://doi.org/10.30482/JHYD.2020.105497

[12] T. S. Behbahan, "Laboratory investigation of submerged vane shapes effect on river banks protection.," *Aust J Basic Appl Sci*, vol. 5, no. 12, pp. 1402-1407, 2011. https://doi.org/10.22059/ijswr.2021.316458.668858

[13] H. N. C. Breusers and A. J. Raudkivi, *Scouring: Hydraulic Structures Design Manual Series*, vol. 2. CRC Press, 1991. https://doi.org/10.1201/9781003079477

[14] A. M. Aly and E. Dougherty, "Bridge pier geometry effects on local scour potential: A comparative study," *Ocean Engineering*, vol. 234, Aug. 2021. https://doi.org/10.1016/j.oceaneng.2021.109326

[15] M. Vaghefi, E. Zarei, G. Ahmadi and A. M. Behroozi, "Experimental analysis of submerged vanes' configuration for mitigating local scour at piers in a sharp bend: Influence of quantity, length, and orientation," *Ocean Engineering*, vol. 289, p. 116267, Dec. 2023. https://doi.org/10.1016/j.oceaneng.2023.116267

[16] A. Mandal, H. Gautam and Z. Ahmad, "Sediment control and flow redistribution with submerged vanes: a review," *Water Pract Technol*, vol. 19, no. 5, pp. 2197-2212, May 2024. https://doi.org/10.2166/wpt.2024.131

[17] B. D. Brian Barkdoll, R. Ettema and A. Jacob Odgaard, "Sediment control at lateral diversions: limits and enhancements to vane use," *Journal of Hydraulic Engineering,* vol. 125, Issue 8, August 1999. https://doi.org/10.1061/(ASCE)0733-9429(1999)125:8(862)

[18] R. Ettema, B. W. Melville and B. Barkdoll, "Scale effect in pier-scour experiments," *Journal of Hydraulic Engineering*, vol. 124, no. 6, pp. 639-642, 1998. https://doi.org/10.1061/(ASCE)0733-9429(1998)124:6(639)

[19] E. V Richardson and S. R. Davis, "Evaluating scour at bridges," United States. Federal Highway Administration. Office of Bridge Technology, 2001.

[20] P. Espa and R. Magini, "Erosione localizzata al piede di ostacoli in alveo: studio sperimentale su un dispositivo di controllo," in *XXVII Convegno di Idraulica e Costruzioni Idrauliche*, vol. 3, 2000, pp. 355-362.

Bioremediation of water contaminated with motor oil by biological surfactants produced by Streptococcus thermophilus, using cheese whey as a carbon source

Ariana Chumi-Pasato[1], *Mary Rueda-Vinces*[2], Giovanni Larriva[3], and Verónica Pinos-Vélez[4]

***Abstract* — The hydrocarbons that contaminate water are difficult to remove, among other things, due to their hydrophobic nature. A surfactant is one way to facilitate contact between the treatment agents. This research prepared a biological surfactant from whey fermentation through Streptococcus thermophilus bacteria. To optimize its production, a complete factorial design was carried out, varying the factors temperature (38, 40, and 42 °C) and time (24, 48, and 72 hours), and the response variable is the amount of surfactant produced. It was found that the highest performance was obtained at 40ºC and 48 hours. The biosurfactant was characterized to determine hemolytic activity, Parafilm, oil dispersion, emulsification index (63.64%), and surface tension (52.7 mN/m). The ecotoxicity test with Daphnia magna confirmed that the biosurfactant is environmentally friendly. Finally, a bioremediation process was applied during the 45 days when more than 50% engine oil removal was achieved.**

***Keywords:* biosurfactants; Streptococcus thermophilus; bioremediation; cheese way valorization.**

***Resumen* — Los hidrocarburos que contaminan el agua son difíciles de remover entre otras cosas por su naturaleza hidrofóbica. Una forma de facilitar el contacto entre el agente del tratamiento es usando un surfactante. En esta investigación se preparó un surfactante biológico a partir de la fermentación de lactosuero a través de las bacterias Streptococcus thermophilus. Para optimizar su producción se realizó un diseño factorial completo variando los factores la temperatura (38, 40 y 42 °C) y el tiempo (24, 48 y 72 horas) y siendo la variable respuesta la cantidad de surfactante producido. Se encontró que el mayor rendimiento se obtuvo a 40 ºC y 48 horas. Se caracterizó el biosurfactante para determinar actividad hemolítica, Parafilm, dispersión del aceite, índice de emulsificación (63.64%) y tensión superficial (52.7 mN/m). La prueba de ecotoxicidad con Daphnia magna corroboró que el biosurfactantes es amigable con el ambiente. Finalmente, aplicando un proceso de biorremediación durante los 45 días donde se alcanzó más del 50% de remoción de aceite de motor.**

***Palabras Clave:* biosurfactante; Streptococcus thermophilus; biorremediación; valorización del suero de queso.**

I. INTRODUCTION

HYDROCARBONS are a severe pollution problem because they are poorly degradable and contain toxic components. Within the hydrocarbons derived from petroleum are motor oils, whose global production uses approximately 2% of the total refined crude oil, corresponding to a consumption of nearly 38 million tons per year. In other words, 0.42 gallons of engine lubricants are produced [1] for every barrel of crude oil. Used massively, once discarded, they are a potential water contamination source [2], [3].

Used engine lubricating oil contains several chemical compounds such as heavy metals, as well as polynuclear aromatic hydrocarbons, benzene, and sometimes there may be the presence of chlorinated solvents, PCBs, etc., producing a direct effect on human health since they can become carcinogenic [4]. As a result of car washing in washing machines and lubricators, up to one million gallons of fresh water are polluted with oils, which has important effects on the exposed ecosystems [5].

In Ecuador, around 54 million liters of used oil are discarded annually, of which only 70% are for domestic use. The rest, equivalent to approximately 4 million gallons, correspond to the automotive and industrial sectors. Currently, in Cuenca, around 34 thousand gallons of used oils are collected per month from washing machines, mechanics, vulcanizers, and industries, representing 55% [6].

Due to the potential contaminants of motorcycle oil, several legislations have regulated the discharge of oils into the water since poor management of these wastes generates considerable environmental problems [7]. For example, in its official standard NOM-001-SEMARNAT-2021, Mexico established maxi-

1. Adriana Chumi-Pasato is with the Universidad de Cuenca, Departamento de Biociencias, Grupo IRCMA, Ecocampus Balzay, C. Victor Manuel Albornoz, Cuenca, Ecuador (e-mail: ariana.chumi@ucuenca.edu.ec). ORCID: https://orcid.org/0009-0009-3330-8005.

2. Mary Rueda-Vinces is with the Universidad de Cuenca, Departamento de Biociencias, Grupo IRCMA, Ecocampus Balzay, C. Victor Manuel Albornoz, Cuenca, Ecuador (e-mail: mary.ruedav@ucuenca.edu.ec). ORCID: https://orcid.org/0009-0004-3234-231X.

3. Giovanni Larriva is with the Universidad de Cuenca, Departamento de Biociencias, Grupo IRCMA, Ecocampus Balzay, C. Victor Manuel Albornoz, Cuenca, Ecuador (e-mail: giovanni.larriva@ucuenca.edu.ec). ORCID: https://orcid.org/0009-0002-8088-9366.

4. Verónica Pinos-Vélez is with the Universidad de Cuenca, Departamento de Biociencias, Grupo IRCMA, Departamento de Recursos Hídricos y Ciencias Ambientales, Grupo Sanitaria, Ecocampus Balzay, C. Victor Manuel Albornoz, Cuenca, Ecuador (e-mail: veronica.pinos@ucuenca.edu.ec, ORCID: https://orcid.org/0000-0001-8278-5873.

Manuscript Received: 05/09/2024
Revised: 30/11/2024
Accepted: 09/12/2024
DOI: https://doi.org/10.29019/enfoqueute.1094
Section Editor: Miriam Recalde

mum permissible limit values for fats and oils of 18 mg/l as a daily average and 15 mg/l as a monthly average [8], [9]. In Directive 75/440/EEC, Spain limits the content of these compounds in the water used for purification, where quality limit values are between 0.05 to 1 mg/l for dissolved or emulsified hydrocarbons and from 0.0002 to 0.001 mg/l. l for polycyclic aromatic hydrocarbons [10]. Within Ecuadorian legislation, Book VI of the TULSMA establishes that the maximum permissible limit for the discharge of compounds such as total petroleum hydrocarbons, oils, and greases are 20 mg/l and 70 mg/l, respectively [11].

Spill treatment methods or discharge to water or soil sources are expensive and/or generate other waste due to the chemicals used, including biological, chemical, physicochemical, thermal, electrical electromagnetic, acoustic, and ultrasonic treatment methods [12]. One of the treatments that turns out to be economical and widely used because it is friendly to the environment is bioremediation, which allows the restoration of contaminated soils or waters, a very interesting biotechnological alternative [13].

Bioremediation is a process that consists of using plants, microorganisms, and enzymes that can be naturally or genetically modified to neutralize chemical and biological contaminants, reducing or eliminating their toxicity for living beings [14]. In addition to being economical, it is environmentally friendly and less invasive than other techniques [15]. For example, effective results have been seen when treating organic and inorganic contaminants with microalgae and plants in wetlands and mangroves that are solubilized in water [16], [17], [18], [19], [20]. However, in the case of hydrophobic contaminants, the efficiency of the treatments is limited by the difficulty involved in contact between the agent that performs the bioremediation and the contaminant [21], [22], [23]. For this reason, in addition to microorganisms, compounds that help increase the efficiency of contaminant removal can be implemented during the bioremediation process, such as biosurfactants, to reduce surface tension, thus allowing the mobilization and reduction of contaminants [24]. Indeed, most of the compounds in hydrocarbons are hydrophobic, making them difficult to degrade by microorganisms; therefore, when using biosurfactants, they allow these compounds to solubilize and increase biodegradation by having greater contact with the contaminant [22], [25], [26].

Some studies demonstrate the effectiveness of using biosurfactants in the bioremediation process. For example, biological surfactants produced by bacterial strains were used together with a consortium of bacteria in water samples contaminated with light crude oil, which was carried out for 90 days and increased the efficiency of the bioremediation process, obtaining 81% remediation [27]. In another study, rhamnolipid and surfactin-type biosurfactants were used together with microorganisms in water contaminated with diesel for 90 days, where the bioremediation efficiency of water and soil contaminated with diesel was improved and had a 94% remediation [28]. Hence, a duo between a biosurfactant and a bioremediation organism is interesting for treating hydrophobic contaminants such as hydrocarbons [21], [26], [28]. An interesting organism for bioremediation is Fungi because they efficiently remove contaminants. The removal mechanism with which they act by adsorption of the contaminant in their biomass or by its use in their metabolism [29], [30].

This research aims to obtain a biosurfactant through the action of *Streptococcus thermophilus* using cheese whey as a carbon source to treat water contaminated with motor oil.

II. METHODOLOGY

2.1 biosurfactant

Activation of microbial strains: The *Streptococcus thermophilus* strain of the CHR HANSEN brand, variety STl–12, was used. The activation temperature was between 37 °C to 45 °C. The strain was activated with a water-serum solution in an 8:2 ratio at an incubation temperature of 37 ºC for 24 hours.

A dilution of up to 10-5 was made for the CFU count, according to the INEN 1529-7:2013 standard. Briefly, culture media were prepared with agar in Petri dishes. Then 0.1 ml of the dilutions of the activated inoculum were placed in each dish, subsequently spreading the inoculum throughout the culture medium. The boxes were sealed with Parafilm and incubated in the oven at 37ºC for 48 h. The number of colonies was counted, then multiplied by the dilution factor and divided by the volume used using the following formula (Eq. 1):

$$\text{UFC/ml} = \frac{\text{colony count} * \text{inverse of dilution}}{\text{Volumen}} \quad (1)$$

- Additionally, the Turbidimeter equipment was used with each dilution to corroborate the results. The higher the dilution factor, the lower the turbidity value. Density, protein, lactose, and fat were determined. The Milkotester equipment (Master Pro model) and a potentiometer were used to measure the pH.
- Cheese Whey: The liquid was sterilized at 121 °C for 45 minutes. After the time was up, a filtering process separated the proteins and fats. A 100 ml aliquot of whey was taken, and the pH was adjusted to 6.8 with 1N NaOH.

Biosurfactant production: A 10% aliquot of activated inoculum was added to the sterilized whey. The fermentation process was carried out for 72 hours at 37 °C. After fermentation, the culture broth was centrifuged at 4000 rpm for 30 minutes. The precipitate was removed. The biosurfactant extraction was done using the acid precipitation method with 96% ethanol. 100 ml culture was taken as a sample; it was acidified with 5 N H_2SO_4 to obtain a pH of 2. An equal volume of ethanol was added to the sample and shaken vigorously until the components were completely mixed. This procedure was modified based on the methodology described in Santos (2017) [31]. After 8 h of rest, the appearance of a white precipitate indicated the presence of the biosurfactant. After that, the sample was separated by centrifugation at 4000 rpm for 10 minutes, leaving the white precipitate, which was washed twice with distilled water and then evaporated for 12 hours in the oven at 45 °C.

Optimization: To optimize production conditions, a complete factorial design with three levels and two factors was carried out, with the response variable being the amount of surfactant obtained. Three replicas of each experiment were carried out. The main effects of the factor's temperature (38, 40, 42 ºC) and

time (24, 48, and 72 h) and their combination were evaluated by ANOVA statistical analysis using the R software version 4.4.0 with the R Studio interface.

2.2 Biosurfactant characterization

Hemolytic Activity was determined to check the presence of the biosurfactant through the breakdown of red blood cells. A colony of Streptococcus thermophilus strains inoculated on Blood Agar plates and incubated at 37 °C for 48-72 hours was obtained [31]. Those strains that presented a clear area around the colonies were considered positive. The presence of a diffuse green area represents a behavior α- hemolytic; if it is a clear area, it is considered β- hemolytic, and finally, if it does not present a change around the colony, it is a behavior γ- hemolytic.

After the fermentation period, the resulting liquid was subjected to a double centrifugation process for 30 minutes to detect the biosurfactant. The precipitate was discarded, and the supernatant was placed in the refrigerator for use in the different biosurfactant detection tests.

For the oil dispersion test (OSM), a modified method of Alkan et al. (2019) [32]. 25 ml of distilled water was placed in a 9 cm diameter Petri dish, and 10 uL of used motor oil was added to the center of the plate; subsequently, 20 uL of the product obtained after fermentation was added to half of the oil. The diameter of the transparent area was measured in centimeters. A theoretical comparison was performed with the diameters of the Tween 80 zone as a positive control sample. The diameter of the transparent zone (cm) was evaluated as "+" for 0.5–0.9 cm, "++" for 1–1.5 cm, "+++" for 1.5–2.1 cm and "++++" for 2.1 cm [31].

For the Parafilm test, 2 ml of the supernatant was taken, and a drop of methylene blue was added. Then, 10 µl of the mixture was taken and placed on a piece of Parafilm, making sure to leave a drop without stirring it. The appearance of the drop was examined 1 minute after being placed on the Parafilm. If the drop maintained its shape, it was estimated as negative, while if it took a flat or "collapsed" shape, it was valued as positive [31].

The emulsifying activity was measured by adding 5 ml of hexane to 5 ml of the aqueous sample and stirring at high speed in a vortex for 2 minutes. Measurements were carried out 24 hours later. The emulsion index (E24) was determined with the Eq. 2 [33].

$$\%E = \frac{\text{Aemulsion layer height}}{\text{Total height}} * 100 \quad (2)$$

A sample of the fermented liquid containing the biosurfactant was used to determine the surface tension. The test was carried out using the ring method following the NTE INEN 834 standard. The maximum thrust exerted by the fluid on the platinum-iridium ring was measured with a dynamometer. The surface tension was calculated from the diameter of the ring and the measured force [34].

An acute test was applied with Daphnia magna (a cladoceran crustacean) to determine ecotoxicity. The average effective concentration (EC50) against the biosurfactant was calculated to evaluate the strains' sensitivity. Twenty neonates under 24 hours old were exposed to different amounts of biosurfactant: 30, 25, twenty, fifteen, 10, 5, and 0 mg/L. The immobilized neonates were counted at 24 and 48 hours. The EC50 value or concentration was calculated, where 50% of the crustaceans were immobilized [35], [36].

2.3 Bioremediation of water contaminated with motor oil

The analyzed samples were prepared from distilled water and used motor oil. Each treatment was prepared by adding the biosurfactant obtained from the strains (10% v/v), the inoculum (10% v/v), and the water contaminated with motor oil for a total volume of 100 ml [27], See table I. The treatments were incubated for 15, 30, and 45 days at 40 °C, with gentle shaking at 40 rpm. In addition, total hydrocarbon analyzes were performed before and after treatment. The results were compared with a standard sample consisting of a mixture of water and motor oil.

TABLE I
DIFFERENT TREATMENTS USED FOR BIOREMEDIATION

Treatment	Water (ml)	Oils (ml)	Biosurfactant (ml)	Inoculum (mil)
Water + Oil (AA)	99	1	-	-
Water + Oil + Inoculum (AAI)	89	1	10	-
Water + Oil + biosurfactant + inoculum (AAIB)	79	1	10	10

Two methods were used to determine the percentage of motor oil removed from water: the gravimetric method based on standard 5520 of the Standard Methods for the Examination of Water and Wastewater and the UV-visible spectroscopy method.

The procedure followed for the gravimetric method consisted of evaporating the water sample with oil from the different proposed treatments in a rotary evaporator and then extracting the oil that remains as a residue with an amount of 10 ml of n-hexane (EMSURE brand), subsequently dry the solvent and weigh. The HTS is calculated with Eq. 3. P1 corresponds to the weight of the empty container in grams, P2 to the weight of the container with the sample residue in grams and V to the sample volume initially measured in ml.

$$\text{HTP(mg/L)} = \frac{(P2-P1) * 1000000}{V} \quad (3)$$

The concentration of hydrocarbons was carried out by UV-visible spectrophotometer (THERMO SCIENTIFIC model GENESYS 180). First, a calibration curve was obtained by measuring the absorbance of a series of solutions of known concentrations, with n-hexane as a standard substance, and worked in a wavelength range between 200 to 400 nm in the case of hydrocarbons [37]. Subsequently, the samples were evaporated in the rotary evaporator and extracted with n-hexane to obtain the concentration of the used motor oil sample.

III. RESULTS AND DISCUSSION

3.1 Obtaining the biosurfactant

After cultivation, ovoid-shaped *Streptococcus thermophilus* bacteria were obtained, and the majority were grouped, forming elongated chains, which developed into pairs known as diplococci [38]; these can be seen in Figure 1a. In the colony count with the dilution of 10^{-4} after 48 hours, $UFC/ml = 1.34\ x\ 10^{7}$

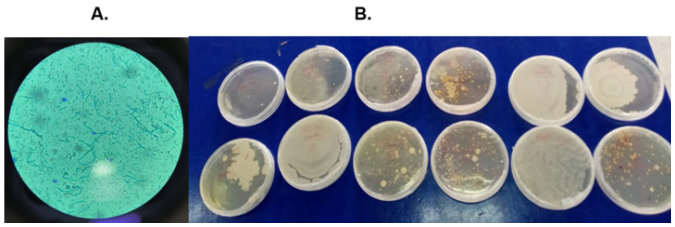

Fig. 1. a. Structure of the studied strain observed under a microscope at 100x. b. Colony count of Streptococcus thermophilus in Petri dish.

Figure 1b shows the growth of Streptococcus thermophilus colonies in the Petri dishes, in which whitish circles of different sizes correspond to the colonies of the bacteria studied. The culture medium used was enriched Agar, so the count values are lower compared to other studies in which M-17 Agar or MRS medium were used [38], [39]. Its characteristic white color was visualized with diameters less than 3 mm.

From measuring the parameters of the fresh cheese whey with the Milkotester equipment, values of 0% fat, 3% protein, 4.5% lactose, and a 1.019 g/cm3 density were obtained. The serum, before being sterilized, presented microorganisms such as Bacillus. Most of the values obtained are close to those reported for other serums, which are between 0.85-1.25% for proteins, 0.94-5.2% for lactose, 0.25-0.7% for fat, 6.45-6.66 for pH, 1.025-1.027 g/cm^3 for density, 3.71% lactose content and 6-7.3% for total solids of sweet whey obtained from homemade cheese production [40]. Only the percentages of proteins and fats differ considerably, presumably due to a poor process in obtaining the cheese.

According to the Ecuadorian standard INEN 2594, which corresponds to the requirements of liquid whey, values of the physicochemical parameters for sweet whey are established of 5% lactose content, 0.8% milk protein, 0.3% milk fat, 6.4-6.8 pH [41]. The measured pH of the serum studied was 6.4, classifying the serum as sweet and being within the established ranges. The fat percentage of the studied whey reflects a lower value than that referred to in national regulations (0.3%), which can be explained by the long resting time of the whey, where the fats form a cream on the surface that is then removed, causing that whey contains little fat. The amount of milk protein is above the norm value (0.8%); this phenomenon is due to the early cutting of the curd, which, being soft, causes premature clot breaks, causing the release of protein and other components in the whey. The amount of lactose present in the study whey was 4.5%, a value close to other studies that reached around 5%, which turned out to be an excellent culture medium for the growth of *Streptococcus thermophilus*, the main source of energy for the bacteria.

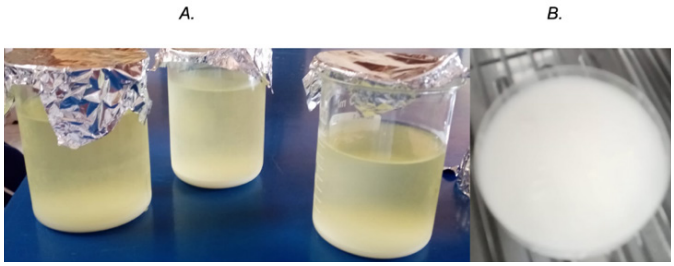

Fig. 2. a. Drying of the biosurfactant. b. Biosurfactant observed under a microscope.

The presence of biosurfactants was verified with quantitative tests such as surface tension and emulsification index. The biosurfactant concentration was 1 g/L, a value similar to that obtained in other studies, where values were between 0.8 and 1.2 g/L [42]. The resulting white powder was observed under a microscope, giving crystalline structures, as shown in Figure 2B.

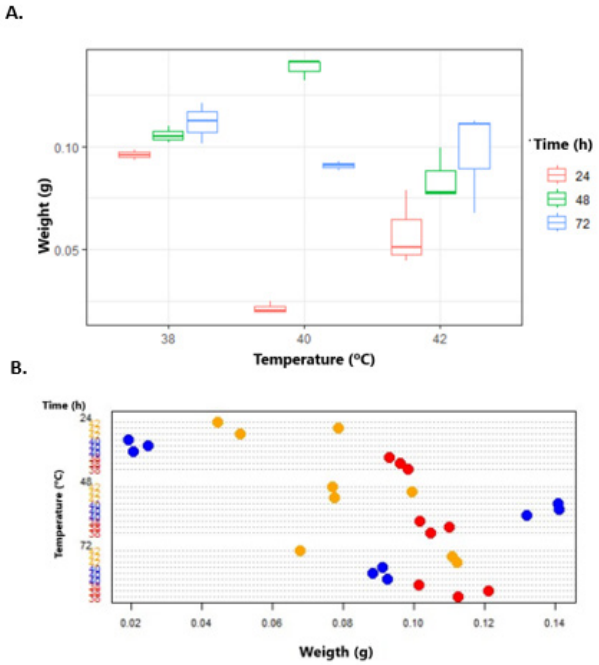

Fig. 3. a. Box plot of the interaction temperature: time vs. Weight. b. Time/temperature plot concerning weight.

For optimization, tests were carried out at different temperatures and times. The weights obtained are shown in Fig. 3, which correspond to the dry whitish residue of surfactant. In Figure 4, you can see the dot scatter plot of the interaction of temperature and time concerning weight. Each color represents a temperature tested (red for 38 °C, blue for 40 °C, and yellow for 42 °C) and the weights obtained. It is observed that the best surfactant production was found at a longer time and temperature. Studies indicate that the influence of time is fundamental for production because bacteria sometimes require more time to process the nutrients present in the carbon source to produce the desired metabolite [31]. It also depends on the microorganisms since each type has its metabolism.

It is important to determine the production time and temperature since it was shown that they influence the concentration of the biosurfactant; during the treatment, the bacteria can run out of the substrate and begin to feed on what they produce, affecting the final amount obtained from the biological surfactant [43], [44]. The optimal time and temperature choice was also based on reducing costs and production times and obtaining a high biosurfactant concentration. Furthermore, the growth temperature range of the chosen bacteria is between 37 °C and 45 °C. The highest yield was a weight of 0.14 g for the conditions of 40 °C for 48 h.

Once homoscedasticity and normality were confirmed through two-way ANOVA statistical analysis, it was confirmed that the factors time p($8.41e^{-08}$) and temperature p(0.00076) and their interaction p($4.63e^{-06}$) were statistically significant. As shown in Figure 3, the temperature and time in which a greater average weight (0.14 g) was obtained were 40 °C and 48 hours, respectively. Therefore, these values have been chosen as the optimal ones, which give better performance in producing biological surfactants. This is also evident when comparing the means of the different combinations of the factors. The total amount obtained from the optimized biosurfactant was 5.6 g/L, which, when compared with the value of the unoptimized biosurfactant (1 g/L), can be said to have increased the amount produced.

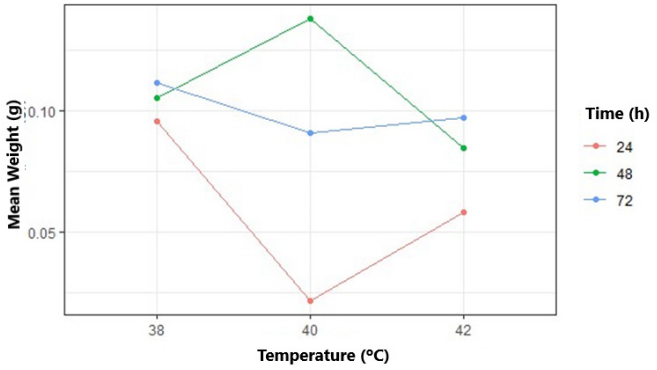

Fig. 4. Factor interaction graph.

The interaction graph shows that the highest surfactant production was obtained at 40 ºC, at 48 h. Also, it can see the interactions between time and temperature.

3.2 Biosurfactant characterization

After 48 hours of incubation at 37 °C, whitish growth areas corresponding to Streptococcus thermophilus were observed. The test was considered positive due to a transparent halo around the colonies generated by the lysis of red blood cells, indicating a decrease in surface tension caused by the secretion of biosurfactants. The light area represents that the bacteria strains studied have a high potential for biosurfactant production [31], and the larger the halo diameter, the greater the concentration of the biosurfactant that is produced [45]. In the case of the strains studied, the observed halo was considered to have β hemolytic behavior since the hemolysis was total or complete due to the presence of a transparent halo.

The hemolytic activity test is performed to verify the absence of production of hemolysins without surfactant properties [46]. It is important to perform these tests to identify false positives, as in one study, the strains showed hemolytic activity, had negative results in the other tests performed (droplet collapse and oil dispersion), and a low reduction in surface tension (greater than 60 mN/m), due to the presence of compounds other than biosurfactants that caused the lysis of red blood cells.

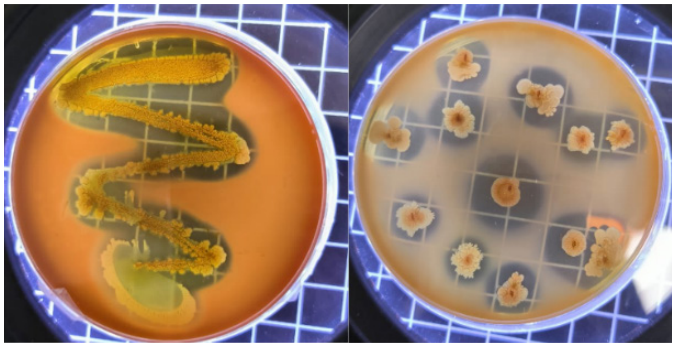

Fig. 5. Hemolytic activity test.

Figure 5 shows the results of the hemolysis test, where the transparent halos formed due to the red blood cell membrane rupture caused by the biosurfactants are observed. The seeding was done by puncture and streaking; the halo was formed similarly in both cases.

The oil dispersion test resulted in a halo diameter of 6.5 cm (++++), confirming the presence of biosurfactant in the sample. The results were compared with those obtained in another study where crude oil was used for the test with a diameter of 5.9 cm for the biosurfactant obtained from lactic acid bacteria [32]. It can be estimated that neither value differed much. In addition, Tween 80 was taken as a positive control sample, this being a chemical surfactant. This test, in addition to helping confirm the presence of the biosurfactant, also demonstrated its ability to break surface tension. There is a linear relationship between the concentration of the biosurfactant and the diameter obtained in the oil dispersion, where the larger the diameter, the higher the concentration, and in turn, it is inversely proportional concerning the surface tension, where the larger the diameter, the lower the surface tension [47].

The Parafilm test studies change in surface tension through the behavior of a drop on a hydrophobic surface [31]. After the estimated time of 1 minute, the shape of the drop placed on the Parafilm was verified. The test was considered positive when a collapse of the placed drop was observed. Additionally, a drop of distilled water was placed on the Parafilm as a blank and was observed to maintain its round shape.

As in the oil dispersion test, there is also a relationship with the concentration of the biosurfactant, where a total and immediate drop collapse will result in a higher product concentration. It may also be due to the carbon source used for production. If fats or oils are used, due to their hydrophobic nature, it is more difficult for bacteria to obtain their nutrients than when sugars are used as a carbon source. Therefore, the concentration of the biological surfactant will vary [31]. After

24 hours, the height of the emulsion was measured, obtaining a value of 2.8 cm out of a total height of 4.4 cm. The emulsification index at 24 h was 63.64%, and it was observed that after a while, the emulsions remained stable since their height did not vary significantly. These results are similar to those of another study where a%E was obtained. 50% at 24 hours and remained stable a week later [32]. A positive test is the presence of emulsion and an emulsification index greater than 40% that remains stable over time. In addition, it was reported that the emulsion is formed depending on the carbon source, as is the case with glucose and acetate of sodium as carbon sources in the production of the biosurfactant, which generated a high positive response when carrying out this test, contrary to what happens with other sources such as diesel where the emulsion was not formed [31].

Research with different microorganisms in different carbon sources found that both variables are relevant when performing the test since it is easier for one strain to adapt to a specific medium than another. Regarding the emulsification index, an investigation reported a higher value for glucose and oil for the *Ralstonia taiwanensis* strain. In contrast, the Pseudomonas veronii strain had a low index in the same substrates. Another investigation that used a synthetic substrate for the strain of Streptococcus thermophilus obtained a lower%E than when using lactic whey, repeating the same with other strains of lactic acid bacteria where the index increased when using whey as a carbon source [32].

The surface tension test result showed a surface tension value of 52.7 mN/m, compared with other studies, which obtained a similar result of 48.85 mN/m [32], using cheese whey as a carbon source and *Streptococcus thermophilus* as a biosurfactant-producing bacteria. Taking pure water as a reference as a control value of 72 mN/m, there is a considerable reduction in surface tension, thus confirming the presence of biosurfactants.

Other studies that used different types of bacteria, obtained surface tension values of between 42 to 71 mN/m, using oil and glucose as culture medium. Likewise, in another study, bacteria and yeast were used to produce a biological surfactant, which managed to reduce the surface tension from 72 to 36 mN/m for the bacteria and 42 mN/m for the yeast [46], [48].

A selection criterion for biosurfactant-producing strains is surface tension values less than 40 mN/m; likewise, higher values are considered emulsifiers [31], [49]. Strains that show values greater than 60 mN/m of surface tension are not considered producers of biological surfactants since there is an inversely proportional relationship between the concentration of the biosurfactant and the surface tension; as long as there is a high reduction in surface tension, the greater will be your concentration [47]. It should be considered that there is an important relationship between the reduction of surface tension with the carbon source, having significant variances between one medium and another, regardless of the strains used, and different carbon sources exert different effects on the production of the biosurfactant [31].

In the different treatments in water for the removal of the oil with the biosurfactant, a concentration of 30 mg/L was used, which is equivalent to 10% of the solution; at the beginning of the study, the test was carried out at that concentration, resulting in the death of 7 neonates of the 20 placed, at 48 hours. But then, by continuing with the standard for the test, they were carried out at different concentrations of the biosurfactant to find out EC50 value. When carrying out the test, it was observed that after 24 hours of having placed the *Daphnia magna* in the solutions with the biosurfactant at a lower concentration, there is low mortality. From 10 mg/L, the mortality increases until all of them die at 48 hours. The EC50 value (mean effective concentration) can be seen in Figure 6, which shows that at a concentration of 14.366 mg/L, p($8.653e^{-10}$), 50% of the neonates die, obtained from the statistical analysis where the value is significant, having a reliability of 97%, and it can be said that the biosurfactant has a low toxicity. Other studies obtained an EC50 of between 3 and 120 mg/l in the evaluation of the toxicity of anionic chemical surfactants, which are generally used in detergents, tested after 24 hours with *Daphnia magna*, demonstrating a low to intermediate toxicity[50]. Although these values do not represent the toxicity of a biological surfactant, they can be used as a reference and allow comparison of both types since they are marketed and widely used.

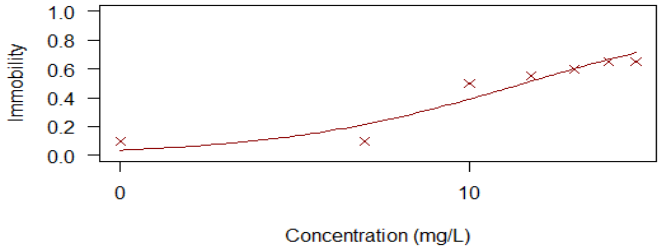

Fig. 6. Biosurfactant concentration concerning immobility rate.

3.3 Application in water bioremediation

The treatments were exposed to different conditions, such as placing them in an incubator with constant shaking at 40 °C and using a bacteria-fungus consortium, in which it was proposed to use the fungus Aspergillus niger. Bioremediation with fungus relies on improved detoxification and degradation of toxic pollutants through intracellular accumulation or enzymatic transformation to less toxic or nontoxic compounds [21], [23].

The different treatments showed a considerable reduction of oil in the water during the incubation time, except the treatment that contained only water with used motor oil, which had a 5% reduction due to losses in the container when performing other tests. Other studies reported a 7% reduction in the standard sample because the water they used was not sterile [27].

The different treatments had an initial concentration of total petroleum hydrocarbons of 8780 mg/L. After the 45 days proposed in the study, final concentrations were between 5348 and 3012 mg/L. The treatment with a higher percentage of removal was that of water, oil, consortium of microorganisms, and biosurfactant (AAIB), achieving 57.68% oil removal. In comparison, the treatment with a lower percentage of bioremediation was the control sample of water and oil, having a 5% reduction. These results were compared with studies that reported removal of 50% in the first 30 days and 81% at 90 days; the treatment with biosurfactant and mixed culture had the highest removal [27]. These results are also compared with

another study, where a high percentage of hydrocarbon removal was obtained (92%) in the third week of experimentation, considering the hydrocarbon concentrations were lower (38.30 mg/l). Likewise, in another investigation, a 39.4% removal of heavy crude oil was obtained for 100 days, where natural mineral nutrients were combined with rhamnolipid biosurfactants. With these values, it is possible to analyze what influences the removal percentage, such as the type of contaminant, the concentration, and the days the treatment lasts [51].

The better removal obtained with the combination of biosurfactant with bioremediation with fungi is because the biosurfactant makes the contaminant available for use by the fungus. This is demonstrated when comparing treatments with (AAIB) or without (AAI) biosurfactants. In all cases, the use of biosurfactants favors bioremediation.

Table 2 shows the results of the weights of the different treatments from day 0 to 45 days.

TABLE II
RESULTS OF THE DIFFERENT TREATMENTS USED FOR BIOREMEDIATION

Days	Micro-organisms	AAI(g)	HTP (mg/L)	% Removal	AAIB (g)	HTP (mg/L	% Removal
0	Bacteria	0.878	8780	0	0.878	8780	0
15		0.6265	6265	25.15	0.6453	6453	23.27
30		0.6009	6009	27.71	0.524	5240	35.4
45		0.5348	5348	34.32	0.4182	4182	45.98
0	Consortium: Bacteria-Fungus	0.878	8780	0	0.878	8780	0
15		0.6107	6107	26.73	0.5202	5502	32.78
30		0.583	5830	29.5	0.4251	4251	45.29
0		0.5075	5075	37.5	0.3012	3012	57.68

Note. AAI: Water, oil and inoculum. AAIB: Water, oil, inoculum, and biosurfactant

The results open the way for this treatment to be used on an industrial scale. Cheese whey is a frequent waste in the local industry. This would justify implementing a system to obtain biosurfactants, which can be used in biological systems such as water treatment plants. Additionally, it can be used in combination with bioremediation to eliminate hydrophobic contaminants such as car wash water or other aqueous waste contaminated with hydrocarbons.

Lubricating oils, in addition to containing hydrocarbons in their composition, also contain other contaminants such as heavy metals, chlorinated solvents, and residual engine dirt, making them difficult to degrade. That said, with the results obtained in this research, it can be concluded that using the biosurfactant and the bacterial consortium removes the hydrocarbon and other types of contaminants in the sample [52]. For example, there is a study where biosurfactants produced by P. aeruginosa were used to remove lead and mercury in marine intertidal sediments, resulting in 62% and 50% of Pb and Hg, respectively. The ionic character of surfactants provides for their use in removing heavy metals due to the affinity of the cations for negatively charged surfactants [53].

CONCLUSIONS

Whey is the main byproduct of the dairy industry and due to its high level of nutrients, it has a high contaminant load and, far from being used, is disposed of in water sources or sewage systems without prior treatment. That said, using whey as a carbon source made it possible to obtain a biological surfactant through whey fermentation by the action of *Streptococcus thermophilus* bacteria. Its extraction was obtained using the acid precipitation method, which was modified since, from the beginning, the solvents used were methanol and chloroform; their risk and cost are known; it was decided to replace them with 96% ethanol, obtaining similar results.

It was demonstrated that time, temperature, and their interaction play a fundamental role in the production of the biosurfactant, where it was evident that at a temperature of 40 ºC and 48 hours of fermentation, the ideal conditions are achieved where *Streptococcus thermophilus* produces a greater amount of biological surfactant improving process performance.

The biosurfactant could be identified thanks to the different qualitative and quantitative tests, thus confirming the product's presence. Furthermore, the ecotoxicity tests and results concluded that the biological surfactant is not dangerous to aquatic fauna if used in water bodies.

The efficiency of the biosurfactants was evaluated in the different treatments carried out for the bioremediation process. The product obtained and the microorganisms that degraded the oil in the contaminated water had a favorable result. Given that the oil is a complex sample, it is recommended that the bioremediation time be increased to improve the biodegradation of contaminating compounds.

REFERENCES

[1] S. Moore, "Lubricantes. ¿Cuánto lubricante hay en un barril de petróleo crudo?," Lubes'N'Greases. Accessed: Apr. 16, 2024. [Online]. Available: https://www.lubesngreases.com/factbook/fbweb/

[2] A. Jurado, "Contaminación y manejo de aceites lubricantes usados," Hoy en La Salle. Accessed: Apr. 17, 2024. [Online]. Available: https://hoy.lasalle.mx/contaminacion-y-manejo-de-aceites-lubricantes-usados/

[3] S. S. Mosquera Romero and J. D. Serrano Mena, "Biorremediación de lodos de una planta regeneradora de Aceites Lubricantes Usados, recuperando el suelo para uso industrial.," Tesis de grado, Escuela Superior Politécnica del Litoral, Guayaquil, 2014. [Online]. Available: https://www.dspace.espol.edu.ec/bitstream/123456789/54972/1/D-99352.pdf

[4] W. Fong Silva, E. Quiñonez Bolaños, and C. Tejeda Tovar, "Caracterización físico-química de aceites usados de motores para su reciclaje," *Prospectiva*, vol. 15, no. 2, pp. 135-144, 2017.

[5] L. F. Barrios-Ziolo, J. Robayo-Gómez, S. Prieto-Cadavid, and S. A. Cardona-Gallo, "Biorremediación de Suelos Contaminados con Aceites Usados de Motor," *Revista CINTEX*, vol. 20, no. 1, Art. no. 1, Aug. 2015.

[6] L. Vásconez, "Convenios en cinco ciudades del Ecuador para reciclar aceites usados," *El Comercio*, Ecuador, 2018. Accessed: Jul. 06, 2023. [Online]. Available: https://www.elcomercio.com/actualidad/ecuador/convenios-ciudades-ecuador-reciclar-aceites.html

[7] D. I. Osman, S. K. Attia and A. R. Taman, "Recycling of used engine oil by different solvent," *Egyptian Journal of Petroleum*, vol. 27, no. 2, pp. 221–225, Jun. 2018. https://doi.org/10.1016/j.ejpe.2017.05.010.

[8] Secretaría de Medio Ambiente y Recursos Naturales, "Norma Oficial Mexicana NOM-001-SEMARNAT-2021. Que establece los límites

permisibles de contaminantes en las descargas de aguas residuales en cuerpos receptores propiedad de la nación.," Diario Oficial de la Federación. Accessed: May 07, 2024. [Online]. Available: https://www.dof.gob.mx/nota_detalle.php?codigo=5645374&fecha=11/03/2022#gsc.tab=0

[9] A. Vidales Olivo, M. Y. Leos Magallanes, and M. G. Campos Sandoval, "Extracción de Grasas y Aceites en los Efluentes de una Industria Automotriz," *Conciencia Tecnológica*, vol. 40, pp. 29-34, 2010.

[10] Ministerio del Medio Ambiente, "Libro blanco del agua," in *Libro blanco del agua*, España, 2000, pp. 205–206. Accessed: May 07, 2024. [Online]. Available: https://www.miteco.gob.es/es/agua/temas/planificacion-hidrologica/libro-blanco-del-agua.html

[11] Ministerio del Ambiente, "Anexo 1 del Libro VI del Texto Unificado de Legislación Secundaria del Ministerio del Ambiente: Norma de Calidad Ambiental y de descarga de efluentes al recurso agua," 2015. [Online]. Available: https://www.ambiente.gob.ec/wp-content/uploads/downloads/2018/05/Acuerdo-097.pdf

[12] I. C. Ossai, A. Ahmed, A. Hassan and F. S. Hamid, "Remediation of soil and water contaminated with petroleum hydrocarbon: A review," *Environmental Technology & Innovation*, vol. 17, p. 100526, Feb. 2020 https://doi.org/10.1016/j.eti.2019.100526.

[13] A. Rodríguez-Gonzales, S. G. Zárate-Villarroe, and A. Bastida-Codina, "Biodiversidad bacteriana presente en suelos contaminados con hidrocarburos para realizar biorremediación," *Revista de Ciencias Ambientales*, vol. 56, no. 1, pp. 178-208, Jun. 2022. https://doi.org/10.15359/rca.56/1.9

[14] H. Contreras and C. Carreño, "Eficiencia de la biodegradación de hidrocarburos de petróleo por hongos filamentosos aislados de suelo contaminado," *Revista Científica UNTRM: Ciencias Naturales e Ingeniería*, vol. 1, no. 1, pp. 27-33, 2018.

[15] V. C. Jiménez Vélez, "Evaluación de bacterias y hongos potencialemente utilizables para la biorremediación de suelos contaminados con hidrocarburos," Tesis de grado, Universidad Agraria del Ecuador, Guayaquil, 2020. [Online]. Available: https://cia.uagraria.edu.ec/Archivos/JIMENEZ%20VELEZ%20VILMA%20CECIBEL.pdf

[16] H. Y. El-Kassas and L. A. Mohamed, "Bioremediation of the textile waste effluent by Chlorella vulgaris," *The Egyptian Journal of Aquatic Research*, vol. 40, no. 3, pp. 301-308, Jan. 2014, https://doi.org/10.1016/j.ejar.2014.08.003

[17] I. Rawat, R. Ranjith Kumar, T. Mutanda, and F. Bux, "Dual role of microalgae: Phycoremediation of domestic wastewater and biomass production for sustainable biofuels production," *Applied Energy*, vol. 88, no. 10, pp. 3411-3424, Oct. 2011. https://doi.org/ 10.1016/j.apenergy.2010.11.025.

[18] K. Larsdotter, "Wastewater treatment with microalgae-a literature review," *Vatten*, vol. 62, no. 1, p. 31, 2006.

[19] V. Matamoros, L. X. Nguyen, C. A. Arias, V. Salvadó, and H. Brix, "Evaluation of aquatic plants for removing polar microcontaminants: A microcosm experiment," *Chemosphere*, vol. 88, no. 10, pp. 1257–1264, Aug. 2012, https://doi.org/10.1016/j.chemosphere.2012.04.004

[20] D. Theuerkauff *et al.*, "Wastewater bioremediation by mangrove ecosystems impacts crab ecophysiology: In-situ caging experiment," *Aquatic Toxicology*, vol. 218, p. 105358, Jan. 2020. https://doi.org/10.1016/j.aquatox.2019.105358

[21] S. S. Cameotra and R. S. Makkar, "Biosurfactant-enhanced bioremediation of hydrophobic pollutants," *Pure and Applied Chemistry*, vol. 82, no. 1, pp. 97-116, Jan. 2010. https://doi.org/10.1351/PAC-CON-09-02-10

[22] E. Z. Ron and E. Rosenberg, "Biosurfactants and oil bioremediation," *Current Opinion in Biotechnology*, vol. 13, no. 3, pp. 249-252, Jun. 2002. https://doi.org/10.1016/S0958-1669(02)00316-6

[23] M. Pacwa-Płociniczak, G. A. Płaza, Z. Piotrowska-Seget and S. S. Cameotra, "Environmental Applications of Biosurfactants: Recent Advances," *Int J Mol Sci*, vol. 12, no. 1, pp. 633-654, Jan. 2011. https://doi.org/10.3390/ijms12010633

[24] V. Frolich, "Evaluación del potencial uso de biosurfactantes producidos por la Pseudomona aeruginosa en la biorremediación de suelos destinados a la agricultura," Trabajo de grado, Universidad de los Andes, 2021.

[25] C. N. Mulligan, "Environmental applications for biosurfactants," *Environmental Pollution*, vol. 133, no. 2, pp. 183-198, Jan. 2005. https://doi.org/10.1016/j.envpol.2004.06.009

[26] E. Eras-Muñoz, A. Farré, A. Sánchez, X. Font, and T. Gea, "Microbial biosurfactants: a review of recent environmental applications," *Bioengineered*, vol. 13, no. 5, pp. 12365-12391, May 2022, doi: https://doi.org/10.1080/21655979.2022.2074621

[27] I. Araujo *et al.*, "Surfactantes biológicos en la biorremediación de aguas contaminadas con crudo liviano," *Interciencia*, vol. 33, no. 4, pp. 245-250, Apr. 2008.

[28] L.-M. Whang, P.-W. G. Liu, C.-C. Ma, and S.-S. Cheng, "Application of biosurfactants, rhamnolipid, and surfactin, for enhanced biodegradation of diesel-contaminated water and soil," *Journal of Hazardous Materials*, vol. 151, no. 1, pp. 155-163, Feb. 2008. https://doi.org/10.1016/j.jhazmat.2007.05.063

[29] S. Skanda, P. S. J. Bharadwaj, S. Kar, V. Sai Muthukumar, and B. S. Vijayakumar, "Bioremoval capacity of recalcitrant azo dye Congo red by soil fungus Aspergillus arcoverdensis SSSIHL-01," *Bioremediation Journal*, vol. 27, no. 1, pp. 32-43, Jan. 2023. https://doi.org/10.1080/10889868.2021.1984198

[30] C. Menacho *et al.*, "Evaluation of some selected antibiotics and dyes removal by fungi isolated from wastewater sludge," *Bioremediation Journal*, vol. 0, no. 0, pp. 1-17, 2024. https://doi.org/10.1080/10889868.2024.2335909

[31] O. Santos, "Detección e Identificación de Biosurfactantes y/o Bioemulsificantes producidos por Aislados Bacterianos asociados a una Fosa Petrolera de la Faja Petrolífera del Orinoco," Tesis de grado, Univrsidad Central de Venezuela, Caracas, 2017. [Online]. Available: http://saber.ucv.ve/bitstream/10872/16817/1/TEG%20Oriana%20Santos%20Mayo%202017.pdf

[32] Z. Alkan, Z. Ergi-Nkaya, G. Konuray, and E. Ünal Turhan, "Production of biosurfactant by lactic acid bacteria using whey as growth medium," *Turk J Vet Anim Sci*, vol. 43, no. 5, pp. 676-683, Oct. 2019. https://doi.org/10.3906/vet-1903-48.

[33] C. Di Martino, "Estudio de bacterias del género Pseudomonas en la degradación de hidrocarburos y síntesis de biosurfactantes: análisis del efecto de los polihidroxialcanoatos," Tesis doctoral, Universidad de Buenos Aires, Buenos Aires, 2015. [Online]. Available: https://bibliotecadigital.exactas.uba.ar/download/tesis/tesis_n5752_DiMartino.pdf

[34] INEN, "NTE INEN 834:2013. Agentes surfactantes. Determinación de las tensiones interfacial y superficial," 2013, *Instituto Ecuatoriano de Normalización*. [Online]. Available: https://www.normalizacion.gob.ec/buzon/normas/nte_inen_834-1.pdf

[35] V. Pinos-Velez, G. S. Araujo, P. Echeverria, M. Abril, S. Acosta, I. Cipriani, G. M. Moulatlet and M.V. Capparelli, "Acute and chronic ecotoxicity of daphnia magna exposed to ash leachate from the Cotopaxi Volcano, Ecuador | Bulletin of Environmental Contamination and Toxicology," *Bulletin of Environmental Contamination and Toxicology*, vol. 113, no. 37, pp. 1-8, 2024, https://doi.org/10.1007/s00128-024-03946-2

[36] V. Pinos-Vélez, G. Araujo, G. M. Moulatley, A. Perez, I. Cipriani, P. Tripialdi and M. Capparelli, "Acute toxicity of daphnia magna neonates exposed to single and composite mixtures of four emerging contaminants," *Bull Environ Contam Toxicol*, vol. 110, no. 1, p. 14, 2023. https://doi.org/10.1007/s00128-022-03663-8

[37] L. Mesa M, J. Falcón, Y. Ruiz, R. Arias and J. Pérez, "Monitoreo de la contaminación de agua por hidrocarburos en el espejo de la bahía de Santiago de Cuba," *Revista Boliviana de Química*, vol. 36, no. 4, pp. 157-172, Oct. 2019.

[38] J. García, "Técnicas moleculares aplicadas a la caracterización y estudio de la supervivencia de bacterias lácticas del yogurt," Doctoral, Universidad Politécnica de Valencia, Valencia, 2010. [Online]. Available: https://m.riunet.upv.es/bitstream/handle/10251/14010/tesisUPV3431.pdf?sequence=6&isAllowed=y

[39] J. M. Rodríguez, M. A. Serna, B. K. Uribe and M. X. Quintanilla, "Aplicación de la metodología de superficie de respuesta para evaluar el efecto de la concentración de azucar y de cultivos iniciadores comerciales sobre la cinética de fermentación del Yogurt.," *Revista Mexicana de Ingeniería Química*, vol. 13, no. 1, pp. 213-225, 2014.

[40] R. R. Montesdeoca and K. Piloso, "Evaluación físicoquímica del lactosuero obtenido del queso fresco pasteurizado producido en el taller de procesos lácteos en la ESPAM 'MFL,'" *Revista Científica de Ciencia y Tecnología El Higo*, vol. 10, no. 1, 2020. https://doi.org/10.5377/elhigo.v10i1.9921.

[41] INEN, "NTE INEN 2594:2011. Suero de leche líquido. Requisitos," 2011.

[42] E. Vasileva-Tonkova and V. Gesheva, "Biosurfactant Production by Antarctic Facultative Anaerobe Pantoea sp. During Growth on Hydrocarbons," *Current Microbiology*, vol. 54, pp. 136-141, 2007. https://doi.org/ 10.1007/s00284-006-0345-6.

[43] L.-M. Whang, P.-W. G. Liu, C.-C. Ma and S.-S. Cheng, "Application of biosurfactants, rhamnolipid, and surfactin, for enhanced biodegradation of diesel-contaminated water and soil," *Journal of Hazardous Materials*, vol. 151, no. 1, pp. 155-163, Feb. 2008. https://doi.org/10.1016/j.jhazmat.2007.05.063.

[44] A. L. Severo Domínguez, M. Á. Hernández Rivera, R. L. Fócil Monterrubio and M. E. Ojeda Morales, "Estudio de la producción de biosurfactantes obtenidos de bacterias fijadoras de nitrógeno y degradadoras de petróleo," *Emerging Trends in Education*, vol. 21, no. 41, p. 4, 2015.

[45] E. P. Martínez and J. A. Osorio, "Estudios preliminares para la producción de un biosurfactante bacteriano activo contra Phytophthora infestans (Mont.) De Bary," *Carpoica. Ciencia y tecnologia Agropecuaria*, vol. 8, no. 2, pp. 5-16, 2007.

[46] M. R. Barrionuevo, "Producción de biosurfactantes bacterianos para su uso en procesos de biotratamiento de efluentes industriales con contenido en metales," Tesis doctoral, Universidad de Buenos Aires, Buenos Aires, 2017.

[47] N. H. Youssef, K. E. Duncan, D. P. Nagle, K. N. Savage, R. M. Knapp and M. J. McInerney, "Comparison of methods to detect biosurfactant production by diverse microorganisms," *J Microbiol Methods*, vol. 56, no. 3, pp. 339-347, Mar. 2004. https://doi.org/10.1016/j.mimet.2003.11.001

[48] M. A. Daniel, M. R. Barrionuevo, S. R. Doyle and D. L. Vullo, "Kinetics of Pseudomonas veronii 2E biofilm development under different nutritional conditions for a proper bioreactor design," *Biochemical Engineering Journal*, no. 105, pp. 150-158, Jan. 2016. https://doi.org/10.1016/j.bej.2015.09.001

[49] M. Martínez Aguilar, "Obtención de un biosurfactante para el recobro mejorado de petróleo," Universidad Nacional de Colombia, Medellín, 2014. [Online]. Available: https://repositorio.unal.edu.co/bitstream/handle/unal/53556/1014217302.2015.pdf?sequence=1&isAllowed=y

[50] E. Jurado, M. Fernández, J. Núñez, M. Lechuga and F. Ríos, "Ecotoxicity of anionic surfactants AKYPO," *WIT Transactions on Ecology and the Environment. Ecosystems and Sustainable Development VIII*, vol. 144, pp. 497-505, 2011. https://doi.org/10.2495/ECO110431

[51] J. García, D. Peñafiel Heredia, and R. Rodríguez, "Bioremediación de hidrocarburos en aguas residuales con cultivo mixto de microorganismos: caso Lubricadora Puyango," *Enfoque UTE*, vol. 10, no. 1, pp. 185-196, Mar. 2019. https://doi.org/10.29019/enfoqueute.v10n1.312

[52] Q. Chen, Y. Li, M. Liu, B. Zhu, J. Mu and Z. Chen, "Removal of Pb and Hg from marine intertidal sediment by using rhamnolipid biosurfactant produced by a *Pseudomonas aeruginosa* strain," *Environmental Technology & Innovation*, vol. 22, p. 101456, May 2021. https://doi.org/10.1016/j.eti.2021.101456.

[53] A. Abalos, Y. Barrios, O. Rodríguez, M. I. López, H. F. Toledo, and I. A. Aguilera, "Surfactante microbiano para la biorrestauración de ecosistemas impactados con hidrocarburos y metales pesados," *Anales de la Academia de Ciencias de Cuba*, vol. 14, no. 4, Art. no. 4, Nov. 2024.

Coca Codo Sinclair Hydropower Plant: A time bomb in the energy sector for Ecuador or a successful project?

Sebastian Naranjo-Silva[1*], Juliana Romero-Bermeo[2]

***Abstract* — In Ecuador, the electricity sector has undergone significant transformation over the past 15 years, with a marked increase in renewable energy capacity, particularly hydropower, which grew from 1,707 MW in 2000 to 5,100 MW in 2022. This shift, driven by the need to diversify the energy grid and reduce fossil fuel dependence. Despite its importance, the Coca Codo Sinclair project with 1,500 MW has faced several technical, environmental, and social challenges, including erosion and structural issues, raising concerns about its long-term sustainability. This article aims to analyze these challenges, their causes, impacts, and potential solutions, providing insights for future hydropower developments in similar regions. Coca Codo Sinclair is an example of the ambition of a government that did not follow the recommendations of technical studies on the maximum capacity that could be generated by a plant that now has more problems than advantages, analyzing all the associated drawbacks that the largest hydropower plant in Ecuador, it is important to understand that technical criteria must prevail over political decisions. In order to keep the more than 3 billion dollars of investment going, urgent action is required on CCS remediation works, with a combination of investments in repairs and maintenance activities, improvements in management and governance of the project, therefore, currently the largest plant in Ecuador represents a time bomb that can collapse due to any of the various problems.**

***Keywords:* Case study, Coca, disadvantages, energy grid, hydropower, Quijos, river.**

***Resumen* — En Ecuador, el sector eléctrico ha experimentado una importante transformación en los últimos 15 años, con un marcado de la capacidad de energía renovable, en particular la hidroeléctrica, que pasó de 1.707 MW en 2000 a 5100 MW en 2022. Cambio, impulsado por diversificar la matriz energética y reducir la dependencia fósil. A pesar de su importancia, el proyecto Coca Codo Sinclair con 1500 MW ha enfrentado varios desafíos técnicos, ambientales y sociales, incluidos problemas de erosión y estructurales, lo que genera preocupaciones sobre su sostenibilidad a largo plazo. Este artículo tiene como objetivo analizar estos desafíos, causas, impactos y posibles soluciones, brindando perspectivas para futuros desarrollos hidroeléctricos en regiones similares. Coca Codo Sinclair es un ejemplo de la ambición de un gobierno que no siguió las recomendaciones de los estudios técnicos sobre la capacidad máxima que genera una planta que ahora tiene más problemas que ventajas, analizando todos los inconvenientes asociados que tiene la hidroeléctrica más grande de Ecuador, es importante entender que los criterios técnicos deben prevalecer sobre las decisiones políticas. Y, para mantener en marcha los más de 3 mil millones de dólares de inversión, se requiere actuar urgentemente en obras con una combinación de inversiones en actividades de reparación y mantenimiento, y mejoras en la gestión y gobernanza del proyecto, pues actualmente la planta más grande del Ecuador representa una bomba de tiempo que puede colapsar por cualquiera de los diversos problemas.**

***Palabras Clave*: Estudio de caso, Coca, desventajas, red energética, hidroelectricidad, Quijos, río.**

I. INTRODUCTION

In Ecuador, a South American country, its electricity sector has been changing for almost 15 years, increasing its capacity in areas of renewable generation, and thus its energy grid grew widely, specifically moving into hydropower development in the year 2000 with 1,707 MW, to 5,100 MW in 2022, means, in 22 years, Ecuador's installed hydroelectricity capacity grew by around 300 % [1], [2].

Ecuador has experienced notable growth in the renewable sector, driven by the need to diversify its energy grid, and reduce dependence on fossil fuels. This development has been an integral part of national energy policies, which seek to meet the growing demand for energy and mitigate the environmental impacts associated with traditional electricity generation [3].

Hydropower has been the keystone of the growth of renewable energy in Ecuador. Emblematic projects such as Coca Codo Sinclair, with a capacity of 1,500 megawatts, have been fundamental to increasing the country's installed capacity [4]. Other important hydroelectric projects include the start-up of: Sopladora, Minas San Francisco and Toachi Pilaton, which have contributed significantly to the generation capacity and the stability of the electricity supply with 487 MW, 270 MW, and 254 MW respectively [5], [6].

The Coca Codo Sinclair hydropower plant (CCSHP), located in the Amazon region of Ecuador (Fig. 1), is one of the largest and most ambitious infrastructure projects in the country. Inaugurated in 2016, this hydroelectric central is the largest in

1. Sebastian Naranjo-Silva* is in the Department of Sustainability, Polytechnic University of Catalonia, Barcelona, Spain; hector.sebastian.naranjo@upc.edu (S.N.-S.); ORCID: https://orcid.org/0000-0002-1430-8140

2. Juliana Romero – Bermeo is in the School of Engineering and Technology, International University of La Rioja, La Rioja, España; evelynromero2007@hotmail.com (E.R.-B.); ORCID: https://orcid.org/0009-0008-8213-2782

*Correspondence author: Tel.: +593-99-8-502974

Manuscript Received: 26/08/2024
Revised: 30/11/2024
Accepted: 06/12/2024
DOI: https://doi.org/10.29019/enfoqueute.1087
Section Editor: Marcelo Mosquera

installed capacity in the country, which makes it a key piece for Ecuador's energy supply [7]. However, since its conception, the project has faced multiple technical, environmental and social challenges that spark widespread debate and concern both nationally and internationally [8], [9].

Fig. 1. Coca Codo Sinclair in Ecuador. Source: [10].

The planning and construction of Coca Codo Sinclair began with the objective of harnessing the hydroelectric potential of the Coca and Quijos rivers to meet the country's growing energy demand and reduce dependence on fossil fuels [11]. Mainly financed by mostly Chinese international loans, and built by the Chinese company Sinohydro, the project promised not only a stable energy supply, but also economic and development benefits for the Amazon region [12], [13].

Despite these promises, the central construction was marked by delays, cost overruns and controversies related to the quality of the materials used and poor project management practices [14]. The need to meet deadlines led to hurried decisions that subsequently resulted in significant structural problems, including cracks in critical infrastructure components [15].

One of the most critical issues facing Coca Codo Sinclair is erosion on the Coca and Quijos rivers, exacerbated by the construction of two dams and natural events such as the San Rafael waterfall slide in 2020 [16]. The alteration of the river channel and the modification of sediment flows have intensified erosive processes, putting both the plant's infrastructure and local communities and ecosystems at risk [17].

Erosion has caused the loss of agricultural land, affected biodiversity and forced the relocation of several communities. Additionally, it has generated significant additional costs for the repair and maintenance of the plant facilities, calling into question the long-term economic and environmental sustainability of the project [18]. The Coca Codo Sinclair hydropower plant has the capacity to supply approximately 30% of the electrical energy consumed in Ecuador, however, since its inauguration, it has faced operational and technical challenges, but remains a crucial component in the country's energy grid [19].

With this background, it observed that there is a technical gap that society is unaware of between the investment made in the Coca Codo Sinclair hydropower plant, and the current problems that must be discussed to generate sustainability for the project, which cost approximately 3.2 billion of american dollars to Ecuador, a figure that includes the cost of construction, equipment, inspection, administration and other aspects until the largest hydropower plant in the country is launched [20].

Thus, this article aims to analyze the problems associated with the Coca Codo Sinclair hydropower plant, exploring the causes, impacts and possible solutions. Through a comprehensive review of literature, and technical data to provide an inclusive understanding of the challenges faced by this project and lessons learned that can be applied to future hydropower developments in similar regions.

II. METHODOLOGY

This study employs a technical-scientific analysis to evaluate the Coca Codo Sinclair Hydropower Plant, focusing on its operational, environmental, and economic implications. Information for this analysis was sourced from official project documentation, including feasibility studies, technical designs, and performance reports published by government agencies, project contractors, and independent auditors. Additionally, data from scientific publications and engineering journals provided a foundation for cross-referencing project outcomes [21], [22].

Key regulations and standards relevant to hydropower and energy infrastructure were reviewed, including Ecuador's legal framework for energy generation, environmental impact assessments, and international hydropower guidelines from organizations such as the International Hydropower Association. These were compared with Coca Codo Sinclair's adherence to ensure compliance and evaluate sustainability.

Technical documents analyzed include structural integrity reports, turbine performance evaluations, and reservoir management strategies. Particular attention was given to assessing compliance with seismic safety codes, given the region's geologic instability. This involved a comparative analysis of global engineering practices in similar projects to identify any deficiencies [23].

Economic data, including construction costs, maintenance expenses, and revenue projections, were analyzed to assess the project's financial viability. Secondary data from government audits and independent financial assessments were incorporated to identify deviations from initial projections and their implications for national energy policy.

Lastly, public records were used to contextualize socio-environmental impacts, focusing on displacement, biodiversity, and downstream water use. This holistic approach ensured a robust understanding of the project's technical, economic, and social dimensions.

III. RESULTS

Through the development of a mega structure like Coca Codo Sinclair, several geomorphological faults, environmental problems, migration of communities, and energy stoppages to Ecuador have been triggered. First there was a 144 meters wa-

terfall called San Rafael, which, due to the manipulation of the direction of the Coca River, now presents pronounced regressive erosion [24].

In Ecuador, in February 2020, a catastrophic reestablishment of the basin upstream and downstream of the hydropower plant began. This sudden failure in river control and regressive erosion continued with processes familiar to geomorphologists that are not previously observed at this scale during the historical era [25].

However, this event is just one more of the problems since 2016 after starting up the plant, problems that have been getting worse, the Coca Codo Sinclair central faced difficulties such as: The location of the plant in a geologically unstable area has caused a phenomenon of regressive erosion in the Coca River. Studies have found that the construction of the plant increased the erosion rate in the area by 42 %, increasing sediments [26], [27].

On the other hand, failures and microcracks have been detected in the plant's infrastructure, which has generated uncertainty about its safety and long-term stability and highlights the importance of a rigorous evaluation of this project. Therefore, the Coca Codo Sinclair hydropower plant has faced several problems since its construction and start-up, following the main problems detected:

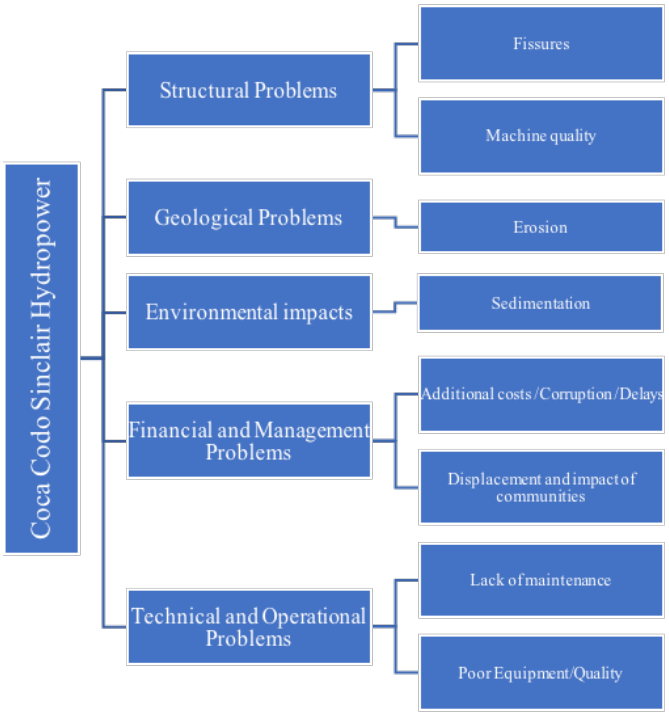

Fig. 2. Problems identified at the Coca Codo Sinclair hydropower plant in Ecuador.

With the references in Fig. 2, the development of each drawback was followed for a better understanding and future discussion in a technical manner:

A. Structural Problems

There are fissures and cracks in the water accumulation and distribution plants, prior to the turbines, as one of the most notable problems. These cracks have raised concerns about the structural integrity and safety of the plant [28].

Likewise, the government entities of Ecuador have still decided not to formally receive the work from the Chinese company Sinohydro due to the quality of construction with criticism about the effectiveness of the materials and labor used in the construction, which contributes to structural problems [29].

These two problems are serious, major and are under discussion in an International Arbitration because these findings are inside the power house, the heart of the hydropower plant, only this part that contains the distributors, water conduits, and turbines required 1.1 billion of dollars, and is the core of the entire plant [30], [31].

In the case of the International Arbitration trial between Ecuador and Sinohydro for the Coca Codo Sinclair hydropower plant, it is carried out under the auspices of the International Chamber of Commerce (ICC). According to the Ecuadorian information, the sponsorship of the lawsuit is in charge of the Attorney General's Office of the State of Ecuador, in coordination with the Electric Corporation of Ecuador. In this specific case, the seat of the arbitration is in Paris, France, it began in 2019, and the main grounds of this arbitration include the following key points:

- Construction Defects,
- Responsibility for Repairs, and
- Additional Costs and Overruns.

B. Geological Problems

The Coca Codo Sinclair plant was built in a geologically unstable area, rather than a more stable zone as is the usual practice for this type of large-scale hydropower projects. It caused a phenomenon of regressive erosion in the Coca River, hence breaking away at the banks of the river and threatens to affect key infrastructure such as the water collection of the plant itself [32].

Additionally, the location of the dam is in an area with seismic activity of the Reventador volcano that poses additional safety challenges. According to an analysis by the United States Army Corps of Engineers from 2023, it was mentioned that pre-construction studies would have used outdated data on water flow and geological risk, without taking into account the effects of climate change, reason for which these physical problems are currently accentuated [33]. The Fig. 3 is a comparative image of the geomorphological displacements in the area.

Fig. 3. Coca River erosion (Before 2020 – Now 2024). Source:[34]

Thus, the landslide near the plant is located in a geologically active area, which resulted in earth movements that affect the infrastructure and access roads. Finally, the induced seismicity due to the construction of the reservoir raises concerns about the possibility of loss of part of the region's infrastructure [35], [36].

C. Environmental impacts

Erosion in the Coca River basin is now evident, the construction of the dam significantly altered the river dynamics, causing erosion problems downstream, which affected, among other things, the San Rafael waterfall, which collapsed in 2020, and it currently no longer exists (Figure 4). It was a 140-meter waterfall and served as a place for tourist visits due to its extensive majesty [37], [38].

Fig. 4. San Rafael Waterfall near CCS (Before 2020 – Now 2024). Source:[34].

In February 2020, the basin upstream and downstream of the hydropower plant presented a sudden failure in river control and regressive erosion that continued with accelerated processes. During the first three years after faulting and rupture (2020-2023), the erosion front migrated almost 13 km upstream, at speeds controlled by the variable resistance of the underlying substrates and the sequence of flows [39].

Erosion of the main valleys and tributaries upstream of the lava dam generated a sediment pulse estimated at 500 MT in three years (one of the largest in modern times), which deposited sediment several meters thick along dozens of kilometers downstream of the dam near the site of the San Rafael waterfall [40], [41].

In contrast, the riverbed at the upstream end of the degraded reach began to open up and form a more channelized flow path, but the Coca River will likely require a decade or more to export most of the sediment. Additional supply from erosion and the presence of sediment storage tracts in the downstream river corridor will slow recovery time [39], [41].

Likewise, another problem is sedimentation, the accumulation of material in the reservoir affects the storage capacity and efficiency of the plant, and has caused several stoppages of Coca Codo Sinclair due to removing these sediments manually in the sand traps. In 2024 there will already be 16 stoppages, as indicated below [42], [43].

TABLE I
STOPPAGES AT COCA CODO SINCLAIR
DUE TO SEDIMENT CLEANING IN THE SAND TRAP

No.	Year	Stoppages	Observation
1	2019	3	-
2	2020	3	-
3	2021	1	-
4	2022	10	-
5	2023	9	-
6	2024	16	Until May 2024*

Source: [44]

Together, these two problems of erosion and sedimentation are serious since the erosion of the surrounding areas, both upstream and downstream of the plant, generates stoppages to release the waste that prevents both the accumulation of water and its discharge.

D. Financial and Social Management Problems

Additional costs in the hydropower plant's development arise from structural and maintenance issues, leading to unforeseen expenses that increase the financial burden on Ecuador, including foreign debt to China's Exim Bank [45].

Likewise, the management of the administration is very questionable, showing variations throughout the contracts, there have been complaints and suspicions of corruption in the awarding of contracts and in the project management, which has affected the transparency and efficiency of the central denoting overprice.

Associating, the Attorney General's Office of the State of Ecuador investigates an alleged network of bribes for approximately 76 million US dollars related to the construction of Coca Codo Sinclair between 2009 and 2018, in which former ex-president of Ecuador, public officials and the company Sinohydro are involved [46].

Finally, there is displacement and impact on communities, the construction of the power plant and its reservoirs (compensation and generation) has affected local communities, both in terms of displacement and in the impact on their traditional livelihoods such as fishing, tourism, hunting and agricultural activities [47].

E. Technical and Operational Problems

One of the main difficulties is the lack of Maintenance, the need for frequent repairs due to structural problems has affected the continuous and efficient operation of the plant, but above all, since there is no structured preventive maintenance plan, it takes its toll throughout of the operation of the hydropower plant.

Likewise, the operating capacity of the plant, although has an installed capacity of 1,500 MW, technical problems have limited its ability to operate at full power, and according to historical data, it appears that it was not adequately sized in capacity, operating at 70 % average energy generation as indicated in Table 2.

F. History of Coca Codo Sinclair

On the other hand, after defining these problems in various schemes, magnitudes, and that in the end determine the efficiency of the plant, it is important to understand where these difficulties came from, wherefore pertinent to mention the history of the Coca Codo Sinclair.

The Ecuadorian Institute of Electrification (INECEL in Spanish), created in 1961, studied the Coca Codo Sinclair Project between 1970 and 1992, with the support of international consulting companies, such as: Hidro Service from Brazil (1976-1980) and Electroconsult from Italy (1986 - 1992), of which concluded that the work would depend on an underground powerhouse built in two phases, 432 MW and 427 MW, totaling 859 MW, with flows of 63.5 m^3/s to generate 6,000 gigawatts/hour each year (GWh/year), with a plant factor of 0.8, in which the total cost of the project was 915 million dollars [48].

After 15 years of Italian, Brazilian and Ecuadorian studies, in 2007 there was talk again of the construction of the Coca Codo Sinclair Project, and in 2008, the company Coca Codo Sinclair EP was created. Where new design parameters were defined for the hydroelectric project, and the power was changed from 859 to 1,500 MW, with a design flow of 222 m^3/s and a plant factor of 0.65 to generate 8,800 GWh/year, with a project cost of 1.6 billion dollars [43].

In general figures from Table 3, it changes and decisions represent a 43 % increase in energy generation compared to the original project, and also an additional 75% investment, without considering all the complementary works, defining this increase as a political proposal, and unrealistic to the current generation data of Coca Codo Sinclair that are later observed with historical generation information [48].

Subsequently, on October 5, 2009, when there was still no firm financing, the Coca Codo Sinclair company and the Chinese company Sinohydro Corporation signed the contract for the construction of the 1,500 MW project, for a value of 1,979,700,000 USD; value that consists of two parts: 85 % Chinese financing, through debt, and 15 % contribution from the Ecuadorian government, that is, 1,682,745,000 USD and 296,955,000 USD, respectively [48].

Next, on May 31, 2011, a Coca Codo Sinclair Management and Supervision contract was signed between Coca Codo Sinclair EP and the company CFE – PYPSA, for a final value of 140,667,692 USD, due to complementary contracts, made for first year of activities, the details of which are not known in detail so far [49].

Also, to transfer the energy from Coca Codo, power lines were needed, for which high voltage transmission lines were installed to carry the electricity generated from the plant to the consumption centers, this included the construction of substations and towers. of transmission. Access Roads and Bridges were also developed to allow access to the construction site and to facilitate the transportation of materials and equipment. And finally, it was spent on Environmental Control measures which included the construction of wastewater management systems, reforestation programs and other actions to mitigate the environmental impact of the project.

Finally, in April 2016 the first four turbines were provisionally received and in November the other four. The new project entered into commercial operation on November 16,2016 and during the last 8 years, it has generated, on average, about 6,551 GWh/year, which means that the hydropower plant provides a value in energy similar to that predicted by INECEL in 1992, but with a smaller plant and cost as indicated in Table 2 in the energy delivered since 2016.

TABLE II
ENERGY DELIVERED FROM
THE COCA CODO SINCLAIR PLANT IN GWH

Years	2016	2017	2018	2019	2020	2021	2022	2023	Average
Energy produced GWh	3,264	6,242	6,488	6,730	7,140	6,969	7,202	8,376	**6,551**
Percentage change %	-	91%	4%	4%	6%	-2%	3%	16%	-

Source: [50]

IV. DISCUSSION

Starting from the fact that to finance Coca Codo Sinclair as the largest work carried out in Ecuador, external credits were required, this project was carried out with Chinese loans and oil agreements were generated that allowed Ecuador to access a large part of the necessary external credit, which became the main source of income to change the electricity sector [45]. However, at the same time it is particular that after generating the credits, the project was built by China.

After understanding that by generating debt, a large-scale work was built, the negotiations became political, and with that, it is assumed that the pressures decided for the construction of China, however, the first finding that since studies, from investigators of China in others cases of energy constructions reveals that quality failures are caused by defaults by workers, inadequate checking procedures, incomplete construction site surveys, wrong design work, and fraud of construction companies that conclude in quality failures [51].

Relating, although rework is a common phenomenon in the Chinese construction industry and significantly affects projects success, an interview with 13 experienced construction professionals in China to prioritize these causes determines that the unclear project process management, poor quality of construction technology, and the poor construction materials are the principal causes [52].

From the compiled history, after generating new calculations from the engineering studies, increasing the capacity of the hydropower plant, the geomorphic adjustment of the Coca & Quijos rivers was not predicted, which now represents an

unusual natural disaster that threatens life, property, important infrastructure and energy security, since it compromises nearby oil pipelines and the largest hydroelectric installation in Ecuador. However, this rare event creates valuable opportunities to learn how a major disturbance and recovery of an autogenous basin evolves, with important lessons for understanding the geomorphic transience and sedimentary record of volcanic landscapes [53], [54].

Nevertheless, after verifying the current problems of the hydropower plant, it is important to discuss how to prevent imminent damage to the works to seek to maintain it, which has a high cost and can establish a risk of paralysis at any time. Thus, based on the 2021-2022 analysis of the United States Army Corps of Engineers in coordination with the Corps of Civil Engineers of Ecuador, options have been generated, especially in nearby works to avoid erosion as the biggest problem that generates stoppages at the moment.

In July 2021, the United States Army Corps of Engineers visited the Coca Codo Sinclair area to inspect the progress of regressive erosion of the Coca River that, since February 2020, has threatened the hydroelectric plant. Among the improvement options there are several discussions, however, the three viable alternatives to mitigate the impacts related to the problems identified so far are considered and updated with investigative criteria:

1. Dredge the river upstream and downstream;
2. Develop sediment retention structures in mountains
3. (foundation walls);
4. Automate sediment tramps (sand filters).

Regarding these three options proposed and discussed, it is considered that they are valid for the current situation of the plant, in which the operational development management could be largely improved for proper operation. Additional to the design of the United States Army Corps of Engineers at the request of the Ecuadorian government, these improvements are the minimum necessary to guarantee the safety and efficiency of the plant, as well as to identify and mitigate any potential problems that could affect its operation, and the safety of nearby communities.

However, again the United States Army Corps of Engineers, during a visit in 2023, generated more recommendations, and as options for aggressive and major changes, in the same study, it was also proposed:

1. Raise the number of machines, which would imply rebuilding this part of the plant;
2. Divert the outlet downstream through a longer tunnel;
3. Change the water reception distributors.

Nonetheless, it is important to mention that what these other three proposed options would do is eliminate the guarantee that the Chinese construction company, Sinohydro, must still cover, because the Ecuadorian State has not yet received officially the plant, and it would also require an abysmal expense, therefore, the first recommendations are the necessary ones, until in international instances, the International Arbitration is resolved, which if it is fair should give Ecuador the reason to grant equipment changes in the powerhouse due to the low quality verified [55].

Though, after discussing these improvement options, it must open the discussion, about how it was abruptly decided to change the initial configuration, in which the original proposed design flow was 63.5 m^3 /s, and when deciding to build step by step 222 m^3 /s, that is, the amount of water needed to generate hydrogeneration increased by more than 220 %, changing the power from 859 MW to 1,500 MW in a bureaucratic manner, without technical criteria or updated data on the possible effects that a work would have. in capacity increased by 75 %, an unreal value to achieve, if one considers that Ecuador has seasonal periods in which the capacity drops even more than the effective designed one. Followed by a comparative table of the dimensioned values before and after construction with the comparison of percentage variation.

TABLE III
COCA CODO SINCLAIR COMPARISONS
(INITIAL AND FINAL PROJECTION)

No.	Parameter	Unit	Initial	Final	Percentage change
1	Design flow	m^3/s	63.5	222	**+250%**
2	Power	MW	859	1,500	**+75%**
3	Investment	Millions -USD	915	1,600	**+75%**
4	Energy	GWh/year	6,000	8,800	**+43%**
5	Plant factor	-	0.8	0.65	**-19%**

Source:[30], [43], [56].

Table 3 discusses the initial and final design criteria and parameters, but the plant factor shows a reduction as a negative percentage variation. However, it is important to understand that the plant factor means that the operating efficiency of the central, and when projecting an increase in power, flow, and investment, it is important to note that the teams were not analytical with the power factor that is ultimately related to the real approved energy that will enter the system [26].

With this background, this research serves as a case study that should be raised to energy policy decision makers, as well as those responsible for the construction of hydropower systems who must act in a committed manner because it is demonstrated that with a good idea that was irresponsibly modified, more problems were generated than solutions, and this shows that the research gap with energy simulations of real efficiency could avoid these current disadvantages, understanding that Coca Codo Sinclair is a plant with a considerable number of failures for a project of only 8 years of operation.

A. Improved Solution Evaluation for Coca Codo Sinclair Hydropower Plant

1. Economic Feasibility: To determine the economic viability of the three proposed solutions—dredging the river, developing sediment retention structures, and automating sediment traps—it's essential to conduct a cost-benefit analysis that assesses funding sources, expected return on investment, and long-term maintenance costs. This analysis should take into account both direct funding opportunities, such as government and international grants, and possible indirect financial im-

pacts, like the protection of surrounding agricultural land and infrastructure from erosion. Given Ecuador's limited budget, prioritizing cost-effective measures that promise a sustainable return of inversion will be crucial to ensure the plant's continued operation without excessive financial burden. However, having already executed the most expensive work in the history of the country, the expenses to maintain its operation are strictly necessary, and indispensable, like this proposal.

2. Technical Feasibility: Evaluating Ecuador's current technical capacity to implement and maintain these solutions is vital. This feasibility check should consider whether local industries and personnel can support complex operations such as automated sediment filtration and construction of large sediment retention walls, or if it will be necessary to introduce external technologies and specialized training programs. Collaborations with international engineering firms, like the U.S. Army Corps of Engineers, may provide insights into necessary adjustments for these solutions to be successful within Ecuador's technological landscape. However, it is believed that for this proposal, there is technical feasibility in Ecuador, therefore, as a recommendation, it could be linked to the academy to form an interdisciplinary group, teachers who know about hydrology, civil engineering, structures, etc. [57].

3. Social Feasibility: Each proposed solution has potential social implications, particularly for communities near Coca Codo Sinclair. Assessing social feasibility means analyzing how these solutions could affect local employment, economic opportunities, and quality of life, as well as identifying any possible social resistance. Local job creation, especially in construction and maintenance, could foster community support; however, it is worth mentioning that most of the impacts have already been deployed, because the work of developing hydropower has already been developed, and what is now proposed are supplementary works.

4. Environmental Feasibility: Long-term environmental impact is a critical factor in the feasibility assessment of the proposed interventions. Dredging, constructing sediment barriers, and adding automated sediment traps all impact the river ecosystem, potentially affecting local flora, fauna, and water quality. A thorough environmental impact assessment would be necessary to predict and mitigate any adverse effects on biodiversity and to ensure that solutions do not unintentionally create new environmental challenges. This evaluation would help Ecuador prevent further degradation of natural habitats while stabilizing the operational environment of the Coca Codo Sinclair plant [58].

5. Community Engagement: Building trust and gaining support from nearby communities are crucial steps in project success. Engaging local stakeholders in the planning process through informational meetings and discussions can help to identify community concerns early on. This engagement would support transparency and ensure that the needs and voices of the local population are integrated into the project's design and implementation, fostering a sense of shared purpose and reducing the likelihood of opposition [59].

6. Monitoring and Evaluation Mechanisms: Once the selected solutions are implemented, establishing a continuous monitoring and evaluation system is essential to assess their effectiveness over time. This system should include performance metrics, regular environmental impact assessments, and a feedback loop to allow for adjustments as needed. The development of a robust monitoring plan would ensure that Coca Codo Sinclair remains a viable and safe power source while protecting the surrounding environment and communities. This proactive approach could serve as a model for future hydropower projects in similar regions [60].

Summarizing, analyzing the long-term impact of the proposed solutions for the Coca Codo Sinclair Hydropower Plant (dredging, constructing sediment retention structures, and automating sediment traps) requires careful consideration of environmental, operational, and community implications. Dredging could reduce sediment buildup and mitigate regressive erosion, yet, if done repeatedly, it risks disrupting aquatic ecosystems and impacting water quality downstream. Building sediment retention structures on mountainous terrain could effectively limit erosion but may alter natural water flow and potentially affect nearby habitats. Automating sediment traps would streamline sediment control with less human intervention, improving efficiency and operational stability, yet this technology requires continuous monitoring and maintenance to ensure long-term functionality [61].

Balancing these interventions with ongoing environmental monitoring would be critical to ensure that the benefits of enhanced plant stability and erosion control are not offset by unintended ecological disturbances.

B. Implementations Costs

Estimating the exact cost of implementing solutions with the nowadays data, would be:

1. Dredging: Costs for dredging depend heavily on the volume and nature of sediment to be removed. For example, dredging a port can range from $15 to $20 million for large projects removing 400,000 to 600,000 cubic meters. Per cubic meter, costs may range from $6 to $8 USD depending on the equipment used. Applying this to Coca Codo Sinclair, 252,286 m^3 of sediment must be removed. This would fill 100 Olympic swimming pools [32], [44].

The volume of sediment to be removed corresponds to an analysis by the Río Coca Executive Commission of the Ecuadorian Electric Corporation in Eq. 1, therefore:

$$\text{Dredging: } 252{,}286\ m^3 \times 8\ \text{USD}/m^3 \quad (1)$$
$$\text{Dredging: } 2{,}018{,}288\ \text{USD}$$

However, since dredging is directly related to other actions such as wall foundations and sand trap automation, an additional 20% of impact that could result from material must be proposed in Eq. 2, therefore, the final cost is considered to be:

$$\text{Total Dredging: } 2{,}018{,}288\ \text{USD} \times 1.20 \quad (2)$$
$$\text{Total Dredging: } 2{,}421{,}956\ \text{USD}$$

2. Sediment Retention Structures: Building sediment retention walls in mountainous regions is costly due to construction challenges and specialized engineering requirements. However, the construction phase involves reinforcing both sides of the

river for 15 km upstream of the intake structure and 10 km downstream after water has passed through the turbines. With an average wall height of 20 meters, the total reinforcement area is estimated at 1,000,000 m^2

The estimated cost per square meter is approximately $55 USD, given the need for specialized equipment for mountain foundation work in Eq. 3. Additionally, 15 % is added to the cost to account for extra civil works, such as soil leveling to prevent future erosion in Eq. 4. Thus, the calculation for the total cost is:

Sediment Retention = 1,000,000 m^2 x 55 USD (3)
Sediment Retention = 55,000,000 USD
Total Sediment Retention = 55,000,000 USD x 1.15 (4)
Total Sediment Retention = 63,250,000 USD

3. Automated Sediment Traps (AST): Automating sediment management requires both initial setup costs and ongoing maintenance. Automated traps are generally less labor-intensive and can reduce operational disruptions, but require technology investments, potentially including sensors and filtration systems, whose costs vary based on technical specifications, which are presented below as approximate costs:

a. Sediment Dredging System (SDS): The cost of a mini dredge for 8 gates of the desander is related to the size and capacity, this desander has 8 water discharge gates, and each part of the mini dredge per gate. Furthermore, it is important to mention that the Coca Codo Sinclair Project consists of a run-of-river development with a capture flow of 222 m^3/s [40].

The Coca Codo Sinclair sand trap is made up of eight chambers with grids to retain solid particles with a diameter greater than or equal to 0.25 millimeters which, at high speed, can cause damage to the turbines. According to inquiries, 17,000 dollars is needed for each grid in Eq. 5:

SDS = 8 gates x 17,000 USD (5)
SDS = 136,000 USD

b. Automatic Sediment Washing System (AWS): Implementing an autonomous sediment washing system requires calculating the amount of sediment removed monthly, and it is necessary to know the time it takes to remove the sediment [56]. Assuming that the removal time is a minimum of 60 minutes each day, the amount of sediment removed monthly is calculated as follows in equations 6 -7-8:

1. Removal time each day: 60 minutes.
2. Water flow: 222 m^3/s.
3. Volume of sediment removed per unit of time each day:
222 m^3/s x 60 minutes/day x 60 s/m = 799,200 m^3/day (6)
4. Amount of sediment removed daily (5%):
799,200 m^3/day x 0.05 = 39,960 m^3/day (7)
5. Amount of sediment removed monthly:
39,960 m^3/day x 30 days/month = 1,198,800 $m^3/month$ (8)

Under this average minimum automatic washing capacity, it is projected that due to the complexity of the system and the evacuation capacity, it would require

Total AWS = 1,500,000 USD

c. Monitoring and Control System, and Information and Analysis (MCS): To install monitoring systems that allow real-time supervision of the sediment level in the sand traps, sensors that detect any problem before a stoppage occurs, alarms and connection to the control system in the powerhouse. The cost of a monitoring system would reach USD 500,000 [18], [62].

In summary, the total cost of automating the Coca Codo Sinclair sediment desander would be as follows in Eq. 9:

Total AST = SDS + AWS + MCS (9)
Total AST = 136,000 + 1,500,000 + 500,000
Total AST = 2,136,000 USD

Each of these solutions would benefit from a tailored feasibility and cost analysis specific to Coca Codo Sinclair's conditions to ensure sustainable and cost-effective implementation, giving the total cost of Eq. 10:

A: Dredging = 2,421,956 USD
B: Sediment Retention Structures = 63,250,000 USD
C: Automation of sediment traps = 2,136,000 USD
Redesign Cost = A + B + C (10)
Redesign Cost = 67,807,956 USD

Finally, due to any inconvenience, such as an additional technical study, supplementary work, external structure to deposit the collected sediments, or other intervention, it is projected that 5% of the total will be projected due to any unforeseen event as show the Eq. 11.

Total Redesign Cost = 67,807,956 USD x 1.05 (11)
Total Redesign Cost = 71,198,354 USD

Once the necessary investment was defined, the estimated loss due to inactivity of the hydropower plant was projected, which contained loss of income, cleaning and maintenance costs, and administrative costs, it represents (Eq. 12):

Installed capacity Coca Codo Sinclair: 1,500 MW (12)

The average rate at the national level with the application of the Tariff Schedule approved at 2024 by the National Electricity Council Board of Directors is 9.20 cUSD/kWh, as shows the Eq. 13.

Average price of electricity: 92 USD/MWh
Maintenance duration average: 1 day (24 hours).
Loss of income = 1,500MW x 24hrs x 92 USD/MWh
Loss of income = 3,312,000 USD/day (13)

In addition, Coca Codo Sinclair sediment cleaning and maintenance costs is 70,000 USD to cover labor, materials and equipment. The administrative costs have an additional cost of 10,000 USD to cover planning, coordination and supervision (Eq. 14):

Total estimated cost = Loss of income + Cleaning and maintenance costs + Administrative costs
Total lost cost = 3,312,000 + 70,000 + 10,000
Total lost cost = 3,392,000 USD (14)

Thus, it is defined for each economic literal in recovery, for which, the following list of payments to the proposed investments of energy optimization is obtained in Eq. 15:

$$\text{Recovery time} = \frac{Total\ proposed\ project}{Total\ losses\ per\ stop} \quad (15)$$

$$\text{Recovery time} = \frac{71{,}198{,}354}{3{,}392{,}000}$$

Recovery time = 21 days

According to Electric Corporation of Ecuador data, the large volume of sediment (composed of silt - soil thicker than clay -, clay and sand) has caused the hydroelectric plant to be shut down 20 times until August 2024. In addition, on some occasions, these shutdowns have been for up to eight hours in a single day, which means that the projected recovery time of the proposal is amply justified due to the need to eliminate said shutdowns [30].

Finally, there is a hidden cost that is much more representative of the stoppages of the largest plant in Ecuador, so, as a second comparison, it has that every time there is a stoppage, Ecuador imports energy from Colombia to supply its demand, however, from journalism data, it is known that the kWh of the neighboring country is much more expensive when requiring this service as show Eq. 16:

Ecuador: Average price of electricity: 92 USD/MWh.
Colombia: Importation 21 cUSD/kWh, it represents 210 USD/MWh.
Import loss = Current average capacity CCS_{2024} x Duration x Import price MWh
Loss of income = 900 MW x 24 hours x 210 USD/MWh
Loss of income = 4,536,000 USD/day (16)

C. International Cooperation for Hydropower Projects

1. Creating an International Quality Supervision Framework: To ensure quality and accountability in large-scale hydropower projects like Coca Codo Sinclair, establishing a collaborative international supervision framework is essential. This framework would define standardized protocols and methodologies for quality checks, involve international experts in periodic project assessments, and incorporate real-time quality monitoring systems. Countries with advanced hydropower experience, such as Norway or Canada, could share best practices in quality control, thereby helping emerging economies like Ecuador implement high standards across construction phases. This cooperative framework would also facilitate timely identification and correction of quality deviations, ensuring the longevity and safety of the project [63], [64].

2. Clarifying Roles and Responsibilities for Quality Control: Effective international cooperation requires that all parties involved—local governments, foreign contractors, and international investors—have clearly defined roles in quality supervision. For Coca Codo Sinclair, this could mean that each stakeholder agrees to a transparent and shared accountability structure, where the quality obligations of engineering firms, environmental consultants, and local authorities are precisely delineated. This structure would facilitate the division of labor, streamline communication channels, and ensure consistent project standards. The experience of other international projects has shown that role clarification fosters accountability, reduces delays, and helps prevent misunderstandings that could compromise project quality and safety.

3. Developing a Sustainable Supervision and Maintenance Mechanism: Beyond construction, establishing international partnerships for the ongoing supervision and maintenance of hydropower projects can be crucial for their long-term success. This might include creating an international committee for regular inspections, utilizing advanced monitoring technology from partner countries, and sharing resources for the training of local engineers. For Coca Codo Sinclair, this ongoing international collaboration could support Ecuador in maintaining operational efficiency, managing environmental impacts, and addressing potential technical challenges proactively [65].

As a comparison, the Three Gorges Dam is a prime example of successful international cooperation in large-scale infrastructure, demonstrating effective strategies for optimizing collaboration across nations. This project benefited from partnerships with international engineering firms, financiers, and environmental experts, each bringing specific expertise to address various challenges. To ensure high construction standards, the project implemented a global supervision framework, involving frequent consultations and assessments by foreign specialists. Additionally, the participation of international environmental organizations encouraged stricter environmental standards, ensuring that project impacts on local ecosystems were minimized and that there was consistent oversight across all stages [66], [67].

The project also emphasized role clarity and transparent communication among all stakeholders, which fostered accountability and efficiency. By creating dedicated committees for quality control, environmental management, and financial supervision, each aspect of the project had specialized international support, reduced delays and increasing operational efficiency [68].

These committees, along with regular audits and transparent reporting, allowed the Three Gorges Dam project to maintain high standards of quality and environmental compliance while optimizing costs through pooled international resources. This approach illustrates the value of structured, specialized international roles and consistent oversight in achieving successful outcomes in complex hydropower projects, best practice that can implement in projects as Coca Codo Sinclair.

V. CONCLUSIONS

- Coca Codo Sinclair is an example of the ambition of a government that did not follow the recommendations of technical studies on the maximum capacity that could be generated by a plant that now has more problems than advantages, hence, when analyzing all the associated drawbacks that the hydropower plant has largest in Ecuador, it is important to understand that technical criteria must prevail over wrong political decisions.
- In order to keep the more than 3 billion dollars of investment going, urgent action is required on CCS remedia-

tion works, with a combination of investments in repairs and maintenance activities, improvements in management and governance of the project, and continued attention to environmental and social impacts.

- The problems of the Coca Codo Sinclair hydropower plant reflect challenges in large-scale infrastructure projects such as migration of populations, surrounding erosion and low quality of equipment that were notably not prevented in Ecuador, and are now risks, especially in this region with high geological activity and complex environmental conditions.
- After verifying the history of Coca Codo Sinclair, exploring the causes, impacts and possible solutions, there must be an exhaustive reflection that the technical data of capacities, infrastructure, reservoir, type of turbines, and other equipment must provide a comprehensive understanding of the challenges that each project will face in the future, therefore, currently the largest plant in Ecuador represents a time bomb that can collapse due to any of the various morphological, environmental, or operational problems.
- Future studies should consider simulation algorithms of the real efficiency of Coca Codo Sinclair, and define the generation capacity to standardize the maximum energy quantity and maintain a homogeneous power that does not require the accumulation of too much water in a place that has too many seismic and geological disadvantages.

ACKNOWLEDGMENT

We would like to express their sincere gratitude to the cited authors of the different articles, web pages, news, and data media.

REFERENCES

[1] International Hydropower Association, "2023 World Hydropower Outlook - Opportunities to advance net zero," Apr. 2024. Accessed: Apr. 10, 2024. [Online]. Available: https://indd.adobe.com/view/4201016f-a51a-4f6f-998b-ec85219d1dfd

[2] Agencia de Regulación y Control de Energía y Recursos Naturales No Renovables, "Annual Statistics for the year 2000 of the Ecuadorian Electricity Sector," Quito, 2001. Accessed: Jul. 27, 2023. [Online]. Available: http://www.controlrecursosyenergia.gob.ec/wp-content/uploads/downloads/2021/03/Estad%C3%ADstica-Sector-El%C3%A9ctrico-Ecuatoriano-2000.pdf

[3] Ministerio de Energía y Recursos No Renovables del Ecuador, "National Energy Efficiency Plan," Ministerio de Energía y Recursos No Renovables del Ecuador. [Online]. Available: https://www.celec.gob.ec/hidroagoyan/images/PLANEE_INGLES/NationalEnergyEfficiencyPlan20162035_2017-09-01_16-00-26.html

[4] S. Naranjo-Silva, L. Rivera-Gonzalez, K. Escobar-Segovia, O. Quimbita-Chiluisa and A. del C. Javier, "Analysis of Water Characteristics by the Hydropower Use (Up-Stream and Downstream): A Case of Study at Ecuador, Argentina, and Uruguay," *J Sustain Dev*, vol. 15, no. 4, p. 71, Jun. 2022. https://doi.org/10.5539/jsd.v15n4p71

[5] S. Naranjo-Silva, J. Punina and J. Álvarez Del Castillo, "Comparative cost per kilowatt of the latest hydropower projects in Ecuador," *InGenio Journal*, vol. 5, no. 1, pp. 1-14, 2022. https://doi.org/10.18779/ingenio.v5i1.473

[6] S. Vaca-Jiménez, P. W. Gerbens-Leenes and S. Nonhebel, "The monthly dynamics of blue water footprints and electricity generation of four types of hydropower plants in Ecuador," *Science of the Total Environment*, vol. 713, p. 136579, 2020. https://doi.org/10.1016/j.scitotenv.2020.136579

[7] National Secretariat of Planning and Development of Ecuador, "Plan Nacional Buen Vivir 2013-2017," 2013.

[8] CELEC, "Presidente del Ecuador inauguró Central Hidroeléctrica Coca Codo Sinclair," Quito, Nov. 2016. Accessed: Jun. 08, 2024. [Online]. Available: https://www.celec.gob.ec/cocacodo/noticias/central-cocacodo/

[9] S. Naranjo-Silva, "A hydropower development perspective in Ecuador: past, present, and future," *La Granja*, vol. 39, no. 1, pp. 63-77, Jan. 2024. https://doi.org/10.17163/lgr.n39.2024.04.

[10] Open Street Map, "Location of Ecuadorian hydroelectric plants," Location of Ecuadorian hydroelectric plants. [Online]. Available: https://www.openstreetmap.org/note/2721104#map=6/-0.754/-73.334

[11] El Comercio, "Coca Codo Sinclair ya abastece de energía a Guayaquil," *Coca Codo Sinclair ya abastece de energía a Guayaquil*, Quito, pp. 1-23, jul. 14, 2019. Accessed: May 30, 2024. [Online]. Available: https://www.elcomercio.com/actualidad/negocios/energia-guayas-santa-elena-napo.html

[12] Banco Interamericano de Desarrollo, "Hydro-BID: Un Sistema Integrado para la Simulación de Impactos del Cambio Climático sobre los Recursos Hídricos," 2019. [Online]. Available: https://publications.iadb.org/publications/spanish/document/Hydro-BID-Un-sistema-integrado-para-la-simulación-de-impactos-del-cambio-climático-sobre-los-recursos-hídricos-Parte-2.pdf

[13] A. Briones Hidrovo, J. Uche and A. Martínez-Gracia, "Estimating the hidden ecological costs of hydropower through an ecosystem services balance: A case study from Ecuador," *J Clean Prod*, vol. 233, pp. 33-42, 2019. https://doi.org/10.1016/j.jclepro.2019.06.068

[14] El Comercio, "Coca Codo-Sinclair tiene más de 40 problemas de construcción por resolver," Quito, p. 10, Sep. 24, 2021. [Online]. Available: https://www.elcomercio.com/actualidad/politica/fiscalizacion-construccion-coca-codo-sinclair.html

[15] J. Cevallos-Sierra and J. Ramos-Martin, "Spatial assessment of the potential of renewable energy: The case of Ecuador," 2018, *Elsevier Ltd*. https://doi.org/10.1016/j.rser.2017.08.015

[16] M. C. Torres, V. Fierro, and M. I. Carrera, "Results of biophysical modeling, economic valuation and policy proposal," Quito, 2018. [Online]. Available: https://www.epn.edu.ec/wp-content/uploads/2018/03/Informe-Final-TEEB-Cuenca-Rio-Coca.pdf

[17] El Comercio, "USD 8 millones de pérdidas debido a fallas del Coca Codo," Quito, p. 16, Sep. 28, 2021. [Online]. Available: https://www.elcomercio.com/actualidad/negocios/coca-codo-perdidas-millonea-rias-fallas.html

[18] A. Gallegos, "Visita técnica a Coca Codo Sinclair," Riobamba, oct. 2015. Accessed: Jun. 20, 2024. [Online]. Available: https://es.slideshare.net/slideshow/informe-centrales-coca-codo/37722313

[19] D. Villamar, R. Soria, M. Império, and P. Carvajal, "Deep Decarbonization Pathways in Latin America and the Caribbean - A case study in Ecuador," in *Conference: 7th ELAEE Buenos Aires 2019 Decarbonization, Efficiency and Affordability: New Energy Markets in Latin America at Buenos Aires, Argentina New Energy Markets in Latin America at Buenos Aires, Argentina*, Buenos Aires, 2019, pp. 1-9. [Online]. Available: https://www.researchgate.net/publication/332179641

[20] R. Rodriguez, "Ecuador as an Exporter of Electricity," *International Journal of Business, Economics & Management*, vol. 3, no. 1, pp. 61-73, 2021. https://doi.org/10.31295/ijbem.v3n1.129

[21] S. Naranjo-Silva and O. Quimbita, "Hydropower and climate change concerning to the implementation of the First National Determined Contribution in Ecuador," *Revista Iberoamericana Ambiente & Sustentabilidad*, vol. 5, no. Sustainable Management of Water Resources, pp. 1-14, Sep. 2022. https://doi.org/10.46380/rias.v5.e268

[22] M. Cárdenas, A. Filonzi and R. Delgadillo, "Finite element and experimental validation of sample size correction factors for indentation on asphalt bitumens with cylindrical geometry," *Constr Build Mater*, vol. 274, 2021. https://doi.org/10.1016/j.conbuildmat.2020.122055

[23] J. E. Sample, N. Duncan, M. Ferguson and S. Cooksley, "Scotland's hydropower: Current capacity, future potential and the possible impacts of climate change," *Renewable and Sustainable Energy Reviews*, vol. 52, no. 2015, pp. 111-122, 2015. https://doi.org/10.1016/j.rser.2015.07.071

[24] E. McDermot, D. Agdas, C. R. Rodríguez Díaz, T. Rose and E. Forcael, "Improving performance of infrastructure projects in developing countries: an Ecuadorian case study," *International Journal of Construc-*

tion Management, vol. 22, no. 13, pp. 2469-2483, Oct. 2022. https://doi.org/10.1080/15623599.2020.1797985

[25] E. Terneus, "Coca Codo Sinclair y la erosión regresiva," Quito, jun. 2020. Accessed: Jun. 08, 2024. [Online]. Available: https://www.uide.edu.ec/coca-codo-sinclair-y-la-erosion-regresiva/

[26] S. Naranjo-Silva *et al.*, "Hydropower Scenarios in the Face of Climate Change in Ecuador," *Sustainability*, vol. 15, no. 13, p. 10160, Jun. 2023. https://doi.org/10.3390/su151310160

[27] P. E. Carvajal, G. Anandarajah, Y. Mulugetta and O. Dessens, "Assessing uncertainty of climate change impacts on long-term hydropower generation using the CMIP5 ensemble—the case of Ecuador," *Clim Change*, vol. 144, no. 4, pp. 611-624, Oct. 2017. https://doi.org/10.1007/s10584-017-2055-4

[28] Primicias, "Erosión: Agencia recomienda reubicar obras de captación de Coca Codo," Erosión: Agencia recomienda reubicar obras de captación de Coca Codo. Accessed: Jun. 08, 2024. [Online]. Available: https://www.primicias.ec/noticias/economia/erosion-agencia-recomienda-reubicar-obras-captacion-coca-codo/

[29] P. E. Solis and J. P. Lozada, "Obras de protección para la Hidroeléctrica Coca Codo Sinclair frente a la erosión regresiva del río Coca," Tesis de grado, Universidad Laica Vicente Rocafuerte de Guayaquil, Guayaquil, 2023. Accessed: Jun. 08, 2024. [Online]. Available: http://repositorio.ulvr.edu.ec/handle/44000/6594

[30] El Universo, "Crisis energética: Coca Codo Sinclair, que provee 30% de la energía del país, está en peligro por la erosión del río Coca," Crisis energética: Coca Codo Sinclair, que provee 30% de la energía del país, está en peligro por la erosión del río Coca. Accessed: Jun. 08, 2024. [Online]. Available: https://www.eluniverso.com/larevista/ecologia/crisis-energetica-coca-coda-sinclair-que-provee-30-de-la-energia-del-pais-esta-en-peligro-por-la-erosion-del-rio-coca-nota/

[31] V. Graw, T. Dedring, R. Hiby, J. Jara-Alvear, P. Guzman and C. Juergens, "Regressive Erosion at River Coca in Northeast Ecuador: Landslide Monitoring with Sentinel-1 to Support Disaster Risk Management," *PFG – Journal of Photogrammetry, Remote Sensing and Geoinformation Science*, vol. 90, no. 5, pp. 457–471, Oct. 2022. https://doi.org/10.1007/s41064-022-00221-z

[32] Primicias, "Con riesgo de apagones encima, Ecuador sigue pagando el costo de las fallas en Coca Codo," Con riesgo de apagones encima, Ecuador sigue pagando el costo de las fallas en Coca Codo. Accessed: Jun. 20, 2024. [Online]. Available: https://www.primicias.ec/noticias/economia/coca-codo-sinclair-sedimentos-cortes-luz/

[33] Mongabay, "Ecuador: gobierno reconoce que la erosión de la cascada San Rafael podría afectar la hidroeléctrica Coca Codo Sinclair," Ecuador: gobierno reconoce que la erosión de la cascada San Rafael podría afectar la hidroeléctrica Coca Codo Sinclair. Accessed: Jun. 08, 2024. [Online]. Available: https://es.mongabay.com/2020/07/erosion-rio-coca-ecuador-hidroelectrica-coca-codo-sinclair/

[34] Fundación EcoCiencia and Amazon Conservation, "Impacto de la Erosión Regresiva del Río Coca (Amazonía Ecuatoriana)," Quito, 2024. Accessed: Jun. 08, 2024. [Online]. Available: https://www.maaproject.org/2024/erosion-regresiva-ecuador/

[35] S. Jimenez-Mendoza and F. Terneus-Paez, "The water-energy nexus: Analysis of the water flow of the Coca Codo Sinclair Hydroelectric Project," *Ingenius*, vol. Jiménez, S, pp. 53-62, 2019. https://doi.org/10.17163/ings.n21.2019.05.

[36] CELEC, "CELEC EP instala sistema de dragado de sedimentos en los desarenadores de la central Coca Codo Sinclair," CELEC EP instala sistema de dragado de sedimentos en los desarenadores de la central Coca Codo Sinclair. Accessed: Jun. 20, 2024. [Online]. Available: https://www.celec.gob.ec/cocacodo/noticias/celec-ep-instala-sistema-de-dragado-de-sedimentos-en-los-desarenadores-de-la-central-coca-codo-sinclair/

[37] Y. Yang, T. Sammut-Bonnici and J. McGee, "LAD Case Study of Funding Coca Codo Sinclair: Correa's Bet on Sustainable Power in Ecuador," *Wiley Encyclopedia of Management*, no. November, pp. 68–69, 2002.

[38] C. Creech, A. McConnell and S. Gibson, "Reconnaissance of the Rio Coca Regressive Erosion and Building the Partnership," in *Sedimentation and Hydrologic Modeling Conference*, Davis, 2021, pp. 29–42. Accessed: Jul. 18, 2024. [Online]. Available: https://www.sedhyd.org/2023Program/_program.html

[39] S. Araujo, O. Guzmán, A. Guamán, R. Espín, I. García and E. Chulde, "Seismic refraction tomography in San Luis, headward Coca River erosion zone," *J Appl Geophy*, vol. 212, p. 104981, May 2023. https://doi.org/10.1016/j.jappgeo.2023.104981.

[40] D. A. Alvarez-Chiriboga, "Prediction model of the energy production of the Coca Codo Sinclair Hydroelectric Plant, based on computational learning techniques," Masters thesis, Army Forces University of Ecuador, 2020. [Online]. Available: http://repositorio.espe.edu.ec/handle/21000/23038

[41] P. D. Barrera Crespo *et al.*, "Major fluvial erosion and a 500-Mt sediment pulse triggered by lava-dam failure, Río Coca, Ecuador," *Earth Surf Process Landf*, vol. 49, no. 3, pp. 1058-1080, Mar. 2024. https://doi.org/10.1002/esp.5751

[42] T. Teräväinen, "Negotiating water and technology-Competing expectations and confronting knowledges in the case of the Coca Codo Sinclair in Ecuador," *Water (Switzerland)*, vol. 11, no. 3, pp. 1-18, 2019, https://doi.org/10.3390/w11030411

[43] La Hora, "La concesión de Coca Codo Sinclair," Quito, Jan. 2023. Accessed: Jul. 16, 2024. [Online]. Available: https://www.lahora.com.ec/esmeraldas/destacado-esmeraldas/la-concesion-de-coca-codo-sinclair/

[44] Primicias, "Coca Codo Sinclair ya suma 18 paralizaciones en lo que va de 2024, ¿cuál es la causa?," Quito, pp. 1-23, Jun. 24, 2024. Accessed: Jul. 21, 2024. [Online]. Available: https://www.primicias.ec/noticias/economia/paralizaciones-coca-codo-sinclair-sedimentos/

[45] G. Escribano, "Ecuador's energy policy mix: Development versus conservation and nationalism with Chinese loans," *Energy Policy*, vol. 57, pp. 152-159, 2013. https://doi.org/10.1016/j.enpol.2013.01.022

[46] J. Oscullo Lala, H. Carvajal Mora, N. Orozco Garzón, J. Vega and T. Ohishi, "Examining the Evolution of Energy Storing in the Ecuadorian Electricity System: A Case Study (2006-2023)," *Energies (Basel)*, vol. 17, no. 14, p. 3500, Jul. 2024. https://doi.org/10.3390/en17143500

[47] E. Méndez and D. Ramírez, "Estudio para la Optimización de la Operación del Proyecto Hidroeléctrico Coca Codo Sinclair mediante el Control Individual de Inyectores de la Turbina Pelton," Tesis de Grado, Escuela Politécnica Nacional, Quito, 2014. Accessed: Jun. 20, 2024. [Online]. Available: https://bibdigital.epn.edu.ec/handle/15000/8755

[48] T. F. Purcell and E. Martinez, "Post-neoliberal energy modernity and the political economy of the landlord state in Ecuador," *Energy Res Soc Sci*, vol. 41, no. June 2017, pp. 12-21, Jul. 2018. https://doi.org/10.1016/j.erss.2018.04.003

[49] D. Icaza, D. Borge-Diez, and S. P. Galindo, "Analysis and proposal of energy planning and renewable energy plans in South America: Case study of Ecuador," *Renew Energy*, vol. 182, pp. 314-342, Jan. 2022. https://doi.org/10.1016/j.renene.2021.09.126

[50] Agencia de Regulación y Control de Energía y Recursos Naturales No Renovables, "Estadística Anual y Multianual del año 2023 del sector Eléctrico Ecuatoriano," Quito, Mar. 2023. Accessed: Apr. 10, 2024. [Online]. Available: https://www.controlrecursosyenergia.gob.ec/estadisticas-del-sector-electrico-ecuatoriano-buscar/

[51] Y. Qi, Q. K. Qian, F. M. Meijer and H. J. Visscher, "Identification of Quality Failures in Building Energy Renovation Projects in Northern China," *Sustainability*, vol. 11, no. 15, p. 4203, Aug. 2019, https://doi.org/10.3390/su11154203

[52] G. Ye, Z. Jin, B. Xia and M. Skitmore, "Analyzing Causes for Reworks in Construction Projects in China," *Journal of Management in Engineering*, vol. 31, no. 6, Nov. 2015. https://doi.org/10.1061/(ASCE)ME.1943-5479.0000347

[53] BBC News, "Coca Codo Sinclair: the problems of the multibillion dollar dam that China built in Ecuador," p. 14, Feb. 19, 2019. [Online]. Available: https://www.bbc.com/mundo/noticias-america-latina-47144338

[54] G. Poveda-Burgos, Z. N. F. Castañeda, E. Á. E. Flores, K. R. Molina and J. G. Ruiz, "Desarrollo local de la nueva matriz energética en el Ecuador desde Coca Codo Sinclair," *Oidles*, vol. 22, pp. 114-144, 2017, [Online]. Available: http://www.eumed.net/rev/oidles/22/coca-codo-sinclair.html

[55] F. D. Riascos and J. C. Cepeda, "Mathematical Modeling of Speed Control System of Generation Units from Coca Codo Sinclair Hydroelectric Power Plant," *Energia*, vol. 18, no. 1, pp. 59-71, 2021.

[56] A. Pala *et al.*, "Desarenadores de Coca Codo Sinclair," Riobamba, Aug. 2021. Accessed: Jun. 20, 2024. [Online]. Available: https://es.scribd.

com/document/502009935/Desarenador-del-Proyecto-Hidroelectrico-Coca-Codo-Sinclair

[57] M. Kattelus, M. M. Rahaman and O. Varis, "Hydropower development in Myanmar and its implications on regional energy cooperation," *Sustainable Society*, vol. 7, no. 1, pp. 42-66, 2015. https://doi.org/10.1016/j.jhydrol.2019.12392210.1504/IJSSOC.2015.068071

[58] E. R. Oviedo-Ocaña, "Hydroelectric Dams: effects on ecosystems and environmental health," *Revista de la Universidad Industrial de Santander. Salud*, vol. 50, no. 3, pp. 191-192, 2018. https://doi.org/10.1016/j.jhydrol.2019.12392210.18273/revsal.v50n3-2018003

[59] S. Pfister, L. Scherer and K. Buxmann, "Water scarcity footprint of hydropower based on a seasonal approach - Global assessment with sensitivities of model assumptions tested on specific cases," *Science of the Total Environment*, vol. 724, 2020. https://doi.org/10.1016/j.jhydrol.2019.12392210.1016/j.scitotenv.2020.138188

[60] L. Scherer and S. Pfister, "Global water footprint assessment of hydropower," *Renew Energy*, vol. 99, pp. 711–720, 2016. https://doi.org/10.1016/j.jhydrol.2019.12392210.1016/j.renene.2016.07.021

[61] S. Kelly, "Megawatts mask impacts: Small hydropower and knowledge politics in the Puelwillimapu, Southern Chile," *Energy Res Soc Sci*, vol. 54, no. April, pp. 224-235, 2019. https://doi.org/10.1016/j.jhydrol.2019.12392210.1016/j.erss.2019.04.014.

[62] M. Dorber, A. Arvesen, D. Gernaat and F. Verones, "Controlling biodiversity impacts of future global hydropower reservoirs by strategic site selection," *Sci Rep*, vol. 10, no. 1, Dec. 2020. https://doi.org/10.1016/j.jhydrol.2019.12392210.1038/s41598-020-78444-6

[63] B. K. Sovacool and G. Walter, "Internationalizing the political economy of hydroelectricity: security, development and sustainability in hydropower states," *Rev Int Polit Econ*, vol. 26, no. 1, pp. 49-79, 2019. https://doi.org/10.1016/j.jhydrol.2019.12392210.1080/09692290.2018.1511449

[64] International Hydropower Association, "Hydropower Sustainability Guidelines on Good International Industry Practice," International Hydropower Association, London, 2018. Accessed: Sep. 09, 2022. [Online]. Available: https://www.hydropower.org/publications/hydropower-sustainability-guidelines

[65] International Commission on Large Dams, "General Synthesis of World register of dams." Accessed: May 18, 2021. [Online]. Available: https://www.icold-cigb.org/article/GB/world_register/general_synthesis/general-synthesis

[66] C. E. Tupiño Salinas, V. P. Vidal de Oliveira, L. Brito, A. V. Ferreira and J. C. De Araújo, "Social impacts of a large-dam construction: the case of Castanhão, Brazil," *Water Int*, vol. 44, no. 8, pp. 871-885, 2019. https://doi.org/10.1080/02508060.2019.1677303

[67] P. Qin, H. Xu, M. Liu, L. Du, Ch. Xiao, L. Liu and B. Tarroja,"Climate change impacts on Three Gorges Reservoir impoundment and hydropower generation," *J Hydrol (Amst)*, vol. 580, no. July 2019, p. 123922, 2020. https://doi.org/10.1016/j.jhydrol.2019.123922

[68] Y. Yao, W. Qu, J. Lu, H. Cheng, Z. Pang, T. Lei and Y. Tang, "Responses of hydrological processes under different shared socioeconomic pathway scenarios in the Huaihe river basin, China," *Water (Switzerland)*, vol. 13, no. 8, Apr. 2021, c10.3390/w13081053

Greenhouse Gas Emissions in Commercial Grills in the Metropolitan Area of the City of Veracruz, Mexico

Manuel Alberto Susunaga Miranda[1], Bernardo Rodríguez Molina[2], Bertha María Estévez Garrido[3], Mario Díaz González[4], Olaya Pirene Castellanos Onorio[5], Juan Francisco Mejía Pérez [6]

***Abstract* — The present work is an effort to determine the generation of greenhouse gases, including carbon dioxide, methane and nitrous oxide, from the cooking process that is developed for chickens, meats, ribs, hamburgers and pizzas, using firewood and coal as a source of thermal energy in the commercial grills of the metropolitan area of the City of Veracruz, which is made up of the municipalities of Veracruz, Boca del Rio, Medellin de Bravo, Jamapa and Manlio Fabio Altamirano, at Veracruz State, Mexico which as a whole They have a population of 882,011 inhabitants, where they exist of 430 commercial establishments of this type exists, making 275 visits to carry out interviews and surveys, showing that 74.18 % use charcoal and 25.81 % use firewood. Using emission factors and caloric indices, it was determined that a total of 2,739.99 tons/year of carbon dioxide equivalent is generated by consumption of firewood and 8,872.66 tons/year of carbon dioxide equivalent by consumption of coal and with a total of 11,612.65 tons/year of carbon dioxide equivalent for all commercial grills facilities, which are involved in constant climate change and the effects that this causes in this metropolitan area on the central coast of the Gulf of Mexico and that must be included in both regulations municipal and in the climate change agenda.[1]**

***Keywords:* commercial grills; emissions, greenhouse gases.**

***Resumen* — El presente trabajo tiene como objetivo determinar la generación de gases de efecto invernadero, específicamente dióxido de carbono, metano y óxido nitroso, derivada del proceso de cocción empleado en asaderos comerciales de la zona metropolitana de la Ciudad de Veracruz. Este proceso incluye la preparación de alimentos como pollos, carnes, costillas, hamburguesas y pizzas, utilizando leña y carbón como fuentes de energía térmica. La zona metropolitana de la Ciudad de Veracruz está conformada por los municipios de Veracruz, Boca del Río, Medellín de Bravo, Jamapa y Manlio Fabio Altamirano, en el Estado de Veracruz, México, con una población conjunta de 882,011 habitantes. En esta región, se identificaron 430 establecimientos comerciales de este tipo. Para el estudio, se realizaron 275 visitas, en las cuales se llevaron a cabo entrevistas y encuestas. Los resultados indican que el 74.18 % de los establecimientos utilizan carbón como combustible, mientras que el 25.81 % emplean leña. Mediante factores de emisión e índices calóricos se determinó que se genera un total de 2,739.99 toneladas/año de dióxido de carbono equivalente por consumo de leña y 8,872.66 toneladas/año de dióxido de carbono equivalente por consumo de carbón y con un total de 11,612.65 toneladas/año de dióxido de carbono equivalente para la totalidad de los asaderos comerciales los cuales son partícipes del constante cambio climático y los efectos que esto ocasiona a esta zona metropolitana en la costa central del Golfo de México y que deben estar incluidos tanto en reglamentación municipal y en la agenda de cambio climático.**

***Palabras Clave:* asaderos comerciales, emisiones, Gases de Efecto Invernadero.**

I. INTRODUCTION

GLOBAL temperatures have increased over the last 50 years, not only due to carbon dioxide emissions (CO_2), but also due to other types of greenhouse gases (GHG) as methane and nitrous oxide [1], Since the intensive use of energy based on the burning of fuels of origin fossil (such as oil, coal and gas) has been one of the main sources of energy, especially in developing countries; the global average combined surface and ocean temperature is estimated to show an increase, in a range of 0.8 to 1.2 °C, during the period 1880-2012 compared to the pre-industrial era [2].

Since 1992, Mexico has signed the United Nations Framework Convention on Climate Change (UNFCCC), with this it committed to comply with the guidelines established in that instrument, among which is the development and updating of a national GHG inventory [2]. This is why in 2012 the General Law on Climate Change was decreed and in 2013 the state law of mitigation and adaptation to the effects of climate change for the state of Veracruz, where the guidelines are established for the regulation of Greenhouse Gas emissions and the obligation to have inventories with estimates of anthropogenic emissions [3],[4].

1. Tecnológico Nacional de México/Instituto Tecnológico de Veracruz, México. Email: manuel.sm@veracruz.tecnm.mx, ORCID: https://orcid.org/0000-0002-5595-0914
2. Tecnológico Nacional de México/Instituto Tecnológico de Veracruz, México. Email: L19020456@veracruz.tecnm.mx, ORCID: https://orcid.org/0009-0008-9461-237X
3. Tecnológico Nacional de México/Instituto Tecnológico de Veracruz, México. Email: bertha.eg@veracruz.tecnm.mx, ORCID: https://orcid.org/0000-0002-8543-3520
4. Tecnológico Nacional de México/Instituto Tecnológico Veracruz, México. Email: mario.dg@veracruz.tecnm.mx, ORCID: https://orcid.org/0000-0002-9281-2190
5. Tecnológico Nacional de México/Instituto Tecnológico de Veracruz, México. Email: olaya.co@veracruz.tecnm.mx, ORCID: https://orcid.org/0000-0003-3510-2640
6. Tecnológico Nacional de México/Instituto Tecnológico de Veracruz, México. E-mail: juan.mp@veracruz.tecnm.mx, ORCID: https://orcid.org/0009-0000-1625-4927
Manuscript Received: 21/08/2024
Revised: 19/11/2024
Accepted: 10/12/2024
DOI: https://doi.org/10.29019/enfoqueute.1085
Section Editor: Miriam Recalde

Firewood is a fuel widely used for cooking in Mexico, with a consumption pattern that reveals implications for climate change, since by 2022 it was estimated that a total of 31.3 million Mexicans, which represents close to 26 % of the population, will total of the country [5], and according to the National Institute of Statistics, in 2018, 11 % of the national population consumes firewood and charcoal in Mexican homes. [6]. This fuel is obtained from various sources, including forests, scrub areas [7], and waste from the construction industry and tree pruning. The use of this fuel has a great impact due to its combustion power, apart from the social and symbolic importance since cooking and preparing food is an activity that is carried out every day [8]. The quality of the wood is the most important factor for use as firewood, since these affect properties such as heating value, ash content and humidity content, among other attributes [9].

Exposure to pollutants generated by the consumption of firewood in the United States has had a great impact on the increase in respiratory diseases, including infections, cancer, asthma and cardiovascular diseases, among others, as well as the deterioration of cognitive functioning in older people [10]. The WHO estimates that 3.8 million deaths occur each year due to air pollution, where the use of firewood takes first place, where women and children are the most affected [11], the use of firewood in commercial grills represents 26 % of total final energy consumption where it is estimated that 2.6 billion people, mainly low and middle income, use traditional biomass (firewood, charcoal, crop residues, livestock manure) to meet your cooking energy needs [12].

The consumption of this type of solid biofuels is an issue of environmental concern, because it arises from the unsustainable production and use of firewood, exerting pressure on the regional and global environment. The unsustainable extraction of firewood has caused deforestation, soil erosion and loss of biodiversity. Traditional biomass, when produced and used from controlled and sustainable sources, represents a reliable and accessible source of energy because it supplies energy in places where access to conventional fuels and technologies is null or limited. Thanks to proposed strategies such as forest codes and certification programs, it has been possible to achieve sustainable production and use of firewood. And now, biofuels and clean cooking technologies are the new alternatives to traditional cooking with biomass. For example: biogas, pellets and briquettes, as well as improved wood stoves [13].

It is important to mention that the use of firewood and charcoal represents a substantial generation of Greenhouse Gases; only the United States Environmental Protection Agency has reported since 1998 that the generation of Carbon Dioxide has been 1,032 and 1,979 grams for each kilogram of Firewood and Coal used as fuel, while for methane it was 4.2 and 7.9 and 0.35 and 0.51 for nitrogen dioxide [14].

The first attempt to determine the emission of greenhouse gases from commercial grills in the metropolitan area of the City of Veracruz was carried out by Lango-Reynoso et al., in 2018, which calculated the CO_2 emissions produced by burning different fuels in grills. commercials, but it is restricted to the City of Boca del Rio, which only represents 16 % of the metropolitan area, concluding that 30 grills in operation emit a total of 134.56 tons/year of CO_2 [15], Diaz-Nigueda et al., in 2022, the calculation of Emissions generated by the consumption of firewood and charcoal in the preparation of roasted chickens in the city of Tuxtla Gutiérrez, Chiapas, Mexico is carried out through the application of emission factors (EF), where they were categorized from establishments based on their production and the infrastructure used for the activity to determine the fuel consumed annually, the results of which indicate that carbon dioxide emissions as a greenhouse gas is 5312.12 tons/year [16].

II. MATERIAL AND METHODS

A. The Metropolitan Area of City of Veracruz, Mexico

The Metropolitan area of City of Veracruz is located in the central part of the State of Veracruz, in the Sotavento Region on the coast of the Gulf of Mexico, it has 1061.9 km^2 (0.3 % of the state territory) and 882,011 inhabitants which represents 7.5 % of the state total and with the municipalities of Boca del Rio, Medellin Jamapa and Manlio Fabio Altamirano form as a whole the most metropolitan area in the state populated metropolitan area in the State of Veracruz [17] (Fig. 1).

Fig. 1. Metropolitan Area of City of Veracruz, Veracruz State, Mexico.

B. identification and location of commercial grills

To account for the commercial grills, an in-person visit was made to the most populated neighborhoods in the month of June 2024 in the municipalities of Veracruz and Boca del Rio because they were the most populated, going street by street, especially the main avenues where Strategy and location Most of the grills are located there. In this tour, a total count and structured interviews were carried out with the owners, managers and employees of these establishments.

Surveys were applied with questions related to establishment data, type of fuel used, fuel consumed (kg), daily production,

days and hours of service. The establishments were classified into three categories with based on its production and infrastructure; identifying national franchises, as well as establishments established on the banks of streets and avenues. The number of establishments surveyed was calculated by [16] (Eq. 1):

$$n_i = \frac{N_i \sigma^2 Z^2}{(N_i - 1)e^2 + \sigma^2 Z^2} \quad (1)$$

Where:

i = category.
n_i = sample size in category i,
Ni = number of establishments in category i,
Z = value of 1.96 for a level of 95 % confidence
σ = population variance in study (0.5).
e = absolute precision level (9 %).

This equation has been used to determine the number of samples that must be taken to be representative with a finite universe, in research carried out for this type of research [16]:

C. Greenhouse gas emission calculation

To calculate pollutants, the annual production of CO_2, CH_4, N_2O (greenhouse gases) was quantified. This was done using the equation [16] (Eq. 2):

$$E_{ij} = (CA_i)(FE_j)\frac{1\,Ton}{10^6 g} \quad (2)$$

Where:

i = category.
j = pollutant.
E_{ij} = annual emission of pollutant j in category i (t year-1).
CA_i = annual fuel consumption in category i (kg year-1).
FE_j = factor of emission of pollutant j by type of fuel (g kg^{-1}).

D. Calculation of the volume of Methane, Carbon Dioxide and Nitrous Oxide from the consumption of firewood and Coal in commercial grills

The emission factors of the greenhouse gases Carbon Dioxide, Methane and Nitrogen Dioxide for charcoal and firewood were obtained from the values tabulated by Díaz-Nigenda and co-authors in 2022, which on average are presented in Table 1 [16].

TABLE 1
GREENHOUSE GAS EMISSION FACTORS

Emission factors (firewood) (g kg^{-1})		
CO_2	CH_4	N_2O
1569.5 (± 104.25)	5.47 (± 2.25)	0.06 (± 0.01)
Emission factors (carbon) (g kg^{-1})		
CO_2	CH_4	N_2O
2 424.26 (± 353.37)	5.62 (± 1.55)	0.20 (± 0.13)

E. Calculation of the Tons of Methane and Nitrous Oxide in Tons of CO2 equivalent

To calculate the tons of Methane and Nitrous Oxide equivalent to Tons of Carbon Dioxide, the formulas proposed by the Institute of Ecology and Climate Change of Mexico in 2020 were used, [18] which establishes (Eq. 3):

$$CH_4\ em\ in\ CO_2eq = (CH_4\ em)(PCGCH_4) \quad (3)$$

Were CH_4 *em* is the total Methane emissions during the reporting year and $PCGCH_4$ is a Global warming potential of methane (Eq. 4).

$$N_2O\ em\ in\ CO_2eq = (N_2O\ em)(PCGN_2O) \quad (4)$$

Were N_2O *em* is the total Nitrous Oxide emissions during the reporting year and $PCGN_2O$ is a Global warming potential of Nitrous Oxide.

Considering the global warming potential of methane at 28 and nitrous oxide at 265 [19].

F. Calculation of the emission of total tons of Carbon Dioxide equivalent of Greenhouse Gases

To calculate the emission of Greenhouse Gases expressed in total tons of Carbon Dioxide equivalent, the following equations are established for the use of coal and firewood. Finally, the total emission results from the sum of the results of both equations (Eq. 5, 6, 7).

$$CO_2eq\ as\ Coal = E_{ij} + CH_4\ em\ in\ CO_2eq + N_2O\ em\ in\ CO_2eq \quad (5)$$

$$CO_2eq\ as\ Firewood = E_{ij} + CH_4\ em\ in\ CO_2eq + N_2O\ em\ in\ CO_2eq \quad (6)$$

$$Total\ CO_2eq = CO_2eq\ as\ Coal + CO_2eq\ as\ Firewood \quad (7)$$

III. RESULTS AND DISCUSSION

To determine the number of commercial grills in the metropolitan area of Veracruz, the commerce directors of the municipalities of Veracruz, Boca del Rio and Medellin were interviewed, who provided the number of commercial grills registered in their respective municipalities, giving a total of 430 establishments of this type, (Table 2).

TABLE 2
TOTAL OF COMMERCIAL GRILLS
IN THE METROPOLITAN AREA OF HE CITY OF VERACRUZ

Municipality	**Use of Firewood**	**Use of Coal**
Veracruz	60	201
Boca del Rio	15	90
Medellin	36	28
Total	111	319

As can be seen in table 2, commercial grills predominantly use coal, since it is used mainly in cooking chicken and meat,

which is more common in the municipalities of Veracruz and Boca del Rio. However, the number of commercial grills that use firewood increases considerably in the Municipality of Medellin de Bravo, this is because in this area there is a gastronomic culture that influences the use of this fuel, especially in the communities of El Tejar and Rancho del Padre, since, as in South American countries, firewood is considered a fuel for cooking [20]. Although the municipalities of Jamapa and Manlio Fabio Altamirano are considered part of the metropolitan area of the city of Veracruz, both municipalities are completely rural and are not part of the urban conglomerate, so the decision was made not to include them in this study.

To determine the number of surveys and interviews necessary for the sample to be representative, equation No. 1 was used for a total population of 430 commercial grills with a confidence level of 95 %, a population variance in study of 0.5 and an absolute precision level of 9 %, resulting in the need to carry out a total of 144 surveys or interviews, 57.58 for commercial grills with the use of firewood and 86.63 for the use of charcoal, these values were adjusted given the complexity of the metropolitan area, for which it was determined that 131 surveys or interviews would be representative of the total number of commercial grills, and that 48 were carried out for those commercial grills that use firewood and 83 for those that use charcoal.

In this study, the consumption of charcoal was separated from that of firewood, since commercial grills do not use both fuels, this is due to the type of food preparation denominated in Spanish A LA LEÑA or LEÑERO y AL CARBÓN. An important point why the number of commercial grills has increased is the change in the stereotypes of traditional Mexican food that considers A LAS BRASAS and AL HUMO as a more gourmet style, where commercial grills offer different gastronomic experiences than the traditional roast chicken, meat, ribs, pizzas and burgers.

The interviews and surveys were carried out through tours of the metropolitan area of the city of Veracruz, from north to south, starting in the municipality of Veracruz from 10:00 a.m. to 2:00 p.m. in the period from Tuesday, 04 June to Sunday, June 9, 2024. It was found that there are commercial grills with restaurant service, in pizzerias, hamburger restaurants and self-service stores, in some of these places they did not have service in the same place, but it was exclusively to go.

For a better understanding of the product of commercial grills and the type of fuel they require, they were divided into Chicken, Beef, Meat, Pizzas and Hamburgers and the use of firewood or charcoal Table 3.

TABLE 3
TOTAL NUMBER OF COMMERCIAL GRILLERS, SURVEYED OR INTERVIEWED BY FOOD CATEGORY

Food Category	Use of Firewood	Use of Coal
Chicken	34	60
Meat	3	6
Ribs	6	9
Hamburgers	2	8
Pizza	3	
Total	48	83

With the information in Table 3, it was possible to identify that the majority of commercial grills in the municipalities of Veracruz, Boca del Rio and Medellin de Bravo are roast chicken grills; and that these consume 70 % of the firewood and 72 % of the charcoal used as fuel, since the state of Veracruz, Veracruz is the main producer of chicken nationwide, and is also the largest consumer of this product. [21]. Meat grills, ribs and hamburgers represent 6.87 %, 11.45 % and 7.63 % respectively, in both cases the use of firewood and charcoal is very similar and there is no considerable difference between them, however in pizzas the use of charcoal is not used. charcoal, because only firewood is used for this food, when we refer to meat, we are considering cuts such as sirloin, bisteck, flank steak, t-bone, longaniza, chistorra, suckling pig

As a result of the surveys and field interviews, it was found that on average commercial chicken grills consume 45 kilograms of firewood per day, this is due to the fact that they are large local chains with restaurants, since this type of preparation is known as firewood chicken. In the case of meat and ribs grills, these are restaurants, they are also wood-fired preparations with less firewood consumption, which on average is 30 kilograms per day. Finally, there are commercial grills that have wood-burning ovens where they prepare pizza and consume on average 20 kilograms of firewood per day and for wood-fired hamburgers on average 15 kilograms of firewood per day are consumed in each commercial grill (Table 4).

TABLE 4
FIREWOOD CONSUMPTION BY COMMERCIAL GRILLS

Food category	Average daily firewood consumption (kg/day)	Total daily firewood consumption (tons/day)
Chicken	45	3.500
Meat	30	0.208
Ribs	30	0.416
Hamburgers	20	0.092
Pizza	15	0.104
Total		4.320

The total consumption of firewood per food category was obtained by multiplying the average daily consumption by the number of commercial units.

As can be seen in table 4, chicken roasters represent the highest consumption of firewood with an average of 1.5 kilograms per chicken, a value that is much less than the 1.85 kilograms of firewood per chicken reported in 2022 for the city of Tuxtla. Gutierrez Chiapas [16], this variation can also be determined given the sensory effects of roasting chickens over wood due to the wood used for cooking and its cost or availability [22].

In the case of commercial grills that use charcoal, the result of field surveys and interviews found that the average consumption in the case of chicken is 30 kilograms of charcoal per day; In this case, we must consider that charcoal grilling occurs both in commercial chains and in small mobile grills in family businesses. An important aspect is that no grill was found that used charcoal to prepare pizzas and the values for

consumption in the case of meat, ribs and hamburgers are presented in Table 5.

TABLE 5
COAL CONSUMPTION BY COMMERCIAL GRILLS
AT METROPOLITAN AREA OF VERACRUZ CITY

Food category	Average daily coal consumption (kg/day)	Total daily coal consumption (tons/day)
Chicken	30	6.89
Meat	25	0.570
Ribs	35	1.215
Hamburgers	18	0.552
Pizza	0	0
Total:		9.227

According to table 5, commercial chicken roasters represent the highest consumption of charcoal with an average of 1 kilogram per chicken. It was not possible to determine the amount of charcoal used for meat, ribs and hamburgers, since this depends on the type of commercial grill, however, it can be seen that for meat and ribs the amount of charcoal increases compared to firewood, if compared in tables 6 and 7, However, studies presented by Melo in 2022 show that beef steak is the meat that emits the most greenhouse gases in its production, with almost 130 kilograms of CO_2 equivalent per kilogram [23], there is a difference in the consumption of firewood and charcoal in commercial grills, this is fundamentally due to the fact that the amount of heat they produce is substantially lower in the case of firewood and greater in the case of firewood. case of charcoal, which allows the cooking time to be shorter and therefore its consumption to be lower.

To determine the annual emission for each of the pollutants (carbon dioxide, methane and nitrogen oxide), equation number 2 was used, for the two categories of firewood and coal, considering the annual consumption per category (which results from the multiplication of the daily emission for 365 days/year) and the emission factors for firewood and coal from table 1, obtaining the values shown in table 6.

TABLE 6
TOTAL GREENHOUSE GAS EMISSIONS
FROM COMMERCIAL GRILLS IN THE METROPOLITAN
AREA OF THE CITY OF VERACRUZ

Category	CA_i Annual consumption (kg/year)	Emission E_{ij} (tons/year)		
		CO_2	CH_4	N_2O
Firewood	1,576,800	2,474.78	8.62	0.09
Coal	3,367,855	8,164.55	18.92	0.67
Total		10,639.33	27.54	0.76

From the data in table 8 we can see that the emission of Carbon Dioxide by commercial grills that use charcoal is 337% greater than what is emitted in grills that use firewood, this is because. The value of the carbon dioxide emission factor of coal is 54 % higher than that of firewood, in the case of Methane the emission values are similar because their emission factor is similar.

Finally using equations 5 and 6 and the values of the global warming potential of methane established by the Institute of Ecology and Climate Change of the Secretariat of Environment and Natural Resources of Mexico [18] and reported by Susunaga-Miranda et al., in 2023 [19] it is obtained that the total equivalent carbon dioxide emitted by the consumption of firewood by commercial grills in the metropolitan area of the city of Veracruz is 2,739.99 tons/year and in the case of the equivalent carbon dioxide by consumption of coal is 8,872.66 tons/year, and with the help of equation number 7, we have that the total amount of equivalent Carbon Dioxide emitted by commercial grills, both firewood and charcoal, for the year 2024 is 11,612.65 tons/year.

Commercial grills facilities contribute substantially to climate change due to the generation of greenhouse gases, since it is known that due to the increase in the amount of Greenhouse Gases in the local atmosphere and given the proximity to the reef zone on the coast of the Gulf of Mexico, contributes to the increase in sea temperature and thus to the bleaching of corals in the Veracruz Reef System National Park due to global warming [19], [24]. In addition, the estimates that have been made by various investigations consider a rise in sea level of between from 19 to 58 cm by the year 2100; Other calculations predict a rise of 0.9 to 1.3 meters for the same period, it should not be ruled out that these variations are not the same in all regions, since some coastal scenarios will present flooding up to the current levels of 10 and 5 meters above sea level, and 5 meters on the coasts. of the municipalities of Veracruz, Boca del Rio, in the low areas of the municipality of Medellin, affecting the habitability conditions of the metropolitan area of the city of Veracruz [25].

V. CONCLUSION

After having carried out the field work, visits, surveys and interviews, it is concluded that in the metropolitan area of the city of Veracruz there are a significant number of commercial grills. The above is due to the ease of acquiring firewood and charcoal as fuel and the little environmental regulation and/or little commercial regulation, which is why the majority of commercial grills use the take-out service, they do not have the infrastructure to provide the service. of restaurants.

Although commercial grills that use firewood or charcoal specialize in chicken, meat, ribs, hamburgers and pizzas, there are other types of restaurants that use these fuels in various preparations of Mexican or international gastronomy and cannot be considered commercial grills, in addition that some supermarkets offer the roasting service with the purchase of products such as meats and vegetables.

Due to the geographical characteristics of the metropolitan area of Veracruz, it is evident that the use of charcoal in commercial grills exceeds those that use firewood, due to the conditions of the territory, firewood is scarce and its cost is much higher than that of charcoal. and due to its dimensions, transporting it presents exponential risk and handling difficul-

ties. For this reason, the consumers of this raw material as fuel for commercial grills predominate those who use charcoal. It is important that city councils do not make isolated efforts to control Greenhouse Gases, since in their respective regulations the subject of regulation is very varied and does not contribute to the metropolitan decrease in the emission of these pollutants.

Although the caloric index of methane and nitrous oxide are very high due to the small proportion present in these fuels, these pollutants do not represent a substantial variation in the tons of carbon equivalent, for which the largest proportion is represented by carbon dioxide.

It can be determined that by making some changes in the cooking of different types of food in commercial grills with the help of renewable energy, implementing solar ovens in these establishments. Through this change, the use of firewood and coal could be reduced, which would therefore result in a decrease in the generation of greenhouse gases, which would be a considerable amount per year, not leaving aside efficiency and heating power. This for the benefit of our environment, thanks to alternatives that can already be implemented.

As final results, there are fundamental characteristics of these fuels (firewood and coal) that determine their performance. On the one hand, charcoal heats up faster, providing higher and more uniform temperatures compared to firewood, which takes longer to reach high temperatures, being more difficult to control, producing more smoke.

The results of this research must be included in the Municipal Climate Change Agendas for the municipalities of Veracruz, Boca del Rio and Medellin de Bravo so that legal provisions are generated to carry out actions that help combat Climate Change, and thus regulate commercial barbecue activities so that they contribute to the reduction of Greenhouse Gases (GHG) and allow adaptation and reduction of the vulnerability of the area to the effects of climate change to its population and territory and thus comply with the provisions of the General Law on Climate Change in the scope of jurisdiction of the municipalities

REFERENCES

[1] G. Hernández, "Emisiones de gases de efecto invernadero y sectores clave en Colombia," *El Trimestre Económico,* vol. no. 350, 523-550, 2021. https://doi.org/10.20430/ete.v88i350.857

[2] H. Catalán-Alonso, "Impacto de las energías renovables en las emisiones de gases efecto invernadero en México. Problemas del Desarrollo," *Revista Latinoamericana de Economía,* vol. 52, no. 204, 59-83, 2021. https://doi.org/10.22201/iiec.20078951e.2021.204.69611

[3] DOF (Ley General de Cambio Climático, Diario Oficial de la Federación del 6 de junio de 2012. Available: https://www.diputados.gob.mx/LeyesBiblio/pdf/LGCC.pdf

[4] GE, Ley Estatal de Mitigación y Adaptación ante los Efectos del Cambio Climático, 2013. Available: http://www.ordenjuridico.gob.mx/Documentos/Estatal/Veracruz/wo77450.pdf

[5] G, Pérez, Jorge M. Islas-Samperio, Genice K. Grande-Acosta and Fabio Manzini, "Socioeconomic and Environmental Aspects of Traditional Firewood for Cooking on the Example of Rural and Peri-Urban Mexican Households" *Energies,* vol. 15, no. 13, p. 4904. 2022. https://doi.org/10.3390/en15134904

[6] Instituto Nacional de Geografía y Estadística, Presentación de Resultados ENCEVI 2018. Available: https://www.inegi.org.mx/contenidos/programas/encevi/2018/doc/encevi2018_presentacion_resultados.pdf (accessed on 16 may 2024)

[7] A. Flammini, H. Adzmir, K. Karl and F. Tubiello, *Quantifying greenhouse gas emissions from woodfuel used in households,* 2022. https://doi.org/10.5194/essd-2022-390

[8] M. Doumecq, N. Jiménez-Escobar, D. Morales and A. Ladio, "Much more than firewood: woody plants in household well-being among rural communities in Argentina," *Journal of Ethnobiology*, vol. 43, 2023. https://doi.org/10.1177/02780771231176065

[9] M. Da Silva, I. Feitosa, R. Cruz, V. De Sá, P. De Medeiros and R. Da Silva, "Use of firewood for artisanal ceramic production in a context of forest scarcity in Northeastern Brazil," *Ethnobiology and Conservation,* 12. 2023. https://doi.org/10.15451/ec2023-11-12.23-1-14

[10] K. Newell, R. P. Cusack, C. Kartsonaki, N. Chaudhary and O. P. Kurmi, *Household air pollution and associated health effects in low and middle income countrieshousehold air pollution and associated health effects in low- and middle-income countries*, 2022. https://doi.org/10.1016/B978-0-12-801238-3.11494-1

[11] M. Ahmed, C. Shuai, K. Abbas, F. Rehman and W. Khoso, "Investigating health impacts of household air pollution on woman's pregnancy and sterilization: Empirical evidence from Pakistan, India, and Bangladesh," *Energy,* vol. 247, p. 123562, 2022. https://doi.org/10.1016/j.energy.2022.123562

[12] REN21. Renewables 2021. Global Status Report; REN21 Secretariat: Paris, France, 2021; ISBN 978-3-948393-03-8.

[13] A. Ghilardi, G. Guerrero and O. Masera, "Spatial analysis of residential fuelwood supply and demand patterns in Mexico using the WISDOM approach," *Biomass and Bioenergy*, vol. 31, pp. 475-491, 2007. https://doi.org/10.1016/j.biombioe.2007.02.003

[14] A. Cimini and M. Moresi, "Environmental impact of the main household cooking systems - A survey," *Italian Journal of Food Science*, vol 34, pp. 86-113, 2022. https://doi.org/10.15586/ijfs.v34i1.2170

[15] V. Lango-Reynoso, J. López-Spiegel, F. Lango-Reynoso, M. D. R. Castañeda-Chávez and J. Montoya-Mendoza, "Estimation of CO_2 emissions produced by commercial grills in Veracruz, Mexico," *Sustainability,* vol. 10, no. 2, p. 464, 2018. https://doi.org/10.3390/su10020464

[16] E. Díaz-Nigenda, W. Morales, A. Sandoval, H. Morales and S. Jiménez, "Emisiones generadas por el consumo de leña y carbón en la preparación de comida rápida," *Ecosistemas y Recursos Agropecuarios*, *8*, 2021. https://doi.org/10.19136/era.a8n2.2962

[17] SEDATU Metrópolis de México 2020. Secretaría de Desarrollo Agrario, Territorial y Urbano. Gobierno de México, 2021. https://www.gob.mx/cms/uploads/sedatu/MM2020_06022024.pdf

[18] Instituto Nacional de Ecología y Cambio Climático INECC, "Metodo-logía para el cálculo de emisiones de gases de efecto invernadero," 2022 Available: https://www.gob.mx/cms/uploads/attachment/file/552726/MetodologiaIPCC180520.pdf

[19] M. A. Susunaga-Miranda, B. Ortiz Muñiz, B. M. Estévez-Garrido, R. M. Susunaga-Estévez, M. Díaz-González and O. P. Castellanos-Onorio, "Greenhouse gas emissions by the biogas from the abandoned solid waste final disposal site in city of Veracruz, Mexico," *Enfoque UTE,* vol. 14, no. 4, pp. 1-8, 2023. https://doi.org/10.29019/enfoqueute.988

[20] A. Benoist, C. Lanvin, O. Lefebvre, C. Godard, H. Ouedraogo. M. Riesgo Saives, P. Martz, S. Ringeissen and J. Blin, "Better practices for including traditional firewood in LCA: Lessons from a shea butter case study in Burkina Faso," *Environmental Impact Assessment Review*, vol. 105, p. 107414, 2024. ISSN 0195-9255, https://doi.org/10.1016/j.eiar.2024.107414

[21] El sitio avícola, "Producción, comercio y consumo avícola de México para 2023 y 2024," El sitio avícola, 2023 Available: https://www.elsitioavicola.com/poultrynews/34470/produccian-comercio-y-consumo-avacola-de-maxico-para-2023-y-2024/

[22] M. Piochi, G. Cabrino and L. Torri, "Effects of different woods in barbecuing: Consumers' sensory perception and liking of grilled chicken meat," *Food Research International*, vol. 163, p. 112295, 2022. https://doi.org/10.1016/j.foodres.2022.112295

[23] F. Melo, "La huella de carbono de los alimentos," *Statista*, 2022. Available: https://es.statista.com/grafico/28549/emisiones-de-gases-de-efecto-invernadero-por-kilogramo-de-alimentos-y-bebidas-seleccionados/

[24] T. Saxena, A. Sahgal, R. Gupta, N. Mehra and L., "Arora coral bleaching: causes, mechanism, consequences, resilience and perspective," *International Journal of Ecology and Environmental Sciences*, vol. 49, 2023. https://doi.org/10.55863/ijees.2023.2717

[25] R. Cabaña, F. Palacios, and S. Espinosa, “Impactos y adaptación al cambio climático en el Puerto de Veracruz,” Rumbos TS, año X, no. 12, pp. 119-129, 2015. Available: https://www.researchgate.net/publication/309791597_IMPACTOS_Y_ADAPTACION_AL_CAMBIO_CLIMATICO_EN_IMPACTS_AND_ADAPTATION_TO_CLIMATE_CHANGE_IN_VERACRUZ

Analysis of Artificial Intelligence Methods for Automatic Bandwidth Adjustment for Wireless Networks

Carrillo Marlon[1], Torres Rommel[2], Barba Luis[3]

***Abstract* — The exponential increase in Internet traffic is mainly due to the proliferation of services such as audio and video streaming, the emergence of applications that require a lot of bandwidth to work optimally and generally the process of digitalization of services. In this context, bandwidth management plays a fundamental role, which translates into a better experience for users. Traffic congestion causes the exchange of information to become deficient, that is why techniques such as automatic bandwidth adjustment have been investigated, which manages the bandwidth according to the traffic demand, therefore in this document a study is made about the automatic bandwidth adjustment, the way in which Artificial Intelligence is integrated with computer networks, finally a comparison will be made of several machine learning methods, cataloged within supervised learning, carrying out several experiments determining that Random Forest is the most effective method to predict the automatic bandwidth adjustment, followed by Naive Bayes, Logistic Regression, and Support Vectorial Machine (SMV), on the other hand K -nearest neighbor (KNN) and neural network do not demonstrate considerable effectiveness, each experiment was carried out taking into account the Quality of Service (QoS).**

***Keywords:* traffic, Internet, Machine Learning, Supervised Learning, Quality of Service.**

***Resumen* — El aumento exponencial del tráfico en Internet se debe principalmente a la proliferación de servicios como el streaming de audio y video, a la aparición de aplicaciones que requieren un alto ancho de banda para funcionar de manera óptima, y, en general, al proceso de digitalización de servicios. En este contexto, la gestión del ancho de banda desempeña un papel fundamental, ya que contribuye a una mejor experiencia para los usuarios. La congestión de tráfico genera que el intercambio de información sea ineficiente. Por ello, se han investigado técnicas como el ajuste automático de ancho de banda, que permite gestionar el ancho de banda según la demanda de tráfico. En este documento se realiza un estudio sobre el ajuste automático de ancho de banda, abordando cómo la Inteligencia Artificial se integra con las redes de computadoras. Además, se presenta una comparación de varios métodos de aprendizaje supervisado en machine learning. A través de diversos experimentos, se determinó que Random Forest es el método más efectivo para predecir el ajuste automático de ancho de banda, seguido por Naive Bayes, Regresión Logística y Support Vector Machine (SVM). En contraste, los métodos K-Vecinos Más Cercanos (KNN) y redes neuronales no demostraron una efectividad significativa. Cada experimento se realizó considerando la Calidad de Servicio (QoS).**

***Palabras Clave:* tráfico, Internet, Machine Learning, Aprendizaje Supervisado, Calidad de Servicio.**

1. Carrillo Encalada Marlon Vicente, is an Information Technology Engineer, graduated from the Universidad Técnica Particular de Loja (e-mail: mvcarrillo2@utpl.edu.ec). ORCID: 0009-0005-1289-3867

2. Torres Tandazo Rommel Vicente. is Torres Rommel, holds a PhD in Computer Science from the Polytechnic University of Madrid, and is currently a research professor in the Department of Computer Science and Electronics at the Technical University of Loja. (e-mail: rovitor@utpl.edu.ec). ORCID: 0000-0003-2313-0118

3. Barba Guamán Luis Rodrigo, holds a PhD in Science and Technology for Smart Citys from the Polytechnic University of Madrid, and is currently a research professor in the Department of Computer Science and Electronics at the Technical University of Loja, (e-mail: lrbarba@utpl.edu.ec). ORCID: 0000-0002-8569-3322

Manuscript Received: 16/10/2024
Revised: 07/12/2024
Accepted: 15/12/2024
DOI: https://doi.org/10.29019/enfoqueute.1105
Section Editor: Marcelo Mosquera

I. INTRODUCTION

TECHNOLOGY has advanced significantly in recent years, today we depend on the Internet for everyday actions such as communication, entertainment, information search, digital services and others. Bandwidth can be defined as: the amount of information that is transmitted through a network connection in each period. It is crucial for proper Internet browsing, because the greater the amount of information transmitted in less time, the better the user experience, for the proper functioning of the services, the availability of bandwidth is crucial [1].

The exponential growth of services such as audio and video streaming, the proliferation of applications that consume a lot of bandwidth, the significant growth of online services and the increase of smart devices that integrate the Internet of Things (IoT), has caused the constant updating of control measures to ensure an adequate quality of service (QoS) to users. The amount of information transmitted on the Internet has gone from bps to Gbps, due to this it is necessary to make changes and implement measures to offer a better service to users [2].

In this research, the integration of Artificial Intelligence methods and algorithms for efficient distribution for bandwidth management is proposed. The objectives of our approach are:

Obtain a set of metrics for bandwidth requirements related to quality of service.

Define scenarios for the generation of dataset information or collect datasets for the use of artificial intelligence tools.

Analysis of artificial intelligence (AI) techniques related to automatic bandwidth adjustment.

Compare AI techniques using QoS requirements for dynamic bandwidth adjustment.

This research is an initial work, its findings will be used for the creation of a wireless network automatic bandwidth adjustment model based on Artificial Intelligence methods with the capacity to predict the required bandwidth.

This paper is organized as follows: State of the art is a review of the most important works on the subject of automatic bandwidth adjustment and Artificial Intelligence, Materials and Methods discusses the tools used to develop this work, Results and Discussion presents the results of the general and specific experiments that were conducted to determine the feasibility of the Artificial Intelligence methods chosen, finally the Conclusions of this work are exposed.

II. STATE OF THE ART

There are some authors who study the automatic bandwidth adjustment and integration with artificial intelligence tools, for example, the impact on ISPs is analyzed in [3], where it is identified that the automatic bandwidth adjustment is a technique that emerged due to the significant increase in the amount of traffic on the network permits adjust the bandwidth of a network, depending on the existing traffic demand, allowing access to products and services that with a fixed bandwidth would not be achieved with the same quality of service such as: Streaming, IP voice calls, online games, etc. Shows also that despite the implementation of the automatic adjustment techniques, ISPs have found it necessary to increase physical bandwidth to support the amount of network traffic generated by the applications and services that are booming.

Automatic adjustment ensures that the network will always have adequate bandwidth to work efficiently when users require it, working with adequate bandwidth is important to avoid problems related to network performance such as packet loss or delays [4].

Working with the appropriate bandwidth to meet the demand of each user, allows the reduction of costs related to increased bandwidth consumption without compromising the required quality of service, i.e. it is not necessary to acquire more bandwidth than is truly required by users [5].

The field of Artificial Intelligence focuses its study to develop theories, techniques and methods to mimic and improve human cognitive ability. The rise of Artificial Intelligence tools and technologies provides a more interesting option in the field of computer networks, since it is more efficient to allocate resources using Intelligence algorithms [6].

The integration of Artificial Intelligence and networks is necessary, since the network industry takes giant steps with each generation, so the combination of these areas permits more efficient, faster networks, with the incorporation of new services and better security. Fields such as wireless networks are influenced by using Artificial Intelligence techniques, which make it possible to exploit multiple opportunities [7], as shown in Fig 1.

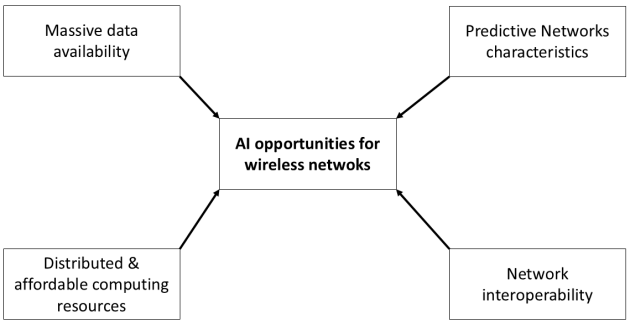

Fig. 1. AI Opportunities in Wireless Networks

Multiple scientific articles have been published referring to the use of Artificial Intelligence methods applied to wireless networks, these mainly analyze how to improve and optimize the performance of networks, in Table 1, shows some methods of Artificial Intelligence, used in the context of wireless networks, for the prediction of various data, ranging from intrusions in the network, resource allocation and network efficiency [8].

TABLE I
AI METHODS USED IN WIRELESS NETWORKS

Method	Characteristics	Result
Vector Machines Support (SVM)	Construct a high-dimensional feature space from the input vectors in terms of the hyperplane and segregate them into two classes, i.e. Positive and negative	Increased accuracy in the classification of abnormal events in the context of networks
Logistic regression	Predicting the occurrence of an event based on the concept of probability.	Minimize the number of specific features, thus improving logistic regression performance.
KNN algorithm	Sorts new data according to similarity and votes on data points according to euclidean distance measurement	It shows a higher accuracy of 15% in classifying data with varied characteristics.
Nayve Bayes	To classify, calculate the probability to determine the likelihood using bayes' theorem.	It showed good accuracy in the data set with highly variable characteristics.
Random Forest	It is mainly based on multiple decision trees, which is one of the key models in the ml architecture.	It shows a fairly good performance, although the time required is longer than that of other sorters.
Neural Network	It is based on the implementation of multiple nodes, connected to each other, to transmit signals, each piece of information goes through these nodes, where it is subjected to different analyses in order to make a decision.	Achieved an overall read bandwidth improvement of 65.7%.

The implementation of Artificial Intelligence algorithms such as Random Forest and Neural Network in short-range 100/400 Gbit/s data transmission networks has allowed constant and effective monitoring of signal quality, especially in heterogeneous optical networks, effectively identifying the modulation format, achieving an astonishing 100% effectiveness [9].

An algorithm based on Naive Bayes has been successfully implemented in 5G wireless networks. This algorithm divides the network into smaller and more efficient network portions, guaranteeing the adequate optimization of resources, being able to predict the best portion of the network even when there are network interruptions [10].

All the Artificial Intelligence methods analyzed in this work demonstrate a considerable degree of efficiency when working with bandwidth data in scenarios such as resource allocation, network security and resource optimization, taking into consideration the appropriate QoS.

QoS focuses on efficiently allocating resources to ensure optimal performance in a network, since not all Internet traffic is equal, QoS prioritizes different types of traffic depending on their importance when browsing. Failure to apply the appropriate quality of service would result in bad user experience, since there would not be adequate concurrence between the different types of traffic present, so it is important to establish the required QoS parameters [8].

The QoS parameters required for multimedia traffic in a network may vary depending on the context in which they are applied [9], but are generally the following:

Packet loss: packets may be dropped when a packet queue overflows, meaning that there are too many packets waiting to be sent, and some must be dropped to avoid further delay in transmission.

Jitter: Jitter occurs because of network congestion, variations in transmission times and changes in data paths.

Latency: The time it takes for a data packet to travel from its point of origin to its destination in a network.

Bandwidth: The capacity of a network communications link to transfer the maximum amount of data from one point to another in a specific time interval.

The present research makes a study of the AI tools to determine which are the most suitable parameters according to the controlled scenario of a 5G wireless network, which has been compiled and is presented in the Dataset.

III. MATERIALS AND METHODS

The use of the right Dataset is of utmost importance when working on an Artificial Intelligence project, because it influences the training capacity of a model, generalization and performance evaluation.

On the Internet there are millions of Datasets available on various topics, it is practically impossible to search every page where Datasets are available, so the use of a good tool that allows the search of Datasets is important, in this research GoogleDataset and Kaggle are used. Tools that allow searching Datasets, the following key phrases were used: “Bandwidth Dataset for used Artificial Intelligence methods” and “Network computers Dataset for used Artificial Intelligence methods”, resulting in a preliminary result of about 100 Datasets founded.

For the selection of the appropriate Dataset, the parameters were established and the variables identified as shown in Table 2.

The analyzed datasets are the following: “Conference Call Bandwidth Consumption” [10] , “International Internet bandwidth per Internet user, kb/s” [11], Dataset 5g Network Metrics High Traffic Event [12]. Of all the Datasets examined, only 1 Dataset met the parameters set out above, this Dataset is called “5g network metrics high traffic event”.

The Dataset has 26 variables where each variable holds 1000 data, giving a total of 26000 data, Table 2 shows the function of each variable selected from the Dataset.

TABLE II
FUNCTION OF DATASET VARIABLES

FUNCTIÓN	VARIABLES
Signal and Quality Indicators	RSRP, RSRQ, CQI
Resource Utilization	BW_Utilization(%), RB_Allocation
Status and User Demand	UE_Demand (kbps)
Traffic and Latency	Traffic_Load (kbps), Latency (ms)
Schemes and Classes	MCS, QoS_Class
Additional Context	Channel_Conditions

Knowing each of the Dataset variables, it is necessary to select the best variables that will be used in the application of experiments to determine the prediction of automatic bandwidth adjustment by means of Artificial Intelligence methods, therefore, using criteria such as: logical discard, knowledge of the subject and correlation analysis, the following variables were chosen:

- Traffic_Load (kbps): Network traffic load.
- Latency (ms): Network latency, measured in milliseconds (ms).
- BW_Utilization (%): Percentage of bandwidth utilization.
- CQI (Channel Quality Indicator): Communication channel quality.
- MCS (Modulation and Coding Scheme): Data rate and signal robustness.
- RSRP (Reference Signal Received Power): Signal quality.
- RSRQ (Reference Signal Received Quality): Signal quality with noise and interference.
- RB_Allocation (Resource Block Allocation): Allocation of resource blocks in the network.
- QoS_Class (Quality of Service Class): Quality of Service Class assigned to the traffic.
- UE_Demand (kbps): Bandwidth demand by users.
- Channel_Conditions: Communication channel conditions.

The analysis of the selected variables shows that there is no variable referring to bandwidth adjustment, which means that the Dataset lacks an objective variable on which, in theory, the necessary predictions should be made to support the research, which is why the decision was made to create such a variable, However, before creating such variable, it should be taken into account that a formula required to calculate the proactive bandwidth adjustment is not a standard formula, since it depends largely on the specific context of the network and the objectives

to be achieved; however, in a 5G network, a weighted combination of different network performance variables can be used to determine the need for a proactive adjustment [13], to calculate the proactive adjustment in this specific network the following variables were taken: Traffic_Load, Latency and BW_Utilization, which through a normalization process and their combination by means of the following Python code shown in Figure 2, allowed calculating the proactive adjustment for each case

```
import pandas as pd
import numpy as np
from Orange.data import Table, Domain, ContinuousVariable, DiscreteVariable

# Convertir los datos de Orange a un DataFrame de pandas
df = pd.DataFrame(in_data.X, columns=[var.name for var in
in_data.domain.attributes])

# Si hay columnas objetivo, añadirlas al DataFrame
if in_data.domain.class_vars:
    target_columns = [var.name for var in in_data.domain.class_vars]
    df_target = pd.DataFrame(in_data.Y, columns=target_columns)
    df = pd.concat([df, df_target], axis=1)

# Normalizar las columnas relevantes
df['Traffic_Load (kbps)'] = (df['Traffic_Load (kbps)'] - df['Traffic_Load
(kbps)'].mean()) / df['Traffic_Load (kbps)'].std()
df['Latency (ms)'] = (df['Latency (ms)'] - df['Latency (ms)'].mean()) /
df['Latency (ms)'].std()
df['BW_Utilization (%)'] = (df['BW_Utilization (%)'] - df['BW_Utilization
(%)'].mean()) / df['BW_Utilization (%)'].std()

# Crear la variable objetivo basada en la suma ponderada de los factores
normalizados
df['Proactive_Adjustment'] = (0.5 * df['Traffic_Load (kbps)']) + (0.3 *
df['Latency (ms)']) + (0.2 * df['BW_Utilization (%)'])
```

Fig. 2. Python code, to calculate the proactive adjustment

In the code the variable "Proactive_Adjusment" stores the amount of bandwidth required at each instant, it is calculated based on latency, traffic load and bandwidth utilization percentage. The variable "Adjusment_Class" stores the categories assigned to each adjustment range, the adjustment ranges and the categories assigned to each range can be seen in Table 3.

TABLE III
CATEGORIES ASSIGNED TO EACH ADJUSTMENT RANGE

ADJUSTMENT RANGE	CATEGORY
Less than -0.5	Low
Enter -0.5 and 0	Moderate
Enter 0 and 0.5	High
Greater than 0.5	Critical

IV. RESULTS AND DISCUSSION

For the present work two sets of experiments were made with 6 training experiments, to determine which is the best AI method to work with the selected dataset based on a list of 6 previously defined methods: Random Forest, Nayve Bayes, Logistic Regression, SVM, KNN and neural network, where cross validation was used to determine the effectiveness of each method. Experiment 1 was validated by 2 folds, experiment 2 was validated by 5 folds, experiment 3 by 10 folds, experiment 4 by 20 folds. From this point onwards the following experiments were performed using random data samples, in experiment 5 a sample of 60% was used and in experiment 6 a sample of 70% was used. Table 4 shows the main results of the training experiments.

TABLE IV
RESULTS OF TRAINING EXPERIMENTS IN ACCURACY

		ACCURACY					
		Ramdon Forest	Nayve Bayes	Logistic Regression	SVM	K-NN	Neural Network
EXPERIMENTS	2 folds	95.8%	95.0%	90.7%	84.5%	22.5%	28.0%
	5 folds	99.1%	95.0%	93.2%	88.8%	22.9%	28.0%
	10 folds	99.2%	95.1%	92.5%	88.3%	22.4%	28.0%
	20 folds	99.0%	94.8%	92.8%	89.4%	22.2%	28.0%
	60 % data random	99.2%	95.7%	91.3%	88.9%	24.4%	28.0%
	70 % data random	98.8%	94.7%	92.0%	84.9%	24.1%	28.0%

In the 6 validation experiments that serve to validate the results of the general experiments, by applying each AI method separately to the dataset, then in the specific experiment 1 the Random Forest method was used, in the specific experiment 2 the Nayve Bayes method was used, in the specific experiment 3 the Logistic Regression method was used, in the specific experiment 4 the SVM method was used, in the specific experiment 5 the KNN method was used and in the specific experiment 6 the Neural Network method was used, in the Table 5 shows the main results of the validation experiments.

TABLE V
RESULTS OF VALIDATION EXPERIMENTS

MODEL	TRAINING: 600 DATES		VALIDATION: 400 DATES	
	Successes	Mistakes	Successes	Mistakes
Random Forest	600 (100%)	0 (0%)	391 (97.8%)	9 (2.2%)
Nayve Bayes	560 (93.3%)	40 (6.7%)	379 (94.8%)	21 (5.2%)
Logistic Regression	567 (94.5%)	33 (5.5%)	368 (92%)	32 (8%)
SVM	587 (97.8%)	13 (2.2%)	349 (87.3%)	51 (12.7%)
KNN	288 (48%)	312 (52%)	89 (22.3%)	311(77.7%)
Red Neuronal	169 (28.1%)	431(71.9%)	111 (27.8%)	289 (72.2%)

A. Training Experiments

The Orange Data Mining environment [14] was used to perform the experiments, firstly, the Testing option is used to test the effectiveness of various prediction models when working with the data stored in the Dataset, then several Artificial Intelligence techniques must be chosen to perform the respective testing, the techniques chosen are: neural network, logistic regression, Random Forest, Support Vector Machines (SVM), Nayve Bayes and k-nearest neighbor (KNN) as shown in Fig. 3. To determine the effectiveness of each model, several evaluation metrics proposed by [15] are used.

Precision (Prec): This metric focuses on the positive and false positive values; it is obtained from the total true positives divided by the sum of true positives and false positives (Eq. 1).

$$Precision = \frac{True\ positives}{True\ positives + False\ Positives} \quad (1)$$

Recall: With the same principle as precision, but with the difference that it focuses on false negatives. It is calculated from the total of true positives divided by the sum of true positives and false negatives (Eq. 2).

$$Recall = \frac{True\ positives}{True\ positives + False\ Negatives} \quad (2)$$

F1 Score (F1): This metric takes into consideration precision and recall. It is obtained from the double product of the multiplication of precision and recall divided by the sum of precision and recall (Eq. 3).

$$F1 = \frac{2 * Precision * Recall}{Precision + Recall} \quad (3)$$

Accuracy (CA): Refers to the number of correct predictions divided by the number of total predictions (Eq. 4).

$$Accuracy = \frac{Correct\ predictions}{Total\ Predictions} \quad (4)$$

Area under the ROC curve (AUC): This metric represents the probability that a randomly chosen positive-valued sample has a higher rating by the model than a randomly chosen negative-valued sample. A perfect model would have an AUC = 1 [16].

Matthews Correlation Coefficient (MCC): It is a statistical metric, widely used in binary classifications, its value ranges from -1 to +1, it returns good results only if the 4 values of the confusion matrix are also good [17].

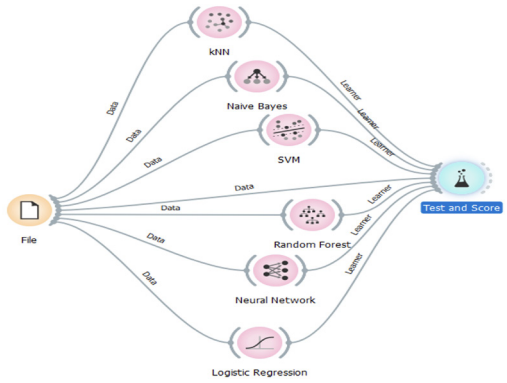

Fig. 3. Testing of Various AI Methods

1. **Experiment 1**
For the present experiment the cross validation was used, with a number of folds of 2, giving as a result what is shown in Table 6, where the models are placed according to the accuracy they showed in the testing, where it can be clearly observed the superiority of the Random Forest model, over the other models, giving a much better performance than the others, while models such as Nayve Bayer, Logistic Regression and SVM show a fairly good reliability, on the contrary, the KNN and Neural Network models show very poor results with respect to the other models.

TABLE VI
RESULTS OF EXPERIMENT 1

MODEL	AUC	CA	F1	PREC	RECALL	MCC
Random Forest	0.999	0.985	0.985	0.985	0.985	0.980
Nayve Bayes	0.988	0.950	0.950	0.952	0.950	0.934
Logistic Regression	0.991	0.907	0.907	0.907	0.907	0.876
SVM	0.979	0.854	0.855	0.856	0.854	0.805
KNN	0.477	0.225	0.220	0.227	0.225	-0.037
Neural Network	0.514	0.280	0.123	0.078	0.280	0.000

2. **Experiment 2**
For the second experiment, cross-validation was used, but this time the number of folds was increased to 5, resulting in the results shown in Table 7, where a clear increase in accuracy can be observed with respect to the previous experiment, leading again the Random Forest model, which remains as the model with the highest accuracy in all aspects, followed by the Nayve Bayes and Logistic Regression models, which remain with a good reliability, the SVM model has significantly increased its reliability, while the KNN and neural network models remain as the model with the lowest accuracy.

TABLE VII
RESULTS OF EXPERIMENT 2

MODEL	AUC	CA	F1	PREC	RECALL	MCC
Random Forest	1.000	0.991	0.991	0.991	0.991	0.988
Nayve Bayes	0.989	0.950	0.950	0.953	0.950	0.934
Logistic Regression	0.994	0.932	0.932	0.932	0.932	0.909
SVM	0.986	0.888	0.888	0..889	0.888	0.850
KNN	0.489	0.229	0.227	0.233	0.229	-0.030
Neural Network	0.518	0.280	0.123	0.078	0.280	0.000

3. **Experiment 3**
For the third experiment the cross validation was used, but this time the number of folds was increased to 10, again there is an increase in the accuracy of the Random Forest model remaining as the model with the highest reliability, followed by the Nayve Bayes, Logistic Regression and SVM models with a very good reliability, while the KNN model and the neural network remain as the models with the lowest reliability, this can be seen in Table 8.

TABLE VIII
RESULTS OF EXPERIMENT 3

MODEL	AUC	CA	F1	PREC	RECALL	MCC
Random Forest	1.000	0.992	0.992	0.992	0.992	0.989
Nayve Bayes	0.989	0.951	0.951	0.954	0.951	0.936
Logistic Regression	0.994	0.925	0.925	0.925	0.925	0.900
SVM	0.986	0.883	0.883	0.884	0.883	0.844
KNN	0.493	0.224	0.221	0.227	0.224	-0.037
Neural Network	0.506	0.280	0.123	0.078	0.280	0.000

4. Experiment 4

For the fourth experiment we used the cross validation which is automatically executed by the Orange Data Minning environment, this time we increased the number of folds to 20, the trend of the previous experiments remains almost the same, but unlike the previous experiments, we noticed a slight decrease in the reliability of the Random Forest, Nayve Bayes and KNN models, a slight decrease in the reliability of the Random Forest, Nayve Bayes and KNN models is noticed, on the other hand the reliability of the Logistic Regression and SVM models has slightly increased, while the neural network remains the same being the model with the lowest reliability, this can be observed in Table 9.

TABLE IX
RESULTS OF EXPERIMENT 4

MODEL	AUC	CA	F1	PREC	RECALL	MCC
Random Forest	1.000	0.990	0.990	0.990	0.990	0.987
Nayve Bayes	0.989	0.948	0.948	0.951	0.948	0.932
Logistic Regression	0.994	0.928	0.928	0.928	0.928	0.904
SVM	0.985	0.894	0.894	0.895	0.894	0.858
KNN	0.488	0.222	0.220	0.226	0.222	-0.039
Neural Network	0.503	0.280	0.123	0.078	0.280	0.000

5. Experiment 5

By using a random data sample of 60% of the Dataset, with 10 test repetitions, we obtained the results shown in Table 10, where maintaining the trend marked in the previous experiments, we note the clear superiority in reliability of the Random Forest model, which shows much higher metrics than the other models, on the other hand models such as Nayve Bayes, Logistic Regression and SVM maintain a very similar level to those shown in the experiments and the KNN and neural network models remain as the models with the lowest reliability.

TABLE X
RESULTS OF EXPERIMENT 5

MODEL	AUC	CA	F1	PREC	RECALL	MCC
Random Forest	1.000	0.992	0.992	0.992	0.992	0.989
Nayve Bayes	0.990	0.957	0.956	0.959	0.957	0.943
Logistic Regression	0.991	0.913	0.913	0.913	0.913	0.884
SVM	0.985	0.889	0.889	0.891	0.889	0.852
KNN	0.490	0.244	0.242	0.250	0.244	-0.009
Neural Network	0.517	0.280	0.123	0.078	0.280	0.000

6. Experiment 6

By using a random data sample of 70% of the Dataset, with 10 test repetitions, we obtained the results shown in Table 11, where we can notice a small decrease in the reliability of most prediction models, except for the Logistic Regression model and SVM, which have experienced a small increase in their reliability, while the neural network remains the same. Data charts which are typically black and white but sometimes include color.

TABLE XI
RESULTS OF EXPERIMENT 6

MODEL	AUC	CA	F1	PREC	RECALL	MCC
Random Forest	1.000	0.988	0.988	0.988	0.988	0.984
Nayve Bayes	0.987	0.947	0.947	0.951	0.947	0.931
Logistic Regression	0.993	0.920	0.920	0.920	0.920	0.893
SVM	0.986	0.894	0.894	0.895	0.894	0.858
KNN	0.495	0.241	0.239	0.248	0.241	-0.014
Neural Network	0.509	0.280	0.123	0.078	0.280	0.000

B. Validation Experiments

Having known the effectiveness of various models through initial testing to see the behavior of the data against each model, it is necessary to validate these results, in order to give credibility to the results given by the general testing.

An abbreviation will be assigned to each word in the tables for better presentation.

- Cat (Category)
- Suma (Summation)
- Hi (High)
- Lo (Low)
- Cri (Critical)
- Mo (Moderate)

1. Random Forest

It is a technique that consists of the creation of multiple decision trees to be trained on a different set of data, and then all the results are integrated to give a final answer. For the present evaluation, the Random Forest model was used on a sample of 60% of the data for training, giving the results shown in Table 12.

TABLE XII
TRAINING RESULTS BY RANDOM FOREST METHOD

	CAT	PREDICTION				SUMA
		HI	LO	CRI	MO	
CURRENT STATUS	HI	164	0	0	0	164
	LO	0	121	0	0	121
	CRI	0	0	146	0	146
	MO	0	0	0	169	169
	SUMA	164	121	146	169	600

Now that the respective model training has been performed, it is necessary to validate the results by evaluating the model by applying 40% of the remaining data, in order to check its efficiency, these new results can be seen in Table 13.

TABLE XIII
EVALUATION RESULTS USING RANDOM FOREST METHOD

	CAT	PREDICTION				SUMA
		HI	LO	CRI	MO	
CURRENT STATUS	HI	94	0	0	2	96
	LO	0	102	0	4	106
	CRI	2	0	85	0	87
	MO	1	0	0	110	111
	SUMA	97	102	85	116	400

The results of the application of the Random Forest technique for the automatic bandwidth adjustment prediction model show that, although in the initial training it was able to get 100% of the predictions right, at the time of validation it made few errors in the predictions.

2. Nayve Bayes

It is a technique that uses Bayes' theorem to determine the most probable membership of a class. For the present training, the Nayve Bayes technique was used, together with a sample of 60% of the data, achieving the results shown in Table 14.

TABLE XIV
TRAINING RESULTS USING THE NAYVE BAYES METHOD

	CAT	PREDICTION				SUMA
		HI	LO	CRI	MO	
CURRENT STATUS	HI	150	0	4	10	164
	LO	0	121	0	0	121
	CRI	0	0	146	0	146
	MO	0	26	0	143	169
	SUMA	150	147	150	153	600

Now the respective validation must be performed, by means of a model evaluation, applying 40% of the remaining data to check the efficiency of the model, when trained, the results of the validation can be seen in Table 15.

TABLE XV
EVALUATION RESULTS USING THE NAYVE BAYES METHOD

	CAT	PREDICTION				SUMA
		HI	LO	CRI	MO	
CURRENT STATUS	HI	87	0	1	8	96
	LO	0	106	0	0	106
	CRI	0	0	87	0	87
	MO	0	12	0	99	111
	SUMA	87	118	88	107	400

The results of the Nayve Bayes technique, after the respective validation, show that, both in the training and in the evaluation, the model made several prediction errors, and it can be deduced that the reliability is quite high because it made few errors.

3. Logistic Regression

It is a technique that, through the use of mathematics, can find relationships between data factors, and then predict one value based on the other value. To train the model based on this technique, a sample of 60% of the data was used, obtaining the results shown in Table 16.

TABLE XVI
TRAINING RESULTS USING LOGISTIC REGRESSION METHOD

	CAT	PREDICTION				SUMA
		HI	LO	CRI	MO	
CURRENT STATUS	HI	149	0	10	5	164
	LO	0	117	0	4	121
	CRI	5	0	141	0	146
	MO	5	4	0	160	169
	SUMA	159	121	151	169	600

As can be seen in Table 16, the prediction model based on the Logistic Regression technique, has made many more errors in the predictions, now it is necessary to make the testing process by using the remaining 40% of data, in Table 17 you can see the results of the test but sometimes include color.

TABLE XVII
EVALUATION RESULTS USING LOGISTIC REGRESSION METHOD

	CAT	PREDICTION				SUMA
		HI	LO	CRI	MO	
CURRENT STATUS	HI	89	0	4	3	96
	LO	0	92	0	14	106
	CRI	5	0	82	0	87
	MO	4	2	0	105	111
	SUMA	98	94	86	122	400

Through the testing process, it has been proven that the model has made several errors in the predictions. It is noteworthy that the model has made more errors in the moderate classification, since it places 17 data wrongly,

which belong to other categories, but the number of correct predictions is much higher than the errors, therefore, the reliability of the model is high.

4. Support Vectorial Machine SVM

It is a technique that helps to predict outliers in different groups, always looking for the best plane to separate these groups in a space of many qualities. For the training of the model based on the SVM technique, a sample of 60% of the available data was used, obtaining the results presented in Table 18.

TABLE XVIII
TRAINING RESULTS USING THE SVM METHOD

	CAT	PREDICTION				SUMA
		HI	LO	CRI	MO	
CURRENT STATUS	HI	160	0	1	3	164
	LO	0	119	0	2	121
	CRI	4	0	142	0	146
	MO	3	0	0	166	169
	SUMA	167	119	143	171	600

Having performed the training process of the SVM-based model for the prediction of the automatic bandwidth adjustment, it is necessary to perform the validation process by applying the respective test using 40% of the remaining data, obtaining the results presented in Table 19.

TABLE XIX
EVALUATION RESULTS USING SVM METHOD

	CAT	PREDICTION				SUMA
		HI	LO	CRI	MO	
CURRENT STATUS	HI	86	0	6	4	96
	LO	1	91	0	14	106
	CRI	8	0	79	0	87
	MO	14	4	0	93	111
	SUMA	109	95	85	111	400

The results of the evaluation indicate that most of the model's errors are concentrated in the assignment of data to the "High" category, while 23 of these data belong to other categories; therefore, it can be said that the reliability of this model is medium-high.

5. K- Nearest Neighbor (KNN)

It is a technique based on the implementation of an algorithm to make predictions by searching for similar data learned in the training stage. To train a model based on this technique, a sample of 60% of the available data was used, obtaining the results presented in Table 20.

TABLE XX
RESULTS OF TRAINING USING KNN METHOD

	CAT	PREDICTION				SUMA
		HI	LO	CRI	MO	
CURRENT STATUS	HI	106	12	29	17	164
	LO	39	50	14	18	121
	CRI	43	24	64	15	146
	MO	48	17	36	68	169
	SUMA	236	103	143	118	600

In the present model, it is observed that the training results are not as expected, since there are many prediction errors, but the corresponding validation should be done by applying a test with 40% of the remaining data, obtaining the results shown in Table 21.

TABLE XXI
EVALUATION RESULTS USING THE KNN METHOD

	CAT	PREDICTION				SUMA
		HI	LO	CRI	MO	
CURRENT STATUS	HI	28	18	24	26	96
	LO	44	20	25	17	106
	CRI	41	15	17	14	87
	MO	35	25	27	24	111
	SUMA	148	78	93	81	400

The results are quite clear, the reliability of this model is very low, since the errors made in each prediction exceed the hits, so it can be deduced that the KNN algorithm is very ineffective for working with this type of data.

6. Neural Network

This technique consists of a set of nodes connected to each other to transmit signals; each piece of information passes through these nodes, where it is subjected to different analyses in order to make a decision. For the training of an automatic bandwidth adjustment prediction model based on a neural network, a sample equivalent to 60% of the available data was used, obtaining the results shown in Table 22.

TABLE XXII
TRAINING RESULTS USING NEURAL NETWORK METHOD

	CAT	PREDICTION				SUMA
		HI	LO	CRI	MO	
CURRENT STATUS	HI	0	0	0	164	164
	LO	0	0	0	121	121
	CRI	0	0	0	146	146
	MO	0	0	0	169	169
	SUMA	0	0	0	600	600

The training results are very unsatisfactory, since the neural network achieved very few predictions correctly, since all the predictions were assigned in the "moderate" category, but only 169 out of 600 are assigned correctly, in this sense, the corresponding validation must be performed by using 40% of the remaining data, Table 23 shows the results of the validation process.

TABLE XXIII
EVALUATION RESULTS USING NEURAL NETWORK METHOD

		PREDICTION				
	CAT	HI	LO	CRI	MO	SUMA
CURRENT STATUS	HI	0	0	0	96	96
	LO	0	0	0	106	106
	CRI	0	0	0	87	87
	MO	0	0	0	111	111
	SUMA	0	0	0	400	400

The validation results confirm the training results, in the new validation predictions the model commits the same errors of the training phase, classifying all the data in the "Moderate" category, of which 111 are correctly assigned out of a total of 400, therefore the reliability of the model is low.

C. Discussion

Once all the general and specific experiments are completed, the results of the experiments are analyzed in each of the tables presented above. It can be observed that the result of the experiments varies very little in each of the AI models used, with the Random Forest, Naive Bayes and Logistic Regression models standing out after having achieved predictions greater than 92% effectiveness in the general and specific experiments, while the SVM model demonstrated good effectiveness reaching 88.8% of correct predictions in the general experiments, varying greatly at the time of performing the specific experiment, rising to 97.8% at the time of training and then having a reduction to 87.3% when completely new data was presented. On the other hand, the KNN and neural network models show an effectiveness of less than 50% of correct predictions in all experiments, all the above can be seen in Table 24.

TABLE XXIV
COMPARISON OF TRAINING AND VALIDATION RESULTS

		ACCURACY		
		5 folds	Training: 600 Dates	Validation: 400 dates
MODELS	Random Forest	99.1%	100%	97.8%
	Nayve Bayes	95.0%	93.3%	94.8%
	Logistic Regression	93.2%	94.5%	92%
	SVM	88.8%	97.8%	87.3%
	KNN	22.9%	48%	22.3%
	Neural Network	28.0%	28.1%	27.8%

Based on the results Random Forest, Naive Bayes, Logistic Regression and SVM models tend to be more efficient in predicting the automatic bandwidth adjustment since they balance well the complexity of the model with the ability to generalize and handle noisy data, on the other hand, KNN and neural network can become inefficient due to the high complexity and computational overhead that is not always necessary for this type of problem.

V. CONCLUSION

Upon careful analysis of the Dataset used for the experiments, it was determined that it partially complies with the required metrics, since it lacks the variable required for automatic adjustment, being necessary to create such variable and assign the adjustment categories to be used as a target variable.

Through the application of the general experiments, it was observed that: Random Forest, Nayve Bayes, Logistic Regression and SVM, demonstrated an effectiveness above 90% measured through the parameters: precision (PREC), classification accuracy (CA), area under the ROC curve (AUC), RECALL and Mathematical Correlation Coefficient (MCC), being that Random Forest demonstrated an effectiveness of 99% in all parameters, being the highest with respect to the other methods, while KNN and Neural Network demonstrated effectiveness below 50%.

The specific experiments showed that the most effective method for the prediction of automatic bandwidth adjustment is Random Forest, since in the training it approached 100% of the predictions, while in the evaluation it got 97.8% of the predictions right, with higher percentages of correct predictions in training and evaluation compared to the other methods,

Comparing the different Artificial Intelligence techniques, taking into consideration the quality of service for the automatic or dynamic bandwidth adjustment, exposes the limitations and strengths that each of the evaluated techniques have when working with certain types of data, although some techniques show a very high prediction effectiveness regardless of the training and validation data, on the contrary, other techniques show that there are variations when exposing the model to training and validation data, being that there is a notable difference between the results of training and validation.

VI. FUTURE WORKS

Future work includes developing an automatic bandwidth adjustment model based on Artificial Intelligence methods, focusing in Analysis of relationship the Random Forest and Neural Network models and the multimedia traffic specially for wireless networks.

REFERENCES

[1] T. Alalibo, O. Sunny and E. Promise, "Bandwidth optimization of wireless networks using," March 2020. [Online]. Available: https://www.irejournals.com/formatedpaper/1702018.pdf

[2] S. C. Madanapalli, H. H. Gharakhieli and V. Sivaraman, "Inferring Netflix user experience from broadband network measurement," 5 August 2019. [Online]. https://doi.org/10.23919/TMA.2019.8784609

[3] S. Rai and A. Kumar, "Dynamic bandwidth allocation in optical networks using Machine Learning," July 2021. [Online]. https://doi.org/10.17605/OSF.IO/5UKBM

[4] A. A. Suham and H. H. Karar, "Optimization of Resource and Bandwidth Allocation in Wireless Networks Performance Analysis using Artificial Intelligence," 2020. [Online]. Available: https://repository.atu.edu.iq/uploads/repo_file_7_23_10_21_51.pdf.

[5] J. Cao, Z. Ma, J. Xie, X. Zhu, F. Dong and Boliu, "Towards Tenant Demand-Aware Bandwidth Allocation Strategy in Cloud Data Center," April 2020. [Online]. Available: https://www.sciencedirect.com/science/article/abs/pii/S0167739X17311834.

[6] K. Lin, C. Li, D. Tian, A. Ghoneim, M. S. Hossain and S. O. Amin, "Artificial-Intelligence-Based Data analytics for cognitive communication in heterogeneous wireless networks," June 2019. [Online]. https://doi.org/10.1109/MWC.2019.1800351

[7] B. L. Khaled, C. Wei, S. Yuanming, Z. Jun and A. Z. Ying-Jun, "The Roadmap to 6G – AI Empowered," 19 July 2019. [Online]. HYPERLINK https://doi.org/10.48550/arXiv.1904.11686; https://doi.org/10.48550/arXiv.1904.11686

[8] T. Sowmya and A. Mary, "A comprehensive review of AI based intrusion detection system," agosto 2023. [Online]. Available: https://www.sciencedirect.com/science/article/pii/S2665917423001630#sec3.

[9] J. Zhao, Z. Su, Y. Yang and T. Xu, "ANN/Random forest based performance monitoring in high-speed short-reach optical interconnections," October 2024. [Online]. HYPERLINK "https://doi.org/10.1016/j.yofte.2024.103941" \t "_blank" \o "Persistent link using digital object identifier" https://doi.org/10.1016/j.yofte.2024.103941

[10] Wezen, "QoS, qué es y cuál es su importancia en la gestión IT," 15 August 2023. [Online]. Available: https://www.wezengroup.com/qos-cual-es-su-importancia-en-la-gestion-it/.

[11] VASExperts, "Cómo utilizar QoS para garantizar la calidad del acceso a Internet," 23 January 2023. [Online]. Available: https://vasexperts.com/es/blog/quality-of-service/how-to-use-qos-to-ensure-the-internet-access-quality/.

[12] D. Young, "Conference Call Bandwidth Consumption. [Dataset]," (2020). [Online]. Available: https://www.kaggle.com/datasets/dikamsiyoung/conference-call-bandwidth-consumption/data.

[13] Union International Telecommunication, "International Internet bandwidth per Internet user, kb/s. [Dataset]," 2016. [Online]. Available: https://www.theglobaleconomy.com/Slovenia/Internet_bandwidth/.

[14] K. Raghunath, "5g network metrics high traffic event. [Dataset]," 18 August 2023. [Online]. https://doi.org/10.21227/1ryt-wb82

[15] L. Mei, J. Gou, Y. Cai, H. Cao and L. Yong, "Realtime Mobile Bandwidth and Handoff Predictions in 4G/5G Networks," 27 April 2021. [Online]. Available: https://doi.org/10.48550/arXiv.2104.12959

[16] O. Schmitz, "Orange Data Mining: Aprendizaje automático de código abierto y visualización de datos," 9 May 2023. [Online]. Available: https://www.linkedin.com/pulse/orange-data-mining-aprendizaje-autom%C3%A1tico-de-c%C3%B3digo-y-schmitz-/.

[17] M. Amer, "Métricas de evaluación de clasificación: precisión, exactitud, recuperación y F1 explicadas visualmente," 7 June 2022. [Online]. Available: https://cohere.com/blog/classification-eval-metrics.

[18] Deepchecks, "Comprensión de las métricas de puntuación F1, precisión, ROC-AUC y PR-AUC para modelos," 13 June 2024. [Online]. Available: https://deepchecks.com/f1-score-accuracy-roc-auc-and-pr-auc-metrics-for-models/.

[19] M. Tech, "¿Qué es el coeficiente de correlación de Matthews (MCC)?," 13 December 2022. [Online]. Available: https://medium.com/@CuttiE_MarU/what-is-matthews-correlation-coefficient-mcc-bb07a-94162ba.